Reactive Transport In Chemically And Physically Heterogeneous Porous Media: Effect Of Non-equilibrium Linear Sorption

by

Anil Kumar Mishra

Submitted in Partial Fulfillment

of the Requirements for the Degree of

Doctor of Philosophy

New Mexico Institute of Mining and Technology

Socorro, New Mexico

June, 1997

To my parents

Prabha and Vishwanath Mishra

for their sacrifices

to nurture my desire of learning

ABSTRACT

Reactive transport of a linearly sorbing solute under kinetically limited conditions is studied. The first-order rates are lumped parameters that combine the effects of both physical and chemical non-equilibrium processes. A probabilistic interpretation of the sorption-desorption phenomena within a Markovian framework is used to develop a recursion-based algorithm in one dimension.

The Markov model is extended to describe sorption site heterogeneity, sites accessed in parallel by the sorbing solute (hyperexponential model) or for sites which are in series (gamma model). The sensitivity of the breakthrough curves is investigated.

A two-dimensional streamline based transport simulator is developed for transport of a linearly sorbing solute in a porous medium exhibiting physical and chemical heterogeneity. The one-dimensional formulation is applied to a two-dimensional steady-state flow field to study plume-scale migration. It is shown that the use of the semi-analytical recursion formulation along the streamlines accurately captures the variability of the concentration in a heterogeneous media. The complex interactions of the spatially varying rates of sorption and desorption with the spatially varying velocity field produces a very irregular pattern of aqueous concentration in the plume. The resulting plume shows areas of high concentration which are discontinuous very much similar to observations made in fields. The spatial moments of the plumes are used to describe the temporal behavior during its advection through the aquifer and are compared with analytical results based on constant K_d. Spatial variability of the rates contributes to an additional spreading of the plume. An ap-

plication to model PCE migration at Borden site is presented. Good agreement of the spatial moments with the field results is obtained when the sorption-desorption rates are modeled as spatially varying random fields.

The Lagrangian framework that has been used throughout this study is further focussed to study transverse spreading of a linearly sorbing solute. For a highly idealized system of stratified aquifer, a new recursion formulation to evaluate transverse dispersion both for a non-sorbing and a sorbing solute is developed. It is shown that inclusion of local dispersion within a Lagrangian framework will lead to transverse spreading of the plume which continues to grow with time.

ACKNOWLEDGMENTS

The guidance, involvement and the continued support of Dr. Allan Gutjahr, my advisor, has been the critical factor in the completion of my dissertation and I wish to express my sincere thanks to him. He was very encouraging and supportive and always available to listen to my various ideas. I would also like to thank him for giving me the opportunity to explore many other areas, like the GXG project, which greatly enriched my knowledge of the subject of reactive transport in groundwater.

I would like to thank my co-advisor, Dr. John Wilson, for his very thorough editing of my dissertation while on a sabbatical as well as his help on the two-dimensional model. Numerous discussions with Dr. Rob Bowman are greatfully acknowledged. Dr. Fred Phillips insightful comments always provided a fresh perspective to my results. The assistance of Dr. Hari Rajaram and his response to my queries with detailed and systematic explanations is greatfully acknowledged. He was very generous with his ideas to our research problem.

I am indebted to my wife, Soni for her love and encouragement during the entire period of my graduate studies. Her inspiration made my PhD a reality as well as her dedication to raising our son, Harsha, almost alone. I want to thank Harsha for constantly reminding me about many other important things in life besides my work. I would also like to thank my numerous friends in the Hydrology Program and at Tech for making our stay at Socorro a very happy and memorable one.

Table of Contents

List of Tables

List of Figures

Chapter 1

Introduction

1.1 Overview

Reactions between solutes and mineral surfaces are important in the study of groundwater flow. In the context of contaminant transport in aquifers, much effort has gone into characterizing the movement of plumes under natural and forced-gradient conditions. The studies done have included both theoretical analyses and field-tests conducted to monitor plume-spreading at the field scale. A major focus has been on evaluating the effect of heterogeneities in the physical and chemical parameters of the aquifer.

In this chapter a brief review of the developments in transport modeling of solute advected by groundwater is presented, first for non-reacting or ideal tracers and then for sorbing solutes. The concept of kinetically limited sorption behavior is introduced to differentiate it from the equilibrium assumptions inherent in most of the transport studies. The central theme of this research work, the effect of spatial variability of the sorption and desorption rates on contaminant transport, is then proposed and outlined.

1.2 Transport Model for Ideal Solutes

For ideal tracers (solutes which do not interact with the rock matrix in any manner) the advection-dispersion equation has been the standard approach for analyzing the movement and spread of solutes as they are transported by groundwater. The advection-dispersion equation is obtained from the continuity equation of mass balance over a representative elementary volume accounting for the advective and dispersive fluxes and relating the flux through Darcy's law. This then allows the equation to be written in terms of the parameters of the permeable medium. The equation in vector notation for a three-dimensional flow domain assuming constant porosity and incompressible fluid and non-deformable matrix is given as

$$\frac{\partial C}{\partial t} + \nabla.(\mathbf{v}C) = \nabla.(\mathbf{D}.\nabla C) \tag{1.1}$$

where C $[M/L^3]$ is the aqueous concentration at a given point $\mathbf{x}$=(x,y,z) at time t, $\mathbf{v}$ is the seepage velocity in [L/T], and $\mathbf{D}$ is the local hydrodynamic dispersion coefficient, $[L^2/T]$.

The advection-dispersion equation given above has been solved for a wide variety of boundary conditions, when the velocity and the dispersion coefficient are considered to be constant. Similarly, an analogous advection-dispersion-reaction equation can be written for many solutes assumed to be in equilibrium with their sorbed fraction. The various equilibrium sorption models will be discussed after reviewing some aspects of non-ideal transport behavior of ideal solutes.

The transport equation in equation 1.1 assumes a homogeneous medium with a constant value of material properties like hydraulic conductivity ($\mathbf{K}$) and porosity. The actual aquifer materials or soils exhibit a large variability in grain-sizes

and the structure of the solid matrix. Often the porous medium may show distinct features such as aggregation, lenses of low conductivity material embedded in the higher conductivity zones or vice-versa. Transport in such medium is termed non-ideal. Non-ideal transport is characterized by early breakthrough and tailing [Anderson, 1979]. The various causes of the non-ideal behavior have been postulated to be physical and chemical factors, which include heterogeneity of hydraulic conductivity and the chemical properties of the aquifer, and non-equilibrium sorption [Brusseau and Rao, 1989a]. For the case of non-sorbing solute transport, physical factors such as soil aggregates have been shown to result in non-ideal transport. A bicontinuum approach has been used to describe the transport process in an aquifer where the heterogeneous structure of the porous medium is simplified to a two-region model. In this model, a mobile region is postulated where the water and dissolved solute can flow and an immobile region where water and solute are stagnant. Mass transfer of the solute between the mobile and immobile region is obtained by a diffusive transfer mechanism. One of the earliest models based on this conceptualization was that of Coats and Smith [1964]. The diffusive mass transfer mechanism was modeled using a first-order equation where the rate of mass transfer is proportional to the concentration difference between the two regions. A number of studies have attempted to find the proportionality constant, known as the mass transfer coefficient, by assuming a given geometry of the aggregate and modeling the diffusive mass transfer as a physical diffusion model [van Genuchten et al., 1984; Rao et al., 1980a, b]. van Genuchten et al. [1984] showed that the mass transfer coefficient, α is related to the lateral diffusion time, $\alpha \propto D_T/a^2$ where a is the characteristic aggregate size, while the studies of Rao et al. [1980a, b] showed that α is related to the solute residence time and is affected by the flow velocity.

The transport of many nonpolar (or weakly polar) organic solutes such as tetrachloroethylene (PCE), polynuclear aromatic hydrocarbons (PAHs) and other hydrocarbons associated with petroleum products are not ideal. These contaminants undergo not only advection and diffusion but also sorption as well as other chemical and biological transformations. The transport of these solutes in groundwater involves a complicated interaction of all the mechanisms above. Often one or more of the mechanisms will be the dominant influence depending on the type of solute, the physical and chemical properties of the porous medium, and (especially for heterogeneous media) the scale of investigation.

For contaminant transport, three scales have been identified to be important, the pore scale, field scale and regional scale [Dagan, 1986]. In this work we do not explicitly address methods of obtaining the sorption and desorption rates at different scales. We assume that for the transport problem at the various scales studied, these rates are known. The problem of relating one scale to another is a very challenging task in itself requiring additional study.

1.3 Reactive Transport in Groundwater

Conceptual models for predicting long-term solute fate and transport need to consider three elements: geological features of the aquifer through which the flow is occurring, events which specify the amount and time of contaminants released and the various processes that occur during the movement of the contaminant through the pore spaces [Tsang et al., 1994] . Transport of solute in groundwater is a complex phenomenon, particularly if the various interactions that are possible between the solid matrix and the dissolved chemical species in aqueous and non-aqueous phases

are taken into account. These reactions could range from precipitation/dissolution reactions, formation of various complex species or sorption onto the solid phase. A detailed description of the reactions, which can be classified as either homogeneous or heterogeneous, is presented in Rubin [1983].

Sorption is a particularly important process occurring at the rock-water interface because it causes significant attenuation of the concentration of the solute during its transport by the advecting groundwater. Sorption phenomenon has been the focus in various fields such as: in soil science, to study the movement of pesticide through the root zone; in chemical engineering to study chromatographic processes and catalysis; and in hydrology and water resources engineering to study contaminant fate and transport. Including the sorption process allows us to predict the arrival of solute at a given location down-gradient of a point from where it was injected and to determine the peak concentration of the solute. Both of these parameters – the arrival time of the solute and the maximum concentration – have implications for regulatory decisions regarding clean-up efforts at various contaminated groundwater sites.

The sorption process reflects the affinity of the solute present in the carrier fluid for selective partitioning onto the solid phase when the carrier fluid is advected through the permeable medium. This process occurs with both the liquid and gaseous phases. In this work, we only consider groundwater flow through aquifer material and thus restrict our attention to saturated conditions. We also use the term 'partition' in a very general sense to mean the transfer from the aqueous to the solid phase, which could be the mineral surface of the rock, an organic coating, or any other solid surface. Sorption is a very complex phenomenon and many different physical and

chemical processes could be the driving forces causing mass to be transferred from the aqueous to the solid phase. For the purposes of our discussion and the realm of this work, we assume sorption to be the main mechanism for interaction of a reactive solute. This interaction then differentiates a reactive solute from ideal tracers - solutes which do not interact with the surrounding rock matrix.

1.4 Equilibrium Sorption Models

The transport of reactive solutes in groundwater is often studied under the assumption of equilibrium conditions for partitioning of the solute between the aqueous and the sorbed phases. The equilibrium conditions that are postulated to exist are then described by a number of phenomenological models which have been developed on the basis of experimental observations.

The general method of equilibrium sorption description uses isotherms such as the Linear, Freundlich and Langmuir isotherms. The linear sorption isotherm is described by [Fetter, 1993]

$$S = K_d C \qquad \text{Linear} \tag{1.2}$$

where S = mass of solute sorbed per dry unit weight of solid (mg/g)
K_d = Distribution coefficient (L/g).

The linear sorption isotherm implies that the amount of solute that can be sorbed onto the solid is unlimited. The Freundlich sorption isotherm also implies this and is defined by the nonlinear relationship

$$S = K_F C^g \qquad \text{Freundlich} \tag{1.3}$$

where K_F and g are constants.

The Langmuir sorption isotherm limits the amount of solute that can be sorbed onto the solid surface and is expressed as

$$S = \frac{\alpha_L \, S_{max} \, C}{1 + \alpha_L \, C} \quad \text{Langmuir} \tag{1.4}$$

where α_L = an absorption constant related to the binding energy (L/mg)
S_{max} = the maximum amount of solute that can be absorbed by the solid (mg/g).

These isotherms relate the aqueous concentration to the sorbed concentration for a given type of mineral surface or a soil type. For sorption described by a linear isotherm, which is defined by a constant value of the slope of the line between the sorbed concentration and the aqueous concentration, the advection-dispersion-reaction equation can be written as

$$\frac{\partial(R\,C)}{\partial t} + \nabla.(\mathbf{v}C) = \nabla.(\mathbf{D}.\nabla C) \tag{1.5}$$

where $R = 1 + \rho \, K_d/n$ is the retardation factor, and n is the porosity. For a non-reactive solute, R equals 1 and we recover equation 1.1. Analytical solutions for the linear sorption conditions are available for various initial and boundary conditions for the case of constant velocity and local dispersion coefficient.

The linear isotherm equation is, however, a very simplified model of the complex sorption process. Two different types of sorption processes can be distinguished: physical sorption and chemisorption. Physical sorption involves the transfer of solute from the aqueous to the sorbed phase either by the process of partitioning or weak van-der Waals interactions and has a typical heat of reaction on the order

of 1 to 10 kcal/mol. Chemisorption may involve transfer of electrons or radicals or rearrangement of the bonds and usually has a higher heat of reaction–on the order of 10 to 100 kcal/mol. Numerous sorption studies on different surfaces have been performed in the fields of material science and chemical engineering where the focus is on the understanding of the mechanisms in greater detail in order to obtain better performance from engineered catalysts. Particularly for heterogeneous catalytic reactions, it is crucial to obtain the rate laws for the various reactions.

From the perspective of groundwater flow and the movement of contaminants that are sorbing on the solid phase, it is imperative that we focus our attention on the equilibrium conditions usually assumed. For the large-scale transport of solute in groundwater which may be of the order of tens to hundreds of meters, the complexity of the porous medium has a larger effect than in column experiments on the overall transport and distribution of the aqueous concentration. If we look at the transport of non-polar organics, which constitute a significant portion of contaminant sources in many areas of the world, sorption behavior has been generally described by linear isotherms assuming equilibrium conditions. Recent field and laboratory studies have, however, indicated that for many pollutants, especially pesticides and other organics, the sorption-desorption reactions are kinetically limited [Pignatello, 1993].

Several studies have shown that the assumption of equilibrium conditions may not always be accurate. Field and laboratory scale experiments often show that sorption rates are quite low and that kinetic effects need to be considered [Nkedi-Kizza et al., 1983; Miller and Weber, 1986; Goltz and Roberts, 1986; Ptacek and Gilham, 1992]. The sorption phenomenon shows two distinct time scales – a short period of very rapid sorption followed by a slower rate which may last for periods

of hours to days. For example, Pignatello and Huang [1991] showed that the distribution coefficient obtained for atrazine and metachlor from field samples collected a few months after the application was about 42 times greater than the value obtained from sorption experiments that lasted 24 hours. Similar non-equilibrium phenomena have been reported for simazine [Scribner, et al., 1992] , tetracholorethylene (PCE), trichloroethylene (TCE), toluene and xylene [Pavlostathis and Mathavan, 1992]. Inference of kinetically limited transport in the field is based on the studies conducted on transport of lithium [Garabedian et al., 1988] and molybdate [Stollenwork, 1995].

1.5 Rate Limited Sorption and Desorption

Transport of a wide variety of chemicals dissolved in groundwater has been studied in several fields, where the main reaction was sorption-desorption of the chemical species under consideration. These studies have been conducted on a wide range of spatial and temporal scales, including both column experiments carried out in the laboratory as well as large-scale field experiments.

The study of the transport problem has proceeded along both Eulerian and Lagrangian lines. In the Eulerian approach it is assumed that on the local scale the following equation for the aqueous concentration holds

$$\frac{\partial C}{\partial t} + \frac{\partial S'}{\partial t} = \nabla.(\mathbf{D}.\nabla C) - \nabla.(\mathbf{v}C) \qquad (1.6)$$

In equation 1.6 S' is the sorbed concentration (defined as sorbed solute mass per formation solid volume). For the case of non-equilibrium linear sorption conditions investigated in this study, the aqueous and sorbed concentrations are related by

$$\frac{\partial S'}{\partial t} = k_f\, C - k_r\, S' \tag{1.7}$$

where k_f and k_r are the sorption and desorption rate coefficients such that $K_d = k_f/k_r$ and K_d is the distribution coefficient of the solute for the assumed linear isotherm conditions.

For reactive solutes, the above two-site concept was extended and non-equilibrium conditions which were identified in solute transport were variously modeled using the multi-process non-equilibrium (MPNE) model [Brusseau et al., 1989] which is based on earlier developments of the two-region models. These models assume an instantaneously sorbing fraction of the solid matrix and another fraction where the sorption occurs over a longer period of time [van Genuchten and Wagnet, 1989; Cameron and Klute, 1977] and consists of two types of sites; the first site is in equilibrium with the aqueous concentration while the second site exchanges solute with the first site and/or the aqueous phase at a rate described by first-order kinetics.

All the formulations discussed above were based on constant values of the different parameters. During the last two decades, a number of studies have focused on the spatial variability of the aquifer parameters and their importance to the transport of solute in groundwater flow. It has been repeatedly shown that there are small-scale and large-scale features of the geologic media which are inherently variable, the probable causes being the deposition mechanisms and post-depositional diagenesis which create a very heterogeneous pattern for various parameters like permeability, organic carbon content, and mineral composition.

The deterministic advection-dispersion-reaction equations which assume known and fixed values of parameters such as velocity, local dispersion and K_d have been

shown to be of limited use in describing field-scale transport. We are now very aware of the heterogeneity of the natural aquifer materials. Various new tools and techniques have been developed to account for the variability and the associated uncertainty in the model predictions. A detailed review of the stochastic theory of transport is presented in the next chapter which also highlights the area of non-equilibrium sorption to be addressed.

Several recent theoretical and computational studies have focused on reactive transport in heterogeneous media. Valocchi [1989] presented an analytical solution for reversible linear kinetic sorption in a stratified aquifer. Cvetkovic and Shapiro [1990], Selroos and Cvetkovic [1992] and Dagan and Cvetkovic [1993] consider the same problem in three-dimensionally heterogeneous media. In none of the above studies was the effect of spatial variability in the individual reaction rates (the sorption rate k_f and desorption rate k_r) considered. Garabedian et al. [1988], Dagan [1989], Chrysikopoulos et al. [1990] and Bellin et al. [1993] did examine the influence of spatial variability in distribution coefficient $K_d(k_f/k_r)$ on sorptive solute transport, demonstrating that a negative correlation between the logarithm of hydraulic conductivity, ln K and ln K_d results in increased macrodispersion. This feature is also evident in field data from the Cape Cod site [Garabedian et al., 1988] and the numerical simulations of Burr et al. [1994] . While these studies incorporate heterogeneity in sorption characteristics of soils, sorption kinetics were not considered. A recent study by Hu et al. [1995], that did incorporate heterogeneity in ln K and in sorption kinetics, revealed a complex interaction between kinetic sorption and the velocity variations.

Evaluation of stochastic theories of solute transport in heterogeneous media

has been facilitated by large-scale numerical simulations (e.g. Tompson and Gelhar [1990], Tompson [1993] and Burr et al. [1994]). These simulation studies identified some limitations of theoretical results, and motivated studies to further refine the theoretical results. In the context of sorptive transport, the relative importance of spatially variable sorption kinetics in explaining features observed from field data has yet to be investigated. A related issue is that of the influence of spatially variable kinetics on clean-up times for sorptive contaminants. To date, no large-scale simulation studies which incorporate spatially variable sorption kinetics have been reported. In this context, there is a need for efficient simulation algorithms for transport involving kinetic sorption.

Particle-tracking algorithms (e.g. Tompson and Gelhar [1990]) are an attractive option for large-scale simulation, primarily due to their computational efficiency. Recently Tompson [1993] extended the particle-tracking approach to model equilibrium sorption by mapping the particle distributions onto a grid for defining local concentrations. Andricevic and Foufoula-Georgiou [1991] and Quinodoz and Valocchi [1993] proposed particle-tracking algorithms that did include kinetic sorption. In their approaches, a particle was allowed to move back and forth between a "sorbed" and "aqueous" state, and the probability density of the times spent in each phase was related to the sorption kinetics. However, spatial variability in sorption kinetics was not considered in those works.

In this dissertation, we focus our attention on non-equilibrium linear sorption characterized by the sorption and desorption rates and their associated variability in the spatial domain. We develop a very general model for contaminant transport of a linearly sorbing solute in a physically and chemically heterogeneous media. The

model is then used to study field-scale transport of a solute. We restrict our investigation to evaluation of the first three spatial moments of the solute concentration distribution.

1.6 Objectives

Processes such as adsorption, precipitation and ion-exchange are key areas of water-rock interactions which affect ground-water quality. Of particular concern is the issue of the slow process of sorption-desorption. This has been variously termed as kinetic sorption, resistant sorption or non-equilibrium sorption.

The overall objective of the study is to evaluate the importance of spatial variability of the kinetically limited sorption-desorption process at different length scales. Most of the results based on stochastic theories of transport assume equilibrium conditions for the sorption process. It has been postulated that the complex interplay of the spatially varying rates of sorption and desorption with the spatially varying velocity field would lead to more realistic descriptions of contaminant plume migration as well as insights regarding spreading. This research focuses on the kinetic aspects of sorption-desorption processes. The implications of slow rates of sorption-desorption on plume evolution are highlighted. In particular we use the standard statistical descriptions of centroid and the second spatial moment which have been thought to provide a complete description.

Specifically the following issues are addressed:

1. We develop a new formulation of the reactive transport with kinetically limited sorption, in which linear sorption is modeled as a Markov process. We first

develop the recursion formulation for the case of constant rates and then consider spatial heterogeneity of the rates and extend the recursion formulation to a spatially varying field.

2. We develop a two-dimensional simulator for modeling transport of a linearly sorbing solute in a heterogeneous medium. The sorption and desorption processes are specified in terms of rates which could be high (denoting equilibrium conditions) or low (signifying kinetically limited conditions). These rates are specified as spatially varying random fields, either independent of the hydraulic conductivity field or correlated with it.

3. We use the algorithm described above to model transport of tetrachloroethylene (PCE), a non-polar organic at the Borden site. We examine transport of non-polar organics at the field-scale referring to distances on the order of tens to hundreds of meters. We evaluate higher moments for the non-equilibrium sorption conditions in order to better describe the plume shape and location.

4. We model the sorption site heterogeneity using a semi-Markov approach.

5. Finally we study the transverse dispersion behavior of a linearly sorbing solute in a stratified aquifer in a Lagrangian framework where we include the local dispersion.

1.7 Outline

This dissertation is divided into the following chapters:

Chapter 1 is the introduction and gives a brief overview of the field of reactive

transport applied to groundwater flow. It also formulates the research questions addressed in this research.

Chapter 2 gives a detailed literature review of the various algorithms and models used for solving the reactive transport equation. Results from stochastic theory of transport are outlined in Chapter 2 along with the assumptions used to obtain the results. We note the need to study non-equilibrium sorptive transport where the rates are spatially varying.

In Chapter 3, a recursion formulation is developed for a one-dimensional flow system. Breakthrough curves for the case of constant and spatially varying sorption and desorption rates are obtained. We also study the effect of the combined processes of sorption and decay in the aqueous or the sorbed phases.

Chapter 4 discusses the application of the Markov model to sorption sites which exhibit heterogeneities and we then develop semi-Markov models of transport.

In Chapter 5, the one-dimensional algorithm is extended to a two-dimensional flow system by applying the recursion formulation along streamtubes. The simulation procedure is described and applied to a field site. In particular we study the transport of PCE in a field setting similar to the Borden site study [Roberts et al., 1986].

Chapter 6 examines the problem of transverse dispersion of a sorbing solute in a stratified aquifer and we present a formulation for dispersion of the plume where the solute undergoes linear kinetic sorption. The transverse spreading of a non-reacting solute is contrasted with that of a sorbing solute where the rates are either constant or spatially varying.

Chapter 7 gives a summary of the main results of this work and outlines some new research areas and questions.

Chapter 2

Literature Review

2.1 Overview

There are a number of solutes that undergo interactions with the rock matrix. These interactions may be of different forms: sorption-desorption, precipitation-solubilization, ion-exchange, etc. The type of interaction depends on the ionic nature of the solute (non-ionic vs cation or anion), the chemical condition of the fluid (presence of other solutes and cosolvents), the pH, and the temperature conditions.

Modeling the coupled processes of reaction and flow in geological media is of interest in subsurface contaminant hydrology, reservoir engineering and geochemistry. Reactive transport involves the hydrodynamic processes of advection, dispersion and diffusion along with a set of equilibrium or kinetic reactions that describe the chemical interactions between the different components present in the fluid phase with the surrounding rock matrix.

The type of reactions that occur in porous media include dissolution, precipitation, oxidation, reduction, hydrolysis, complexation, sorption, desorption, decay and degradation. These reactions are termed homogeneous if there is no phase change involved and heterogeneous if the chemical species is transferred from the aqueous to the solid phase or vice-versa (see James and Rubin [1979]).

In developing these theories a number of important issues have been identified. The foremost is the identification of the most dominant process: hydrological, chemical or biological. The problem is complicated by the variation in the degree of interaction between these three processes at different spatial and temporal scales. The second most important aspect is the considerable spatial variability of the subsurface environment.

Heterogeneity in groundwater flow is observed at many different scales. These range from the pore scale to Darcy scale (which is on the order of cm) to the regional scale (few tens to hundreds of kilometers). One challenging problem in subsurface contaminant hydrology is to examine transport at scales smaller than the regional scale but larger than the Darcy scale. The range of this problem varies from a few meters to a few kilometers. This scale for purposes of discussion will be referred to as the inter-well scale.

This chapter provides some background information about the theory developed in the general area of solute transport in groundwater, particularly emphasizing the models of stochastic theory developed along two broad avenues, Eulerian methods of analysis and Lagrangian approaches. Stochastic theory provides a framework of analysis where the natural variability of the formation is explicitly taken into account to predict ensemble average behavior of contaminant plumes. In the next section a brief overview of some of the terminology is given.

The porous medium through which the groundwater flow occurs is considered to have spatially varying parameters such as permeability and porosity. Heterogeneity of these parameters has been well documented and has been been the starting point of many studies [Freeze, 1975; Bakr et al., 1978] . Two very com-

monly employed assumptions in modeling these spatial random functions (SRF) are stationarity and ergodicity. Stationarity assumes that the various moments of the parameter (say hydraulic conductivity, **K**) are independent of the spatial locations. In particular, a weaker form of stationarity is "second order stationarity", which requires that the second moment depend only on the separation distance and not on actual locations. The issue of ergodicity is a more complex matter which allows us to treat the data available from a field site to be equivalent to the ensemble mean and thus representative of the SRF.

Allowing for heterogeneity of **K** field, water moving under a prescribed gradient has a velocity **v** which is a SRF. In the very general case, a mixture of dissolved species with composition different from that of groundwater enters the aquifer either as a pulse input or a continuous injection. The variable velocity of the groundwater leads to the development of a plume with an erratic front. Having satisfied ourselves that the variability of the permeable medium is indeed a common natural phenomenon, we can now look at the effect of variability of hydraulic conductivity on predicting flow and transport. The two most common models for studying flow and transport, Darcy's law and the convection-dispersion equation, relate hydraulic head (h), hydraulic conductivity (**K**), pore-water velocity (**v**) and concentration (C). It is then obvious that variability of **K** would lead to variability of h and C.

The primary dispersive mechanism for a non-reactive solute is likely associated with the spatial fluctuation of the velocity field caused by the local-scale variations in the K field. For a reactive solute, additional processes of intra-particle diffusion and/or kinetic sorption have also been hypothesized to influence solute dispersion. Stochastic continuum theory has been used to describe the transport of

solute in a heterogeneous media. Gelhar and Axness [1983] used a Fourier-Stieltjes formulation of the perturbed head linearized steady flow and transport equations to study the asymptotic behavior of nonreactive solutes. Dagan [1982, 1984, 1988], using a Lagrangian approach based on the Taylor's theory of diffusion [1921], formulated a relation between the time rate of growth of the second moment of the mean concentration field with the variance and correlation length of a statistically anisotropic K field. In Dagan's work, local dispersion is neglected and it is shown that for longitudinal second moment analysis the effect of the local dispersion is negligible [Cushman et al., 1996]. Naff [1990] presents an analysis of the dispersion of the solute plume by incorporating local-scale mixing. Garabedian [1987], Dagan [1989] and Kabala and Sposito [1991] have studied reactive solute migration and provided analytical results describing the asymptotic dispersive behavior of a sorbing solute. All the results however assume K_d to be either constant or fully correlated with the K field.

We now present some of the results of the Eulerian and Lagrangian analyses for non-reactive solute for flow in a heterogeneous medium to describe the spreading of a plume as it migrates down-gradient under a spatially varying velocity field. Both of the methods relate hydraulic conductivity variability to macrodispersion by obtaining expressions for fluid velocity correlation with that of hydraulic conductivity and head. Expressions for the spatial moments and that of macrodispersion coefficient are the final results.

2.2 Eulerian Approach

Assuming the different variables, C, h, $\mathbf{K}$ and $\mathbf{v}$ to be stochastic processes, a stochastic partial differential equation for the concentration field C, can be written

as follows:

$$n\frac{\partial C}{\partial t} + \mathbf{q}.\nabla C = -\nabla.(\mathbf{D}.\nabla C) \qquad (2.1)$$

where $\mathbf{q}$ is the specific discharge and for constant porosity n is related to the velocity field by $\mathbf{q} = \mathbf{v}/n$. The random velocity field $\mathbf{v}=\mathbf{U} + \mathbf{u}$, $\mathbf{U}$ is the mean velocity, $\mathbf{u}$ is the local fluctuation in velocity. Similarly, the concentration field C(x,t)= E(C) + c(x,t), where E(C) is the mean concentration and c(x,t) is the fluctuation. $\mathbf{D}$ is the pore scale dispersion tensor.

In the Eulerian approach, the spectral representation theorem is used to find the different moments of C. First and second-order perturbation techniques are used to characterize the ensemble average of C. Some of the earliest work in stochastic theory related to quantifying variability of $\mathbf{K}$ [Bakr et al., 1978], studying the variance of h [Mizell et al., 1982] , and studying mean concentration and variance of c [Gelhar et al., 1979; Vomvoris, 1986]. In deriving the variance of c, we have to evaluate an added macrodispersive flux term ($\mathbf{u}c$) which is often approximated using a Fickian relationship

$$\overline{c\mathbf{u}} = -\mathbf{A} \,.\, \nabla c \qquad (2.2)$$

where $\mathbf{A}$ is the macrodispersion tensor. Great effort in Eulerian analysis has been expended in obtaining expressions for $\mathbf{A}$ in terms of the statistics of $\mathbf{K}$, h and $\mathbf{v}$. Details of the analysis can be obtained from the work of Gelhar et al. [1979], and Gelhar and Axness [1983] .

For example in the simplified case of stratified aquifer, the asymptotic value of the macrodispersivity, A_∞ is given by Gelhar et. al. [1979]

$$A_\infty = \frac{\sigma_k^2 \, l^2}{3 \, \bar{K}^2 \, a_T} \tag{2.3}$$

where K=$\bar{K}$+k is the physically isotropic hydraulic conductivity with a constant mean, $\bar{K}$ and perturbation, k such that E[k]=0; l=length scale of k, σ_k^2 = the variance of k; and a_T=local transverse dispersivity. The results obtained in the above-mentioned studies were applicable for small variances of ln K and were viewed as an asymptotic large time limit valid for plumes with large spatial extent.

For the early times, **A** has been postulated to be time dependent and expressions for time-dependent **A** have been developed by Koch and Brady [1988], Graham and McLaughlin [1989a, b] and Naff [1990] . Their approach was based on some simplifying assumptions where dropping some cross-terms leads to simplification of the solution. However, Dagan and Neuman [1991] showed that such an analysis may lead to an underestimation of the higher-order spatial moments.

2.3 Lagrangian Approach

In the Lagrangian approach, the movement of individual particles is analyzed by assigning a particle position $X(t; x_0, t_0)$ at time t, given it was at x_0 at t_0. Each particle is associated with a mass, m given by

$$C(x,t) = \frac{m}{n}\delta \left(x - X(t; x_0, t_0)\right) \tag{2.4}$$

where n denotes the porosity of the medium and δ is the Dirac delta. $X(t; x_0, t_0)$ is related to the velocity field by

$$X(t; x_0, t_0) = \int_{t_0}^{t} v[X(t'; x_0, t_0)] \, dt' \tag{2.5}$$

Using a stochastic model for the random velocity field, $X(t; x_0, t_0)$ and C(x,t) can be calculated. The above equation allows computation of the various moments of X and for the calculation of a time-dependent, preasymptotic macrodispersion coefficient (see Dagan [1987] for a review). The expected values of the first two spatial moments of a non-reacting solute advected in a three-dimensional isotropic heterogeneous flow domain assuming an exponential covariance structure for the log K field, are given by [Dagan 1982, 1984]

$$X_1 = U\,t = \frac{K_G\,J}{n}t; \quad X_2 = X_3 = 0 \tag{2.6}$$

$$X_{11} = 2\,U^2\,I^2\,\sigma_Y^2[t' - 8/3 + 4/t' - 8/t'^3 + 8e^{-t'}(1 + 1/t')1/t'^2] \tag{2.7}$$

$$X_{22} = X_{33} = 2\,U^2\,I^2\,\sigma_Y^2[1/3 - 1/t' + 4/t'^3 - e - t'(1/t' + 4/t'^2 + 4/t'^3)] \tag{2.8}$$

where X_1 is the mean displacement in the flow direction, and X_{ij} are the variances in the x, y, and z directions, with $X_{ij} = 0$ for i≠j. The dimensionless time t' is defined as t/t_h where t_h, the characteristic time of the formation heterogeneity, is I/U; I is the integral scale of the formation and U is the mean velocity.

In both approaches the effective dispersion coefficients related to the rate of growth of the solute plumes increase initially with the travel distance from the source, showing non-Fickian behavior, and are much larger than the pore-scale dispersion coefficients.

2.4 Reactive Transport

The stochastic methodology above was developed for ideal tracers – namely, solutes which do not interact with the surrounding rock matrix. At the same time, a

parallel development has occurred in simulating deterministic multi-component systems where reactions influence transport and vice-versa. These models were developed for idealized equilibrium conditions and varying degrees of complexity [Yeh and Tripathi, 1991; McNab and Narshimhan, 1994] . The reactive transport model generally considers a two-phase heterogeneous porous formation. Groundwater forms the mobile continuous phase. The immobile phase is the solid rock matrix consisting of minerals, organic matter, etc.

Considering N_c mobile species and N_s immobile species with M components, a total of $N_c + N_s$ species are present in the system. The stoichiometric equations for the system are [Friedly and Rubin, 1992]

$$\sum_{i=1}^{N_c} \mu_{ri} C_i = \sum_{j=1}^{N_s} \nu_{rj} S_j, \quad r = 1, M \tag{2.9}$$

where the mobile species C_i (i=1, N_c) undergo homogeneous and heterogeneous reactions with the immobile species S_j (j=1, N_s), and μ, ν are stoichiometric coefficient matrices. In the above formulation all of the reactions are linearly independent and each of the reactions has a forward and a backward reaction rate.

The above formulation is very general for a multi-component system undergoing many different types of reactions. We will however study just one reaction, the linear sorption process. Often reactions are considered to occur at equilibrium conditions although there is evidence that non-equilibrium reactions may exist for many solutes at different sites. In particular, our research focuses on the relevance of slow sorption-desorption which has been variously termed as kinetic sorption, resistant sorption or non-equilibrium sorption in the context of long-term predictions.

2.5 Results for Equilibrium Linear Sorption

As discussed in Chapter 1, sorption of solutes is an important attenuating mechanism in groundwater flow. The simplest representation of sorption uses linear kinetics and assumes constant rates for the sorption and desorption. Equilibrium conditions are often assumed in which case the time scale of the transport process is much larger than the time of sorption/desorption. Analytical results for linear sorption models in heterogeneous media have been presented in Garabedian [1988]; Cvetkovic and Shapiro [1990]; Kabala and Sposito [1991]; Chyrsikopoulos et al. [1992]; Quinodoz and Valocchi [1993]; and Cvetkovic and Dagan [1994]. In all cases above K_d was considered to be constant or spatially varying.

The analytical results obtained by various methods have been tested for their accuracy and limitations by applying them to results obtained from field-scale observations. The Borden site tracer test [Roberts et. al., 1986], the Cape Cod site test [LeBlanc et. al., 1991], and the MADE site test [Adams and Gelhar, 1992] are three examples of large-scale experiments carried out in the fields to validate the stochastic theory results both for ideal and reactive tracers. We will discuss the comparison of stochastic theory results with field data of the Borden site test in greater detail in Chapter 5.

2.6 Large-scale Numerical Simulation

Evaluation of stochastic theories of solute transport in heterogeneous porous media has also been done by large-scale numerical simulations [Tompson and Gelhar, 1990; Tompson, 1993; Burr et al., 1994]. A common approach is to study the effect of the heterogeneity using Monte-Carlo methods. Monte-Carlo methods are used to

solve the above equation for different realizations of **K** and **v** to obtain the entire probability distribution function of C and then to calculate the mean and variances of C. Two of the most popular techniques used are the Laplace Transform Galerkin approach [Sudicky, 1989; 1990] and the particle tracking method [Tompson, 1993].

The particle-tracking algorithms discussed below are generally used in numerical simulations. We focus our attention on the particle tracking algorithms in particular because we will develop an algorithm which is conceptually similar to particle tracking but computationally more efficient.

2.7 Particle Tracking Algorithm

Particle tracking algorithms constitute an important class of methods for solving transport problems. Their applications have been used in wide variety of fields including plasma physics, astrophysics, estuary flow and heat flow. The basic idea is to discretize the total mass that is being transported into a large number of particles subjected to advection by the flow, sorption-desorption or other reactions and an additional Brownian motion process to account for dispersion. The random walk particle method has been used in many studies to simulate both conservative and reactive transport [Prickett et al., 1981; Uffink, 1985; Tompson, 1987; Tompson and Gelhar, 1990; Tompson, 1993] .

The random walk method from statistical physics has been used in the analysis of diffusion and dispersion in porous media [Scheidegger, 1954]. Early work on the formulation of the particle tracking code was by Pricket et al. [1981]. The advection-dispersion equation was solved by simulating the movement of a large number of particles advected with the constant flow velocity U and subject to a Brownian

motion with a given dispersion, **D**.

$$\frac{\partial C}{\partial t} + U\frac{\partial C}{\partial x} = \mathbf{D}\frac{\partial^2 C}{\partial x^2} \tag{2.10}$$

$$x(t+\Delta t) = x(t) + U\Delta t + (2D\Delta t)^{1/2}\zeta \tag{2.11}$$

The second equation gives the position of a particle for one-dimensional flow where x(t) is the location at time t, U is the constant advective velocity, **D** is the dispersion coefficient, and ζ is an independent normally distributed variable with zero mean and unit variance.

The frequency distribution f of the particles obtained from the random walk (equation 2.11) satisfies in the limit of large particle numbers the Ito-Fokker-Planck equation [Uffink, 1985]

$$\frac{\partial f}{\partial t} + U\frac{\partial f}{\partial x} = \frac{\partial^2 Df}{\partial x^2} \tag{2.12}$$

If the dispersion coefficient is space independent, the Fokker-Planck equation is identical to the transport equation. It is this identity that allows us to interpret the advection-dispersion equation as a Fokker-Planck equation with a corresponding equivalent random walk of the form given in equation (2.11) [Uffink, 1985; Kinzelbach, 1988] .

However, the formulation is changed for spatially varying **D** case. Consider the advection-dispersion equation where the velocity and dispersion coefficient vary in space.

$$\frac{\partial C}{\partial t} + \frac{\partial (\mathbf{v}C)}{\partial x} = \frac{\partial}{\partial x}\left(\mathbf{D}\frac{\partial C}{\partial x}\right) \tag{2.13}$$

The particle tracking formulation in this case includes the addition of the "drift" term to the advective velocity:

$$x(t+\Delta t) = x(t) + [u(x) + \frac{1}{2}\frac{dD}{dx}]_{x=x(t)+(\frac{\Delta t}{2})}\Delta t + [2D(x(t))\Delta t]^{1/2}\zeta \tag{2.14}$$

The "drift" term involves the derivative of the dispersion coefficient in space and was introduced by Kinzelbach and Uffink [1991] who found that a simple extension of the earlier approach to the spatially varying velocity field led to accumulation of mass in low-dispersion areas. The presence of the drift term results in the low-dispersion areas repelling particles while high dispersion areas tend to attract them. The above can be theoretically justified in terms of the theory of stochastic differential equations. There are two slightly different approaches known as the Ito and Stratonovich formulations. Stratonovich defined his stochastic integrals in a different way than Ito – further details about the "Ito-Stratonovich dilemma" are contained in Van Kampen [1981] and Gardiner [1990] . Kitanidis [1994] has produced a method of moments analysis to explain the significance of the "drift" term.

In the next section we outline some of the advantages of the particle tracking code which has made it a very popular modeling tool and then discuss its limitations for reactive transport with non-equilibrium sorption.

2.8 Advantages and Limitations of Particle Tracking Codes

A major advantage of the particle tracking method is that it performs well for large Peclet numbers, unlike most classical numerical methods of solute transport. The grid Peclet number is the ratio of the advective velocity times the grid dimension divided by the dispersion coefficient. When this number is large, the transport equation behaves as a hyperbolic partial differential equation for which solutions obtained from the classical finite difference or finite element formulations are prone to numerical dispersion or oscillations [Huyakorn and Pinder, 1983]. In problems dominated by advection, numerical dispersion may cause errors unless the grid is highly resolved.

The particle tracking method is computationally appealing because it is grid independent and therefore requires little computer storage relative to the finite element, finite difference, and method of characteristics procedures. The particle tracking method conserves mass at both the local and global scale. Discontinuities in the velocity yield a dispersion tensor that is discontinuous in space, which if neglected will result in local mass conservation error. The particle-tracking code does not require the solution of a large system of equations. Techniques for applying the particle tracking code in the case of spatially varying velocity field are given in LaBolle et al., [1996]. The method is well suited for evaluating the bulk-averaged characteristics, such as the location of the centroid of the plume.

A disadvantage of the particle tracking algorithm is that the concentration is not smooth and usually requires the application of a smoothing function which varies with the dimension of the flow field. For a large-scale simulation, we would need a very large number of particles to be able to accurately resolve concentration fluctuations. Thus the particle tracking algorithm is still a computationally intensive approach. The time discretization would need to be exceedingly small for small rates of sorption-desorption. We propose a recursion algorithm for a linearly sorbing solute which will provide a fast and accurate resolution of the breakthrough curve, especially at the tail portion where particle tracking algorithm is prone to erratic numerical behavior.

2.9 Ideas Generated for Research

Non-equilibrium sorption is an important process affecting field-scale transport of reactive solutes. For linearly sorbing solutes, there are some studies which

have explicitly modeled the variability of K_d. Spatial variability of rates, however, are important aspects that remain to be addressed.

This research looks into some aspects of modeling transport of linearly sorbing solutes at a number of different scales. We will first look at the transport on a column scale and develop an algorithm for transport of a sorbing solute subject to kinetically-limited conditions. The algorithm is very general and can accommodate a whole spectrum of rates ranging from very high rates which denote equilibrium conditions to very low rates signifying rate-limited behavior.

The issue of heterogeneity of the chemical parameters of the aquifer is addressed next. We will extend the formulation developed for the constant rate case to spatially varying rates with a prescribed covariance structure. We will study the effect of the variability of the rate parameters on the breakthrough curves and correlate the variability to physical processes. We will also study the effect of the combined processes of sorption and decay of a solute. This is an important process because many solutes show natural degradation during transport. We will look at methods to model sorption site heterogeneity where we can specifically identify various types of sorbing sites.

We will develop a multi-dimensional transport simulator based on the recursion formulation which is in essence a semi-analytical formulation of the solute transport of a linearly sorbing solute. This approach provides a very fast method for generating the plume-scale migration of contaminants. Accurate resolution of the aqueous and the sorbed concentration distribution is of critical importance in the design and implementation of remedial projects.

We will show that our formulation of the transport of a sorbing solute in

terms of the probabilistic framework is very general and conceptually simple. Using the basis of transitions from the aqueous to the sorbed phase and back again, an analytical expression for the breakthrough curve at a given time can be obtained which is then used to compute the spatial moments. Our approach gives results similar to Dagan and Cvetkovic [1993] for the case of constant K_d and rates. We will then outline a procedure to obtain the moments for the case of spatially varying rates as an extension of the constant rates case.

The recursion formulation will also be used to study transverse dispersion of a solute plume, in particular the effect of local dispersion on the spreading of the plume in a direction transverse to the mean flow direction. There have been some interesting observations about the asymptotic behavior of transverse dispersion [Hu and Cushman, 1997] where the Eulerian and the Lagrangian moments differ substantially. We will address this problem of inclusion of local dispersion in the Lagrangian framework and study the second transverse moment variation with time for the simplified problem of a stratified aquifer.

Chapter 3

A Recursion Formulation For Non-equilibrium Transport

3.1 Overview

In the previous chapters we showed transport of a linearly sorbing solute under non-equilibrium conditions is an important problem in issues related to contaminant migration. Non-equilibrium conditions have been postulated to exist both in the laboratory and in the field. In particular, the effect of heterogeneity in the chemical parameters on solute transport has been the subject of much debate and conjecture. In this chapter, we develop an efficient recursion formulation approach for simulating transport with spatially variable kinetic sorption. The recursion formulation is derived by assuming a Markov process model for unimolecular reactions. This approach provides a way for computing concentration breakthrough curves semi-analytically, without resorting explicitly to particle-tracking. Effectively, the transport of an infinite number of particles is simulated. The recursion formulation does not include any local dispersion. We illustrate the approach with simulations of one-dimensional transport, which clarifies the influence of spatially variable kinetic sorption on the concentration breakthrough curves. The approach presented in this chapter can be extended to multi-dimensional transport simulations by applying the recursion formulation along pathlines or streamtubes, which is the topic of Chapter 5.

This chapter is organized as follows : in the next section (3.2), the Markov process model of sorption-desorption is described, followed by the development of the recursion formulation. In section 3.3, comparisons to analytical solutions for transport with constant kinetic parameters are presented. In section 3.4, the influence of spatially variable sorption kinetics on concentration breakthrough is examined through parametric studies, and comparisons to analytical results are presented for the case of fast sorption reactions. In section 3.5, the combined processes of sorption and degradation of the solute, either in the aqueous or the sorbed phase, is formulated. The chapter concludes with a discussion of the results.

3.2 Markov Process Model of Sorption-Desorption

Markov process formulations for studying adsorbing solutes with constant rate parameters have been presented previously in the literature. Andricevic and Foufoula-Georgiou [1991] modeled the sorption process as a birth-death process with constant rate parameters. In the birth-death model, the number of transitions between the aqueous and sorbed phases during a fixed time period will be a Poisson process.

We examine this case below first for constant rate coefficients and then for spatially varying coefficients. For the constant rate case, the breakthrough curves are discrete analogs of results presented by Giddings and Eyring [1955] . We model the one-dimensional column as a collection of small discrete segments and consider the fate of the sorbing mass advected through the column allowing for sorption-desorption processes. The rate at which the solute is sorbed onto the solids is defined as k_f while the rate of desorption is defined as k_r. In the case of a linear sorption isotherm, the

distribution coefficient is $K_d = k_f/k_r$.

The probability that a particle is sorbed during a time interval Δt is related to k_f and the time step size, Δt. Specifically, the probability that a particle is sorbed during a time-step Δt is given by [Andricevic and Foufoula-Georgiou, 1991]

$$Pr(sorption) = \frac{k_f}{k_r + k_f}\left[1 - e^{-(k_f+k_r)\Delta t)}\right] \tag{3.1}$$

which can be simplified using a first-order approximation, as follows

$$Pr(sorption) = k_f\ \Delta t + \mathcal{O}(\Delta t) \tag{3.2}$$

where the term $\mathcal{O}(\Delta t)$ is used to indicate a negligible component as Δt approaches 0; namely

$$Lim_{\Delta t \to 0}\frac{\mathcal{O}(\Delta t)}{\Delta t} = 0. \tag{3.3}$$

If solute is sorbed, the time spent in the sorbed phase will be assumed to have an exponential distribution with mean $1/k_r$. This again implies

$$Pr(desorption) = k_r\ \Delta t + \mathcal{O}(\Delta t) \tag{3.4}$$

The exponential assumption implicit above and in equation 3.1 implies that the resulting process that describes the number of particles in each state (sorbed or mobile) is a Markov process [Ross, 1989].

3.3 Development of A Recursion Formulation

For linear kinetic models where the sorption-desorption process only depends on the forward and backward rate coefficients, we develop recursive equations for the

probability distribution of the number of time steps taken to reach the effluent end. The probability distribution of the travel time is then related to the concentration breakthrough curve.

In the discrete formulation used here, time is discretized into steps of length Δt and space into steps of length Δx. For simplicity, the velocity v is assigned a value of 1 in the arguments presented below, while in the general case, $\Delta x = v\ \Delta t$. Later the recursion formulation is extended to incorporate velocity variations along a flowpath, as would be encountered in a heterogeneous medium.

We denote the state of a solute particle as either mobile (j=1) or sorbed (j=2). Let $P_{n,k}^{(j)}$ denote the probability that it takes k time-steps for a solute particle to move n space steps, starting from state j. The probability that the solute remains in the aqueous phase during a time-step is denoted by r_{11}, and $r_{12} = 1 - r_{11}$ is the probability that the solute moves from the aqueous to the sorbed phase. Similarly, the probability that solute initially in the sorbed phase remains in the sorbed phase after a time step Δt is denoted by r_{22} , and $r_{21} = 1 - r_{22}$ is the transition probability for moving from the sorbed to the aqueous phase.

The transition probabilities for fixed Δt are given by

$$r_{12} = 1 - r_{11} = k_f\ \Delta t + \mathcal{O}(\Delta t) \cong k_f\ \Delta t \tag{3.5}$$

$$r_{21} = 1 - r_{22} = k_r\ \Delta t + \mathcal{O}(\Delta t) \cong k_r\ \Delta t \tag{3.6}$$

in the discrete approximation adopted here. In equations 3.2 and 3.4 we have assumed Δt is small and $\mathcal{O}(\Delta t)$ denotes terms of order Δt^2 and higher, which are negligible.

We can then derive the probability $P_{n,k}^{(j)}$ that a solute particle has traveled n space steps in k time steps and is in state j. For j=1 (namely starting in state 1, the mobile state) the following cases arise:

(a) the solute particle stays mobile during the next time step: This occurs with probability r_{11}, in which case we now need to move n-1 space steps in the next k-1 time steps;

(b) the solute particle becomes sorbed during the next time step. This occurs with probability 1-r_{11} in which case we need to move n space steps in the next k-1 time steps.

In addition we assume that the "decision" about sorption/desorption occurs at the beginning of the time step. We thus arrive at the following recursion relation, for $k > n$,

$$P^{(1)}_{n,k} = r_{11}\, P^{(1)}_{n-1,k-1} + (1 - r_{11})\, P^{(2)}_{n,k-1} \tag{3.7}$$

By a similar argument,

$$P^{(2)}_{n,k} = r_{22}\, P^{(2)}_{n,k-1} + (1 - r_{22})\, P^{(1)}_{n-1,k-1} \tag{3.8}$$

Before these recursion equations can be solved, we need appropriate boundary conditions. These can be derived directly as follows:

$$P^{(1)}_{n,n} = r^{n}_{11} \tag{3.9}$$

$$P^{(2)}_{n,n} = r^{n-1}_{11}\,(1 - r_{22}) \tag{3.10}$$

$$P^{(1)}_{1,k} = (1 - r_{11})\, r^{k-2}_{22}\,(1 - r_{22}), \quad k \geq 2 \tag{3.11}$$

$$P^{(2)}_{1,k} = r^{k-1}_{22}\,(1 - r_{22}), \quad k \geq 2 \tag{3.12}$$

$$P^{(1)}_{n,k} = 0, \quad k < n, j = 1, 2 \tag{3.13}$$

For example, equation 3.10 refers to the case where n time steps are needed to travel n space steps when the solute starts from the sorbed state. This can only occur if

(a) the solute enters the mobile state in step 1 and

(b) never leaves the mobile state in the next (n-1) steps.

The other boundary conditions can be derived in a similar manner. While the equations are derived for transitions occurring at the beginning of a time step, they can also be derived with minor changes for transitions at the end of a period.

The procedure for obtaining the breakthrough curve at a given location is now described. Given the distance of the effluent point from the inlet, say 1 m, a velocity of 0.1 m/day and a Δt of 0.1 day, the distance moved in one time unit is 0.01 m. The total number of steps required to cover a distance of 1 m is 100 space steps and the earliest time at which a particle can reach the effluent end is 10 days or 100 time steps if it was never sorbed. For the results reported in pore volumes, 1 pore volume (PV) equals 10 days in this example. Thus we need to calculate $P_{n,k}^{(1)}$ for n=100 and values of $k \geq 100$ up to a suitably large number (kmax) where the concentration reaches a negligible value. Starting from the boundary conditions, we can obtain $P_{1,k}^{(1)}$ and $P_{1,k}^{(2)}$ for k=2 to kmax and then go through the recursion formulation for n=2 to 100, i.e. till we have reached the end of the flowpath. We have then obtained $P_{n,k}^{(1)}$ for n=100 and for k=100 to kmax, which describes the breakthrough curve in normalized concentration units. In the examples below we take kmax=1000.

The breakthrough curves for various different values of k_f and k_r are shown in Figure 3.1. It is evident that the equilibrium condition is just an end-member of the whole spectrum of possible breakthrough curves. As can be seen from the

graphs, small values of k_f and k_r, corresponding to slow sorption/desorption rates lead to breakthrough curves with a sharp peak followed by a long tail. As the rates are increased and equilibrium conditions are approached, the curves have a Gaussian shape (Note that in the seminal work of Giddings and Eyring [1955], the approach to Gaussian shape is discussed further).

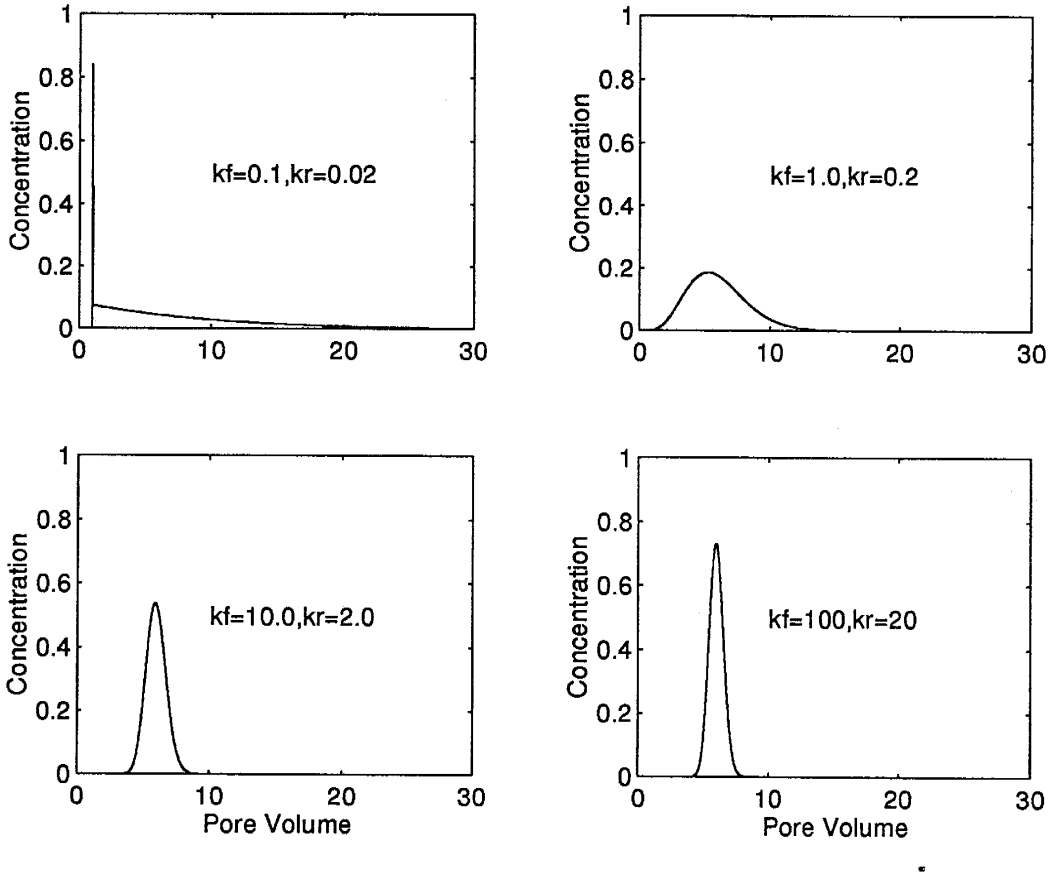

Figure 3.1: Breakthrough curves for k_f, k_r varying from 0.1 and 0.02/day to 100 and 20/day obtained by recursion formulation. Note that K_d =5 in all the cases, 1 Pore volume is equivalent to 10 days.

A novel feature of the recursion formulation is that it effectively simulates the transport of an infinite number of particles through the flowpath. In the traditional particle-tracking algorithm, a finite number of particles are tracked through the flowpath in discrete steps. The resolution and smoothness of the breakthrough curve obtained using the particle-tracking approach depends on the number of particles used. This is especially true in the case of nonequilibrium sorption, in which case the breakthrough curves exhibit a long tail. Accurate resolution of the tail will require a very large number of particles, and even if a large number of particles were used, oscillations would be observed. On the other hand, the recursion formulation is capable of resolving the tail very accurately, since it effectively simulates an infinite number of particles. This feature is further illustrated in Figure 3.2, where the breakthrough curve obtained using the recursion formulation is compared to those obtained with particle-tracking simulations using 1000, 2000 and 5000 particles. The k_f and k_r values in this case are 0.5 and 0.1/day. The other parameters are the same as discussed above.

As expected, the breakthrough curve obtained using the recursion formulation is very smooth, in contrast to the noisy behavior of the breakthrough curves obtained with particle-tracking. In addition, the recursion formulation is computationally more efficient than direct particle-tracking. This is illustrated in Table 3.1 where a comparison of the number of operations required to obtain the breakthrough curves in Figure 3.2 is given. The number of operations required to obtain the breakthrough curve by the recursion formulation depends on the time step chosen and the maximum time to which we want to compute the breakthrough curve. The time step, Δt will determine the number of times the recursion formulation is evaluated to arrive at the effluent end (in our example it is 1 m). The choice of Δt also dictates

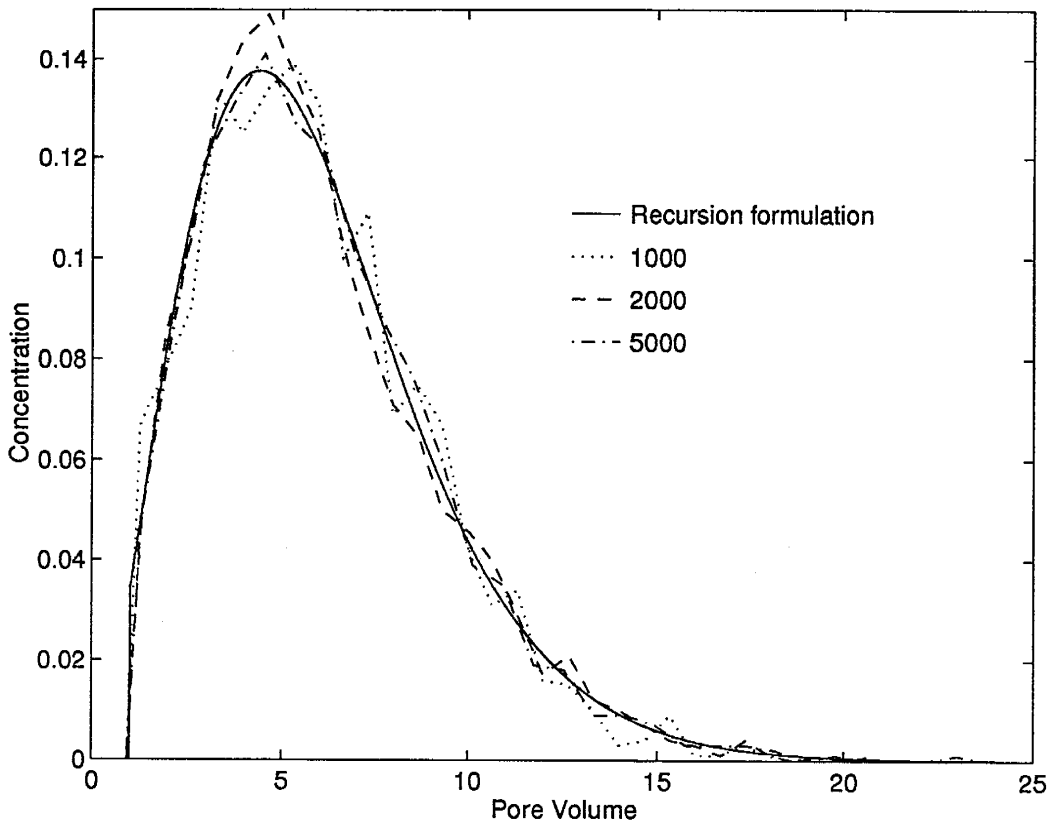

Figure 3.2: Comparison with particle tracking code. Breakthrough curve for k_f, k_r equal to 0.5 and 0.1/day obtained by recursion formulation is compared with a particle tracking code where the number of particles are varied from 1000, 2000 and 5000. (1 Pore Volume $\equiv$ 10 days)

the resolution of the breakthrough curve. The values of $P_{n,k}^{(j)}$, which denote the concentration, are obtained at a given spatial location at time intervals Δt units apart. For the results presented in Table 3.1, a time step of 0.5 day and a maximum time of 250 days (25 PV) was chosen for the recursion formulation. For the particle tracking algorithm a time step of 0.1 day was used to obtain the breakthrough curve. It is evident that there is an order of a magnitude difference in computational effort between the recursion formulation and the particle tracking method. The superior resolution and computational efficiency achieved with the recursion formulation are especially important in the context of transport with spatially variable sorption kinetics, when multiple-realization simulations are necessary for quantifying the ensemble average behavior.

Description	Number of flops
Recursion Formulation	28,406
Particle Tracking (1000 particles)	774,624
Particle Tracking (2000 particles)	1,541,241
Particle Tracking (5000 particles)	3,899,537

Table 3.1: Comparison of flops for obtaining the breakthrough curve between recursion formulation and particle tracking. (1flop = 1 computational operation)

3.3.1 Constant Rate Parameters: Comparison to Analytical Solution

For the constant k_f and k_r case, the recursion formulation presented here is a discrete analog of the results of Giddings and Eyring [1955]. The results are shown for the case of sorption and desorption rates of 1.0 and 0.2/day, respectively for breakthrough obtained at a distance of 1 m from inlet, with a velocity of 0.1 m/day. The results from the model were compared with the analytical solution obtained by Giddings and Eyring [1955] and agreed very closely (Figure 3.3). In the recursion formulation, a time-step of 0.1 day was used, which is about $(0.1/k_f)$. It is our experience that with a choice of Δt of $0.1/k_f$ to $0.5/k_f$, the simulated breakthrough curves are practically identical to the analytical breakthrough curves of Giddings and Eyring [1955].

We have developed the recursion formulation for transport of a linearly sorbing solute where the rates of sorption and desorption, k_f and k_r are constant. We have demonstrated the computational efficiency of the algorithm in comparison to the particle tracking approach and shown that the long tail observed for kinetically limited conditions is accurately obtained by this formulation. However, we need to account for spatial variability of k_f and k_r which has been hypothesized in some other studies [Hu et al., 1995]. Our main aim in this work is to go beyond the constant rate coefficient case and the recursion formulation is extended below to incorporate spatial variability in sorption rates in the next section.

3.4 Influence of Spatially Variable Kinetics

The sorption phenomenon, in simplified terms, is a mass transfer mechanism from the aqueous to the solid phase of the porous medium and is generally modeled

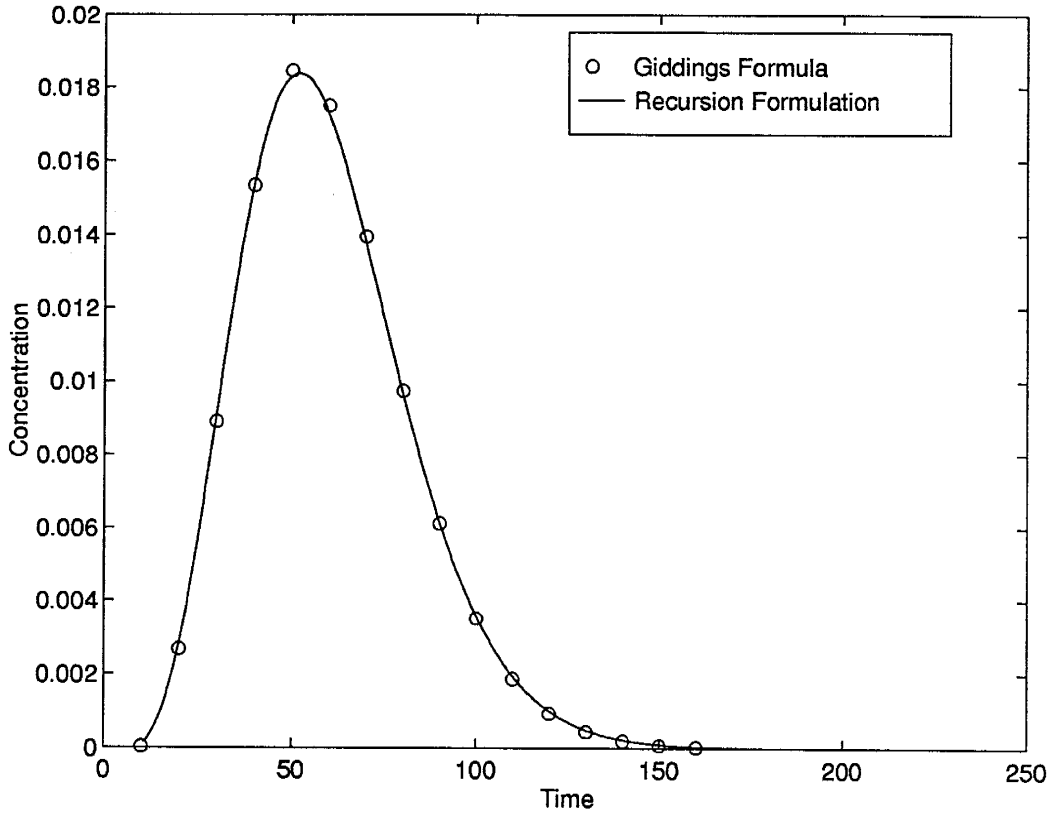

Figure 3.3: Breakthrough curve for k_f, k_r 0.1 and 0.02/day obtained by recursion formulation is compared to Giddings and Eyring [1955] analytical result.

as a first-order process for the linear sorption case. The actual sorption-desorption process is much more complicated, with the rates of mass transfer between the aqueous and the sorbed phase related to the small-scale variations in aquifer properties. The aquifer materials may contain a wide range of particle sizes and aggregates. It was this explicit recognition of the heterogeneity that led to extension of the one-site model to a two-site model [Coats and Smith, 1964; Cameron and Klute, 1977] and its variants. While these models had some success in explaining the laboratory scale behavior [Wu and Gschwend, 1986; Ball and Roberts, 1991], they are not accurate in predicting the breakthrough curves in a heterogeneous aquifer [Harmon et al., 1992].

In the chemical engineering literature, the effects of variability in the particle size and sorption properties on solute transport have long been known [Dougharty, 1972] and have been modeled using a transfer function approach [Villermaux, 1981, 1987, 1990]. The first-order transfer function approach has been applied in groundwater studies of solute transport by Valocchi [1990] and Sardin et al. [1991]. This was followed by the development of a MPNE [Brusseau et al., 1989] which consists of three first-order mass transfer reactions operating simultaneously, two in parallel and one in series with one of the first two. A more recent study along these lines is the multirate model [Haggerty and Gorelick, 1995] where a series of first-order equations are used to represent each of the mass transfer process.

We can see the increasing complexity of the models to account for the multitude of the processes and scales that contribute to rate-limited mass transfer. The variations in the rate limited behavior can be attributed to some of the following:

1. The type of minerals and their spatial distribution including the coatings on the surfaces of the aquifer particles [Barber et al., 1992; Pignatello, 1990];

2. The quantity and distribution of organic material [Grathwohl, 1990; Barber et al., 1992];

3. The chemistry of the water and contaminant [Curtis et al., 1986; Weber et al., 1991];

4. Variations in hydraulic conductivity within the aquifer including the external and internal geometry of low permeability materials [Quinodoz and Valocchi, 1993; Cvetkovic and Shapiro, 1990];

5. The volume, size and geometry of macro- and micro-porosity in individual grains and aggregates of particles [Ball and Roberts, 1991; Harmon and Roberts, 1994].

The various factors which could affect mass transfer rates exhibit significant spatial variations and it would be an extremely difficult task to be able to account for each of the processes individually. However, all these multiple rates of mass transfer present at the small scale significantly affect larger-scale transport [Weber et al., 1992].

We approach this problem by assuming the rates to be a spatial random function. This simplification allows us to retain the ease of modeling the rates as a random variable while at the same time accounting for our imprecise knowledge of all the small-scale processes controlling the rate limited mass transfer. We can now develop a recursion formulation where the rates are spatially varying.

3.4.1 Recursion Formulation with Spatially Variable Rates

The derivation of the recursion equations in the case of spatially variable k_f and k_r is a simple extension of the equations 3.5 to 3.8 above. The boundary

conditions are a little more complicated, though still similar to the conditions in equations 3.9 through 3.13. The probabilities r_{11} and r_{22} now need to be replaced by $r_{11}(n)$ and $r_{22}(n)$ where n indicates spatial location. Basically, we index the parameters starting from the influent end. Thus for $k > n$,

$$P^{(1)}_{n,k} = r_{11}(n)\, P^{(1)}_{n-1,k-1} + (1 - r_{11}(n))\, P^{(2)}_{n,k-1} \tag{3.14}$$

$$P^{(2)}_{n,k} = r_{22}(n)\, P^{(2)}_{n,k-1} + (1 - r_{22}(n))\, P^{(1)}_{n-1,k-1} \tag{3.15}$$

where $r_{11}(n) = 1 - k_f(n)\ \Delta t, r_{22}(n) = 1 - k_r(n)\ \Delta t$. Here, $k_f(n) = k_f(n\Delta x)$ is the sorption rate $(n\Delta x)$ units from the influent end, with similar indexing for the other variables.

The boundary conditions now become

$$P^{(1)}_{n,n} = r_{11}(1)r_{11}(2)...r_{11}(n) = \Pi^{n}_{i=1} r_{11}(i) \tag{3.16}$$

$$P^{(2)}_{n,n} = \Pi^{n-1}_{i=1} r_{11}(i)\ (1 - r_{22}(n)) \tag{3.17}$$

$$P^{(1)}_{1,k} = (1 - r_{11}(1))\, r_{22}(1)^{k-2}\ (1 - r_{22}(1)), \quad k \geq 2 \tag{3.18}$$

$$P^{(2)}_{1,k} = r_{22}(1)^{k-1}\ (1 - r_{22}(1)), \quad k \geq 2 \tag{3.19}$$

$$P^{(1)}_{n,k} = 0, \quad k < n, j = 1, 2 \tag{3.20}$$

Breakthrough curves in a single realization of spatially variable k_f and k_r can be obtained directly by using the recursion formulation. The ensemble average breakthrough curve is readily obtained by repeating the same procedure in a number of realizations. The direct particle tracking method would be more computationally intensive and unless many particles were used, would exhibit more variability in the

breakthrough curves. Illustrative computations of breakthrough curves are presented below, for the case of spatially variable k_f and k_r.

In the examples presented below, a Fast Fourier Transform random field generator [Gutjahr et al., 1994] was used to generate independent realizations of k_f and k_r. It is also possible to generate cross-correlated random fields of k_f and k_r [see Gutjahr et al., 1996] with an adaptation of this algorithm. However for simplicity, the cross-correlated case is not included here.

For the results presented here, the recursion formulation is used to obtain the breakthrough curves in 30 realizations . The parameters used are the length of the column, L=1 m, velocity of the fluid, v=0.1 m/day, Δt=0.1 day. The covariance function for ln k_f and ln k_r is an exponential function of the form

$$C(\xi) = \sigma^2 \, e^{\frac{-|\xi|}{\lambda}} \tag{3.21}$$

The correlation length λ used for the simulations is 0.2 m. The mean values of k_f and k_r are 1.0/day and 0.2/day, identical to the values of the constant rates used in Figure 3.1(b), to facilitate comparison.

The ln k_f and ln k_r processes are generated so as to ensure that the mean values of k_f and k_r are as desired, by using the following relationships between the statistics of lognormal and normal distributions:

$$e^{F+\sigma^2/2} \;=\; \mu_{k_f} \tag{3.22}$$

where F and σ^2 are respectively the mean and variance of ln k_f. Similar conversions are made for k_r.

In Figure 3.4 the breakthrough curve for the case of constant rates is compared to the ensemble mean breakthrough curve obtained for the spatially variable rates for a variance of 0.5 of ln k_f and ln k_r. The ensemble mean curve for the spatially variable rates shows a small shift in the position of the peak concentration compared to the constant rate case signifying a slight reduction in the effective retardation factor. The mean curve also shows a larger spread, i.e. extensive tailing of the breakthrough curve caused by the spatial variability of the rates. This illustrates the importance of understanding the heterogeneity of the rates and its impact on the breakthrough curve. Also shown in the figure are the one standard deviation bounds on the mean breakthrough curve showing the extent of variability among the realizations. This point is further illustrated in the next figure.

Breakthrough curves from 5 different realizations out of 30 that were used to calculate the ensemble mean curve in Figure 3.4 are presented in Figure 3.5. Note that individual realizations vary significantly from the mean ensemble curve as well as from each other. The peak concentrations (presented as normalized units relative to the input concentration) show a wide variation from 0.044 to 0.005 and the time of complete breakthrough ranges from 90 days to over 250 days (9 PV to 25 PV).

Going back to Figure 3.4 , we see a peak concentration in the ensemble mean breakthrough curve of about 0.01 compared to about 0.02 for the constant rates case. In addition, the breakthrough curve ends at about 15 PV for the constant rate case while for the spatially variable rates it continues up to 25 PV. Also to be noted is the greater variability in the arrival times and the peak concentration shown by the one standard deviation bounds. At later times, the bounds are narrower. The most important consequence of spatially variable rates, evident from Figures 3.4 and 3.5,

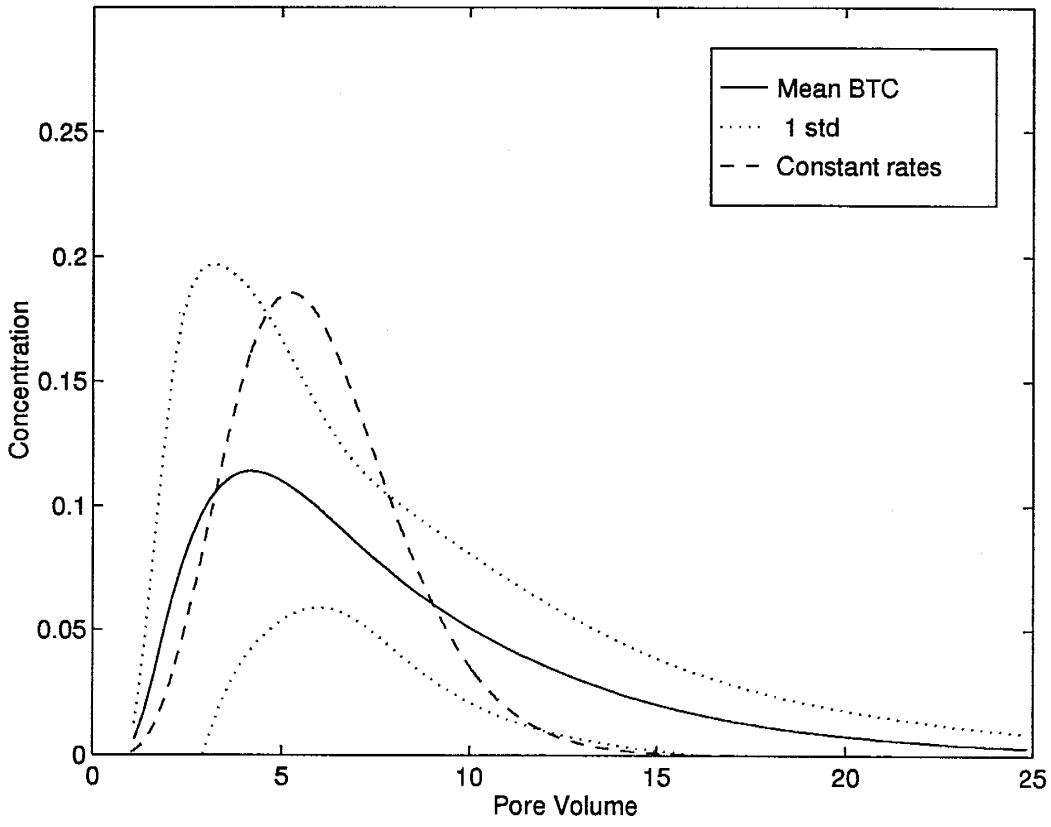

Figure 3.4: Mean breakthrough curve for spatially varying k_f, k_r. Mean k_f, k_r are 0.1 and 0.02/day, with an exponential correlation structure of scale 0.2 m and variance of 0.5.

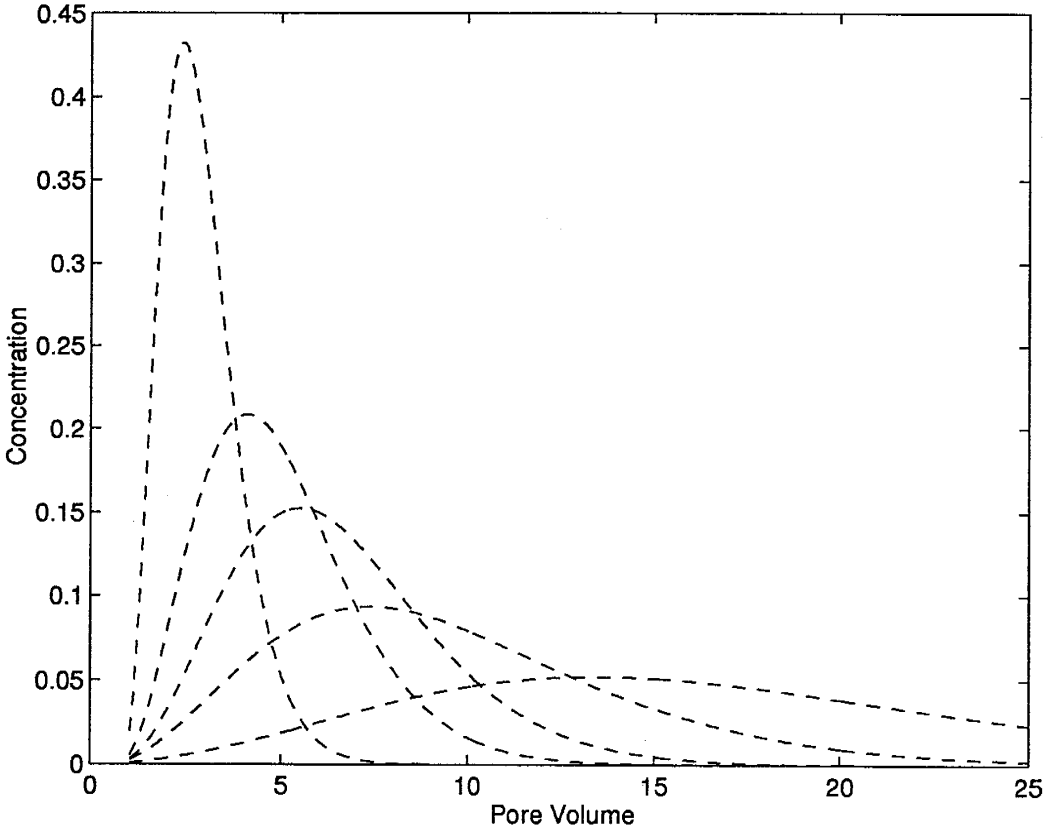

Figure 3.5: Five individual realizations shown for the Monte Carlo simulations done to obtain the mean breakthrough curve in Figure 3.4.

is that the breakthrough curves show longer tails than in the constant rate case.

3.4.2 Comparison with an Analytical Solution for Spatially Variable K_d

In the previous section, the recursion formulation was applied to situations where the sorption and desorption rates were spatially variable. The sorption and desorption rates were treated distinctly. In most applications however, it is typically the distribution coefficient K_d or the retardation factor which is modeled as a random process. An analytical solution for the mean concentration of a sorbing solute has been developed by Chyrisokopoulos et al. [1990], using a perturbation approach. In their analysis, equilibrium conditions were assumed for the sorbing solute and the retardation factor was assumed to be spatially variable. An expression for the mean concentration was developed based on a first-order perturbation analysis, in the form of an integral which had to be evaluated numerically.

We extend their results to include the effect of sorption kinetics. Modeling the sorption and desorption rates independently, leads to a covariance function for K_d which is not of the exponential form. The form of the covariance function which results from modeling the variations of k_f and k_r distinctly is presented in Appendix B. This revised covariance (eqn. B8) is used in the mean concentration expression of Chyrisokopoulos et al. [1990] and the resulting mean breakthrough curve is shown in Figure 3.6 as CKFKR. The analytical expression for mean concentration as presented by Chyrisokopoulos et al. [1990] for a Pe=72 is also shown in Figure 3.6 as CKD. As a consequence of the modified covariance function, the peak concentration is shifted, showing a slight increase in the effective retardation factor. Note however this is still a one-parameter model consistent with essentially a single K_d but one that takes into

account a different covariance structure.

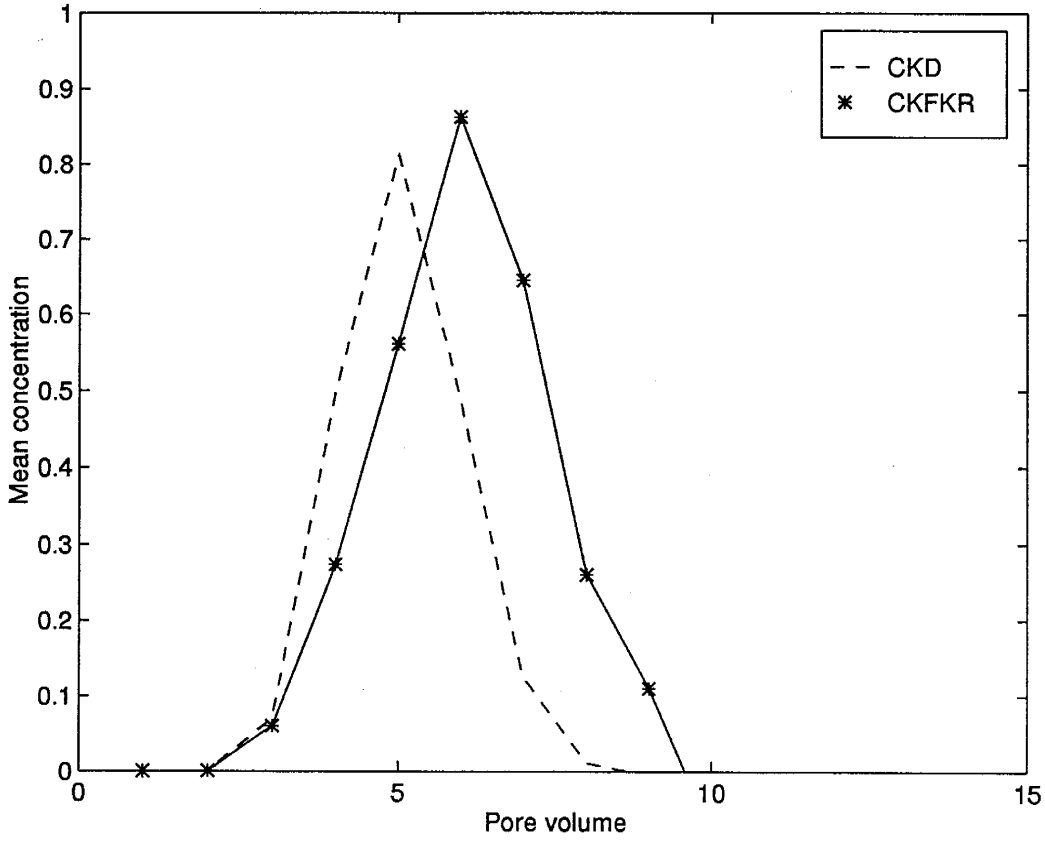

Figure 3.6: Mean breakthrough curve for spatially varying k_f, k_r (CKFKR) are compared to results obtained from spatially varying K_d (CKD).

We next present a comparison between the ensemble average breakthrough curves obtained using the recursion formulation with different cases of spatially variable rates. Consequently our formulation does not incorporate the influence of local dispersion. To do the comparison, we chose a Peclet number of 72, so that the effect of local dispersion is minimized. In addition, a dimensionless parameter, the Damkohler number is used to represent the rates. This nondimensionalization is in

terms of a characteristic advection time. We will use DaI and DaII, Damkohler number I and Damkohler number II [Bahr and Rubin, 1987] to quantify the effect of the sorption and desorption rates with respect to the advection time, using the following relationship

$$DaI = \frac{k_f L}{v} \tag{3.23}$$

$$DaII = \frac{k_r L}{v} \tag{3.24}$$

DaI and DaII, the dimensionless Damkohler number I and II, have the following physical interpretation: they are ratios of the time-scale of advection to a characteristic reaction time-scale and small numbers represent a situation where the reaction rate is slower than advection time whereas large DaI and DaII represent fast reaction rates where the assumption of equilibrium sorption is applicable.

For the spatially variable rates, the mean values of k_f and k_r are used to calculate DaI and DaII. Two different sets of mean k_f and k_r values corresponding to mean DaI values of 170 and 1.7 and DaII values of 45 and 0.45 respectively are chosen. The two parameters k_f and k_r are assumed to have an exponential covariance structure with a variance of 0.1 and an correlation scale of 6 m. With these parameter values, K_d has a mean value of 3.8 and a variance of 0.1, identical to the values used by Chyrisokopoulos et al. [1990]. Ensemble average breakthrough curves are obtained based on 30 realizations for each of the two values of DaI, and are shown in Figure 3.7. The two different breakthrough curves obtained using the recursion formulation illustrate the effect of kinetics on transport of a sorbing solute. Note that in the two cases presented in Figure 3.7 the mean value of K_d is 3.8. For DaI= 1.7, i.e. for slow rates (k_f=0.38 [1/day] and k_r=0.1 [1/day]), the ensemble mean breakthrough curve with the recursion formulation shows a smaller peak and longer tail. As DaI is

increased to 170 (equivalent to equilibrium conditions), the mean breakthrough curve approaches the analytical solution depicted in Figure 3.6 by CKFKR. These results emphasize the importance of explicitly modeling the sorption and desorption rates under kinetically limited conditions.

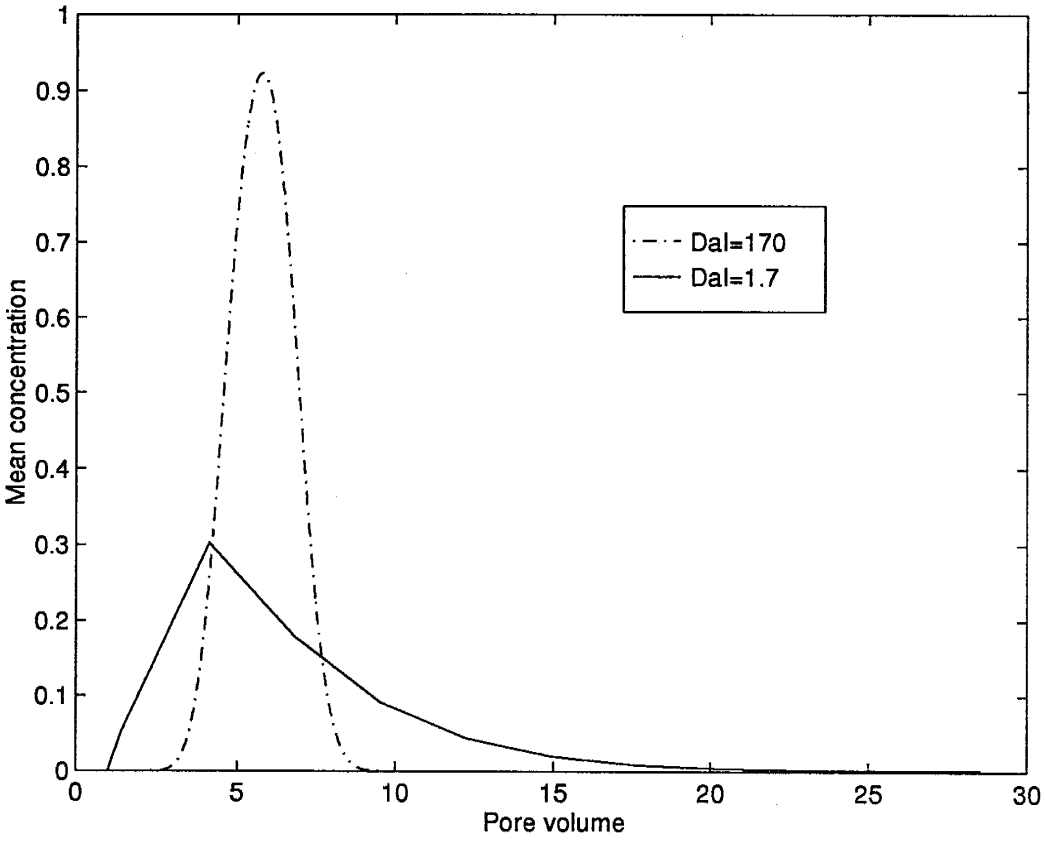

Figure 3.7: Mean breakthrough curve for spatially varying k_f, k_r obtained by using the recursion formulation. Non-equilibrium conditions (small DaI) lead to a longer tail on the breakthrough curve.

3.4.3 Sensitivity of Breakthrough Curves to Spatially Variable Sorption Kinetics

In this section, we examine the sensitivity of the breakthrough curves to the mean and variance of the non-dimensional sorption rates. In the first sensitivity study, the effect of increasing variances of both of the rates is examined. The flow column considered in this case is 2 m long, with a flow velocity of 0.1 m/day. Two different mean rates of 0.1/day and 50/day for k_f and 0.02/day and 10/day for the corresponding k_r values were evaluated. We assume that the sorption and desorption processes are two independent processes with the prescribed mean and variances and an exponential correlation structure with a correlation scale of 0.2 m. The rates chosen were such that the first set represented slow rates compared to the advection time, and the second set fast rates (equilibrium conditions). Note that in all these cases, the values of the distribution coefficient K_d are the same. Approaches which assume equilibrium adsorption will predict the same behavior in all the above cases. The variances of ln k_f and ln k_r were assumed to be the same, and we have considered two different variance values: 0.05 and 0.5.

The ensemble average breakthrough curves corresponding to each of the two cases are shown in Figure 3.8. The top panel presents the results for a case where the characteristic time-scale for sorption is moderately faster than the advection time-scale, while that for desorption is moderately slower (DaI=2, DaII=0.4). The bottom panel corresponds to a case where sorption-desorption rates are much faster than the rate of advection (DaI=1000, DaII=200). For the small DaI and II represented in the top panel, the rates of sorption are very small and most of the solute is advected out of the column at the velocity corresponding to the non-sorbed solute, represented by

the spike of large concentration seen in the initial section of the breakthrough curve. There is still a small amount of solute sorbed and once sorbed it is desorbed slowly, resulting in a very long tail extending to about 25 PV. As the variance is increased to 0.5, the magnitude of the spike decreases and the tail extends beyond 40 PV. As the rates are increased (DaI increases to 1000), the familiar Gaussian breakthrough curves corresponding to equilibrium sorption are seen.

The kinetically limited sorption case leads to breakthrough curves with much longer tails than those obtained under equilibrium conditions. This feature is of special significance in designing remediation schemes and the duration of remedial action. For very slow rates, the variances of the rates affects the peak concentration significantly (the magnitude of the peak concentration decreases as the variance increases). For the large rates equivalent to equilibrium conditions, an increase in the variance of k_f and k_r also leads to changes in both the peak concentration and the length of the tail of the breakthrough curve. The time taken for complete removal of a sorbing contaminant is about 40 PV, when the means of k_f and k_r are 0.1 and 0.02/day and the variances are 0.5, compared to about 6 PV if constant rates and equilibrium conditions are used. The spatial variability of sorption-desorption rates have a significant influence even when the rates are fast.

It is also of interest to examine the relative importance of variability in sorption and desorption rates. To examine this issue we study the effect of partitioning the variance of K_d unequally between k_f and k_r. Note that in all the previous simulations, the variances of k_f and k_r were equal. A number of studies have shown that the desorption rate has a major influence on the breakthrough behavior [Pignatello and Huang, 1991; Pignatello, 1993; Pavlostathis and Mathavan, 1992]. The sorbed

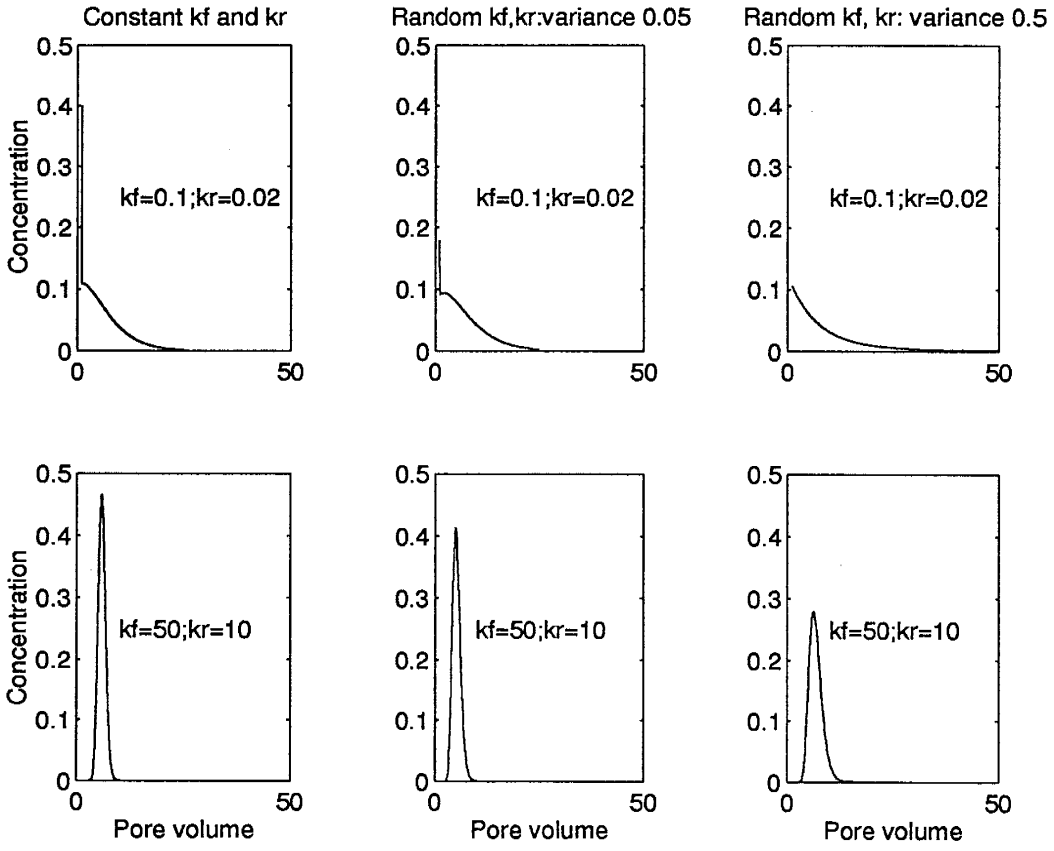

Figure 3.8: Sensitivity study to variance of sorption and desorption rates. DaI and DaII for the top panel is 2 and 0.4 respectively and for the bottom panel is 1000 and 200 respectively.

mass stored in the solid phase acts like a source of contaminant which is then released at varying rates depending on the interactions between the sorbed mass and the solid matrix. We next study the sensitivity of the breakthrough curves to the means and variances of the desorption rates.

For the same flow conditions as in Figure 3.9, the total variance of 1.0 of ln K_d is partitioned in three different ways:

(a) $\sigma^2_{ln\,k_f} = \sigma^2_{ln\,k_r} = 0.5$,

(b) $\sigma^2_{ln\,k_f} = 0.9$ and $\sigma^2_{ln\,k_r} = 0.1$, and

(c) $\sigma^2_{ln\,k_f} = 0.1$ and $\sigma^2_{ln\,k_r} = 0.9$.

A total of 30 realizations were used to compute the ensemble average breakthrough curves for each case (Figure 3.9). For DaI=2 (kinetically limited sorption conditions), the variability of desorption rate has a small effect on the breakthrough curve, both in the peak concentration which decreases and in the longer tail which extends to about 50 PV. However, for a higher DaI value of 1000 (corresponding to equilibrium conditions), increasing the variance of k_r significantly changes the breakthrough curve leading to both a reduction in the peak concentration and a longer tail.

It is evident from Figure 3.9, that the variance of k_r is the controlling factor in the increased tailing seen in the breakthrough curve. Other sensitivity studies have also indicated that variability in desorption rates is an important parameter to be considered in the design of remediation studies [Haggerty and Gorelick, 1994].

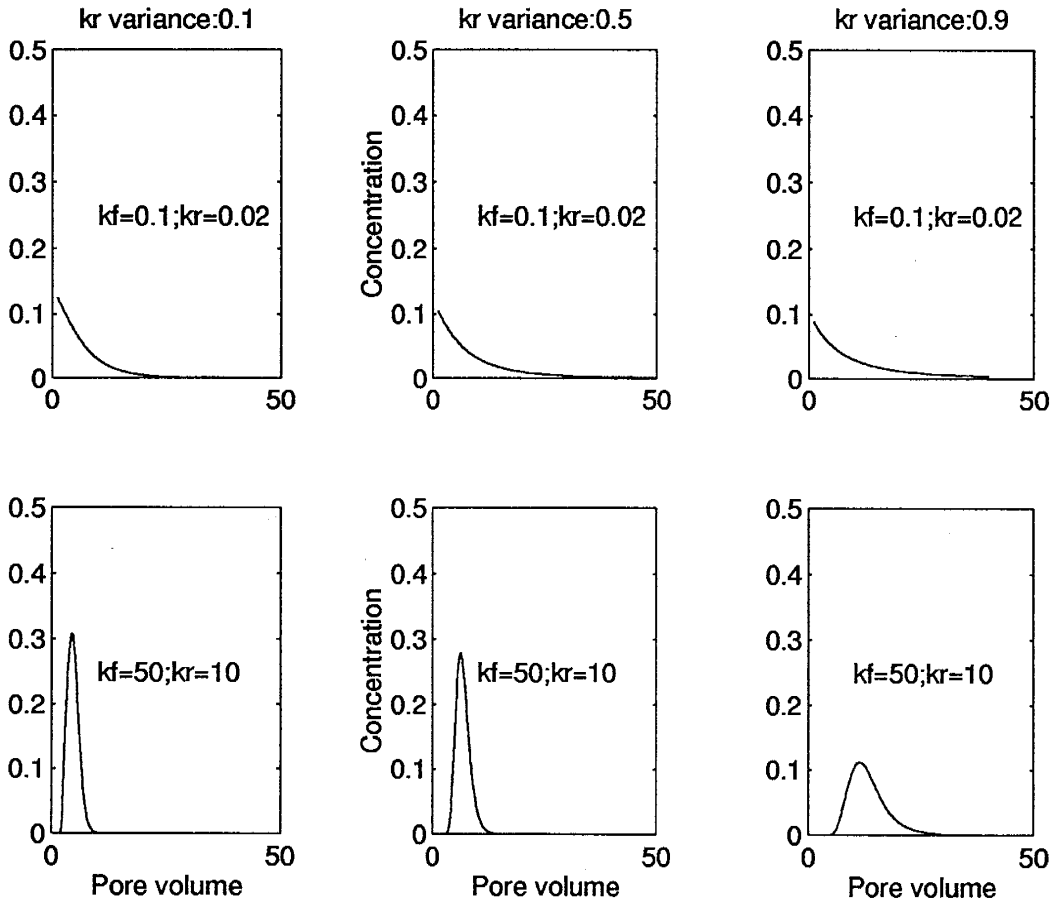

Figure 3.9: Sensitivity to the variance of desorption rate. DaI and DaII for the top panel is 2 and 0.4 respectively and for the bottom panel is 1000 and 200 respectively.

3.5 Combined Processes of Decay and Sorption

In this section we develop a semi-analytical solution for calculating the breakthrough curve of a reactive solute undergoing decay along with sorption-desorption. The recursion formulation previously developed to account for the kinetically limited sorption rate parameters is extended to include decay of the solute either in the aqueous or sorbed phase.

With this formulation we can model the biodegradation of contaminants where the solute particles are first sorbed on a thin biofilm layer followed by transformation of the solute. Once again spatial variability of the rate parameters is incorporated as an extension of the basic model.

3.5.1 Decay of Solute in Aqueous Phase

For a number of solutes, especially radionuclides, the solute can undergo natural decay specified by a first order rate coefficient. The decay rate, d, is easily incorporated in our recursion formulation to obtain the breakthrough curve. Once again we define $P_{n,n}^{(1)}$ as the probability that the solute particle starting from the aqueous phase stays in the aqueous phase for n time steps and moves a distance of n space steps. The probability for a particle to remain in aqueous phase is represented by r_{11} and in the sorbed phase by r_{22}. We similarly define $1 - r_{11}$ and $1 - r_{22}$ to represent the transition probabilities to move to the sorbed phase and the aqueous phase respectively: these are related to the sorption rate k_f and the desorption rate k_r via

$$(1 - r_{11}) = k_f \, \Delta t \tag{3.25}$$

$$(1 - r_{22}) = k_r \, \Delta t \tag{3.26}$$

As before the general notation is $P_{n,k}^{(j)}$ which denotes the probability that a particle moves n space steps in k time steps starting from phase j, where j=1 is the aqueous phase and j=2 is the sorbed phase. If the solute undergoes decay at a rate given by d, then

$$P_{n,n}^{(1)} = r_{11}^{n} \, e^{-d\, n\, \Delta t} \tag{3.27}$$

$$P_{n.n}^{(2)} = r_{11}^{n-1} \, (1 - r_{22}) \, e^{-d\, n\, \Delta t} \tag{3.28}$$

The aqueous concentration is decaying at a rate d and the total amount of decay is proportional to $n \, \Delta t$ where Δt is the time interval for each step. The probabilities $P_{1,k}^{(j)}$ that a particle moves one space step in k time steps starting in state j (j=1, the aqueous state and j=2, the sorbed state are

$$P_{1,k}^{(1)} = (1 - r_{11}) \, r_{22}^{k-2} \, (1 - r_{22}) \, e^{-d\, \Delta t}, \quad k \geq 2 \tag{3.29}$$

$$P_{1,k}^{(2)} = r_{22}^{k-1} \, (1 - r_{22}) \, e^{-d\, \Delta t}, \quad k \geq 2 \tag{3.30}$$

$$P_{n,k}^{(j)} = 0 \;\; for \;\; k \ll n, \;\; j = 1, 2 \tag{3.31}$$

The following recursion formulations are then used to calculate $P_{n,k}^{(j)}$ for any given n or k, $k \gg n$

$$P_{n,k}^{(1)} = r_{11} \, P_{n-1,k-1}^{(1)} \, e^{-d\, \Delta t} + (1 - r_{11}) \, P_{n,k-1}^{(2)} \tag{3.32}$$

$$P_{n,k}^{(2)} = r_{22} \, P_{n,k-1}^{(2)} + \, (1 - r_{22}) \, P_{n-1,k-1}^{(1)} \, e^{-d\, \Delta t} \tag{3.33}$$

Figure 3.10 shows the breakthrough curve obtained by the recursion formulation for a solute undergoing decay at two different rates of 0.1/d and 0.05/d for a column of length 1.0 m, constant velocity 0.1m/d and the sorption (k_f) and desorption (k_r) rates being 1.0/d and 0.2/d to give a K_d of 5. The breakthrough curve for a solute which does not decay is also given for comparison. The figure shows that increasing values of the decay rates cause a sharp reduction in the maximum (peak) concentration.

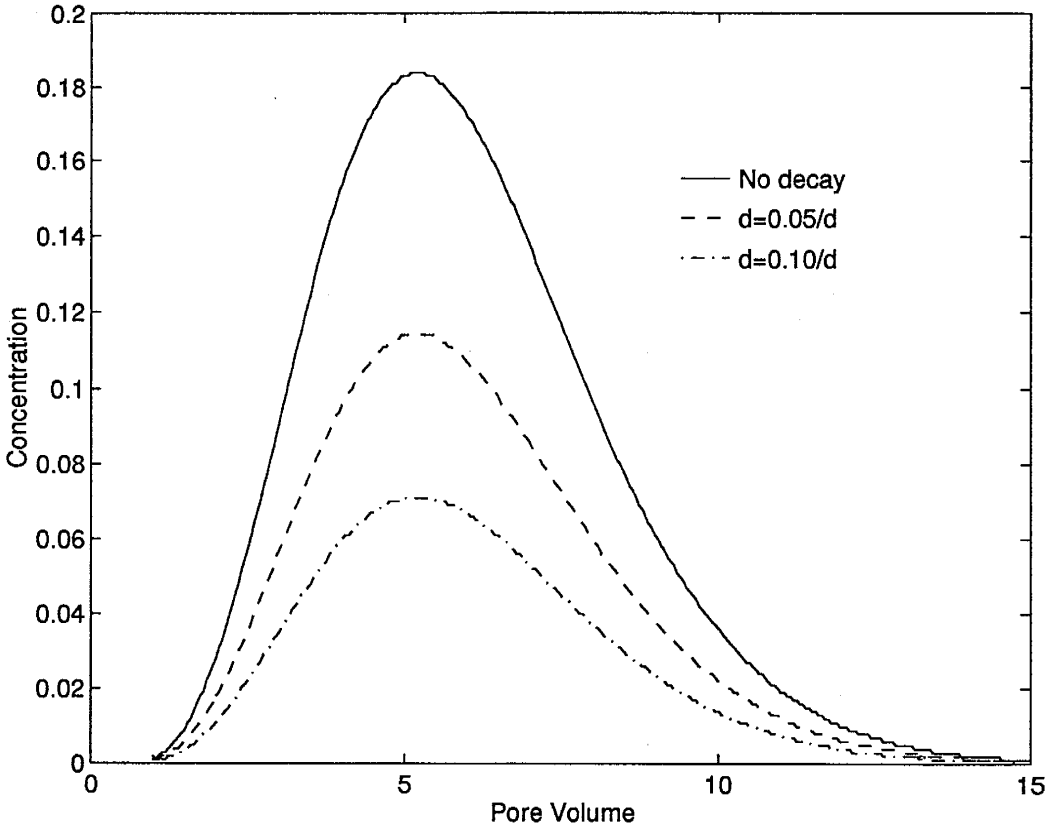

Figure 3.10: Breakthrough curves for decay rates of 0.05 and 0.1 obtained by recursion formulation and comparison with solute undergoing no decay.

3.5.2 Biodegradation

Biodegradation of contaminant is currently a major area of research. It is of special significance as it provides a natural attenuation mechanism for the breakdown of toxic contaminants into less toxic or harmless byproducts by in-situ living organisms. In addition, engineered bioremediation techniques are being used to introduce specific microbes to enhance the concentration of the existing ones for efficient cleanup processes.

A possible mechanism by which these organisms use the contaminants is the sorption of the solute molecules into the thin biofilm surrounding the rock surfaces [Dykaar and Kitanidis, 1996] where the solute is then broken up through enzyme action or metabolized by the organism. We are not interested in studying the specific mechanism of biodegradation but only present a model which allows for the removal of the solute phase to a stationary phase (biofilm) where the degradation can occur. We use the recursion formulation developed in the earlier section to model the effect of biodegradation which occurs in the sorbed phase. The biodegradation process is described both for constant and spatially varying rates. The following three scenarios are studied.

Constant k_f, k_r and constant biodegradation rate, d

The recursion formulation in this case of decay occurring only in the sorbed phase which is specified in terms of a rate parameter, d leads to the following set of recursion formulations:

$$P_{n,n}^{(1)} = r_{11}^{n} \tag{3.34}$$

$$P^{(2)}_{n.n} = r_{11}^{n-1}\,(1-r_{22}) \tag{3.35}$$

$$P^{(1)}_{1,k} = (1-r_{11})\,r_{22}^{k-2}\,(1-r_{22})e^{-d\,(k-1)\,\Delta t},\quad k \geq 2 \tag{3.36}$$

$$P^{(2)}_{1,k} = r_{22}^{k-1}\,(1-r_{22})\,e^{-d\,(k-1)\,\Delta t},\quad k \geq 2 \tag{3.37}$$

$$P^{(j)}_{n,k} = 0 \quad for\ k \ll n,\ \ j = 1,2 \tag{3.38}$$

The following recursion formulations are then used to calculate $P_{n,k}$ for any given n or k, $k > n$

$$P^{(1)}_{n,k} = r_{11}\,P^{(1)}_{n-1,k-1} + (1-r_{11})\,P^{(2)}_{n,k-1}\,e^{-d\,\Delta t} \tag{3.39}$$

$$P^{(2)}_{n,k} = r_{22}\,P^{(2)}_{n,k-1}\,e^{-d\,\Delta t} + (1-r_{22})\,P^{(1)}_{n-1,k-1} \tag{3.40}$$

Figure 3.11 shows the breakthrough curve obtained for the two different biodegradation rates of 0.1/d and 0.05/d obtained by using the above formulation. Comparing it to Figure 3.10, the peak concentrations are substantially lower in Figure 3.11 where the decay occurs in the sorbed phase than the case where decay is occurring in the aqueous phase. Note that the breakthrough curves for the non-zero decay rates in the sorbed phase show an earlier peak. This can be explained by the fact that a rapid decay in the sorbed phase will imply that a large fraction of the breakthrough curve is due to material that is never sorbed. Considering a particle tracking interpretation, the conditional travel time for a particle given it is not sorbed will be substantially shorter than the one that is adsorbed.

Spatially variable k_f, k_r and constant biodegradation rate, d

The rate parameters k_f and k_r can be modeled as random processes; $k_f(x)$ and $k_r(x)$, that vary in space. An alternative interpretation is that spatially variable

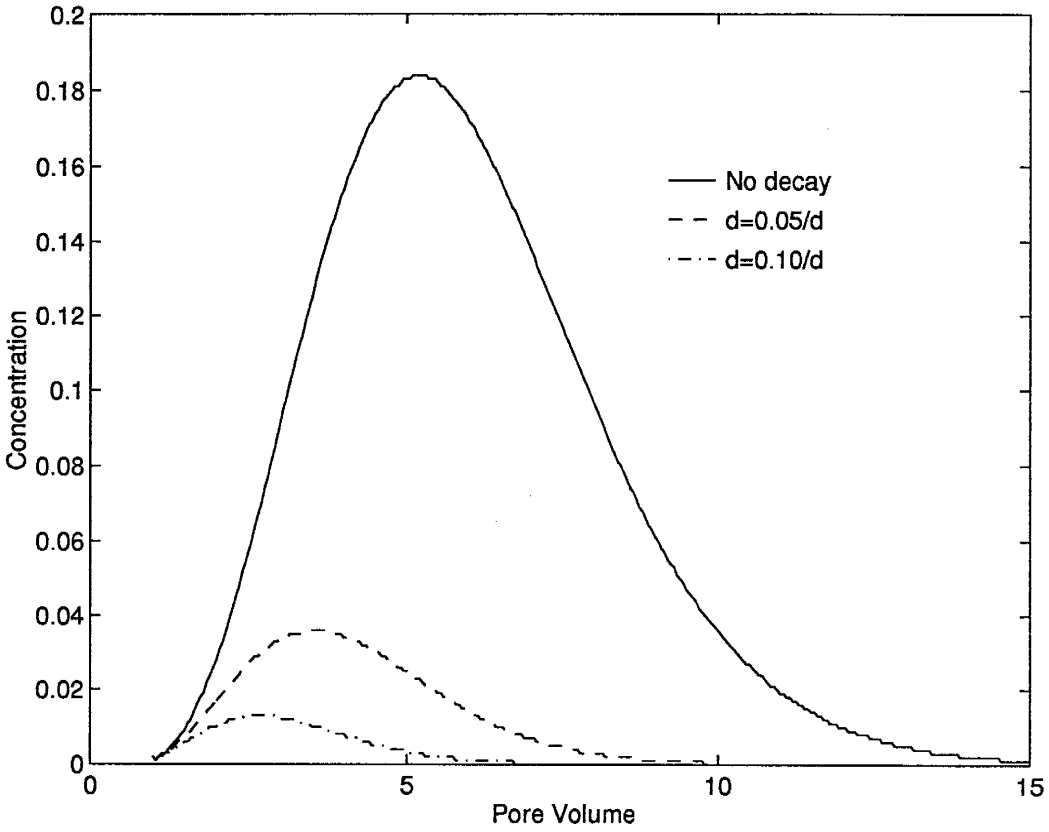

Figure 3.11: Breakthrough curves for the biodegradation process for two different rates of 0.05 and 0.1. The flow parameters are the same as those in Figure 3.10.

k_f and k_r could represent variations in the thickness or areal extent of the biofilm [Rittmann, 1993]. The issue of the continuity of the biofilm is still a matter of debate. Some researchers are of the opinion that the microbial population forms a continuous film [Taylor and Jaffe, 1990; Cunningham et al., 1991] while others believe that it forms isolated patches or colonies [Vandervivere and Baveye, 92]. The recursion formulation described in the earlier section is easily extended to account for spatial variation of the rate parameters and to include the biodegradation process occurring in the sorbed phase.

The mean breakthrough curve for the case of spatially variable k_f and k_r is shown in Figure 3.12. A variance of 0.05 for both ln k_f and ln k_r and a constant biodegradation rate of 0.05 are used. The two processes k_f and k_r are assumed to have a exponential correlation structure with a correlation scale of 0.1 and are generated at spatial discretization of 0.01 m to obtain 100 points over 1.0 m length. A total of 50 individual realizations of the breakthrough curve were generated. The mean values of k_f and k_r are the same as that used earlier, i.e. 1.0 and 0.2, respectively. Spatial variability of the rates leads to a larger spread of the breakthrough curve and the peak concentration is also reduced. Also shown are the one standard deviation values from the mean.

Comparison of Figure 3.11 and 3.12 reveals some interesting features. The peak concentration exits the column at about 4 pore volume showing a small shift from the case of constant rates. The long tail observed in Figure 3.12 shows that solute concentration is significant even for time beyond 10 pore volumes.

Another series of simulation were run where the k_f and k_r were kept constant and the decay rate was modeled as a spatially variable process with a exponential

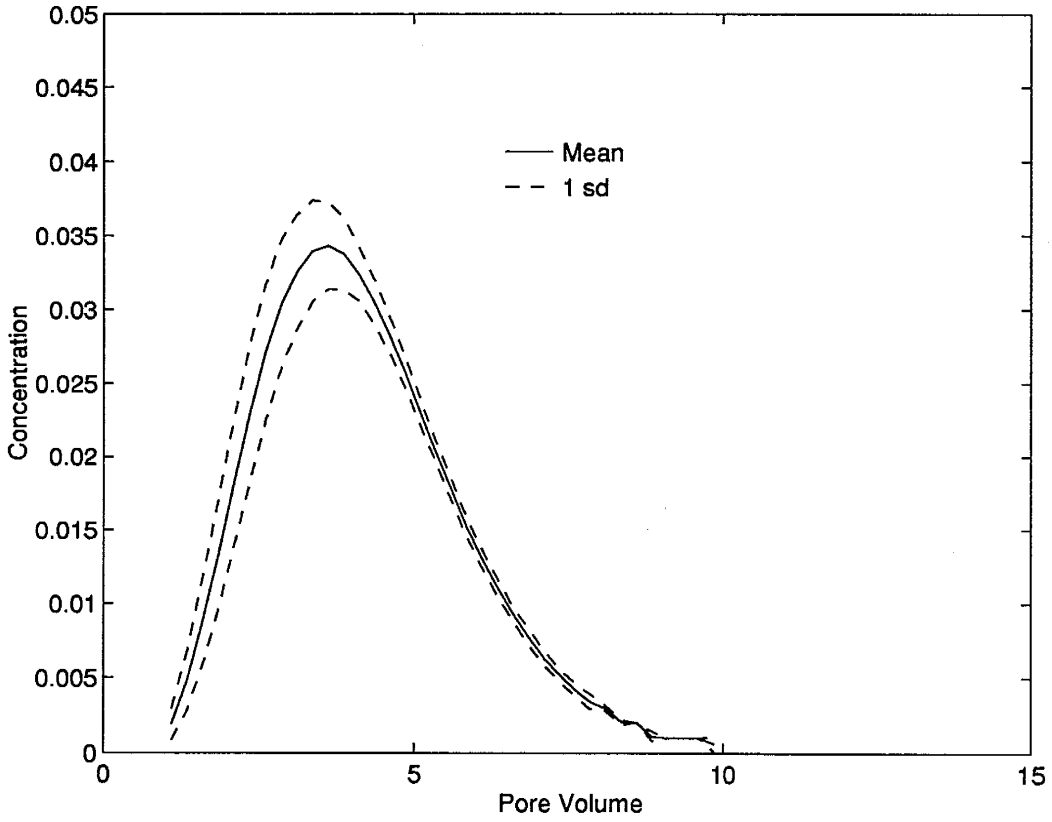

Figure 3.12: Mean breakthrough curve for spatially variable sorption and desorption rates. A constant value of 0.05 is used for the biodegradation rate. Also shown as dotted lines are the one standard deviation results from the mean breakthrough curve.

correlation structure. Two different variances of 0.01 and 0.05 with the mean value fixed at 0.05 did not show a large difference in the breakthrough curves. This indicated very little sensitivity to the decay rate variations for the parameter values studied for the given flow system.

Spatially varying k_f, k_r and d

In the final case all the variables (k_f and k_r and d) are assumed to be random functions with a exponential covariance and correlation scale of 0.1. The breakthrough curves are calculated for two different variances of 0.1 and 0.5 for the three processes, k_f and k_r and d (Figure 3.13). The breakthrough curves are very similar to the ones obtained in Figure 3.11 with regard to the arrival of the peak concentration. The only difference is in the spread of the breakthrough curve, especially at the larger variance of 0.5 which signifies that the combined effect of sorption and degradation where all the three rates are spatially varying leads to a longer tail of the breakthrough curve.

3.6 Discussion and Conclusions

In this chapter we developed a recursion formulation for modeling transport with linear kinetic sorption. The recursion formulation is derived from a Markov process model of sorptive transport, previously presented by Giddings and Eyring [1955], Andricevic and Foufoula-Georgiou [1991], and Quinodoz and Valocchi, [1993]. The recursion formulation is relatively easy to implement and effectively mimics particle-tracking involving an infinite number of particles. For this reason, it is very efficient and holds promise in connection with large-scale simulations of transport involving

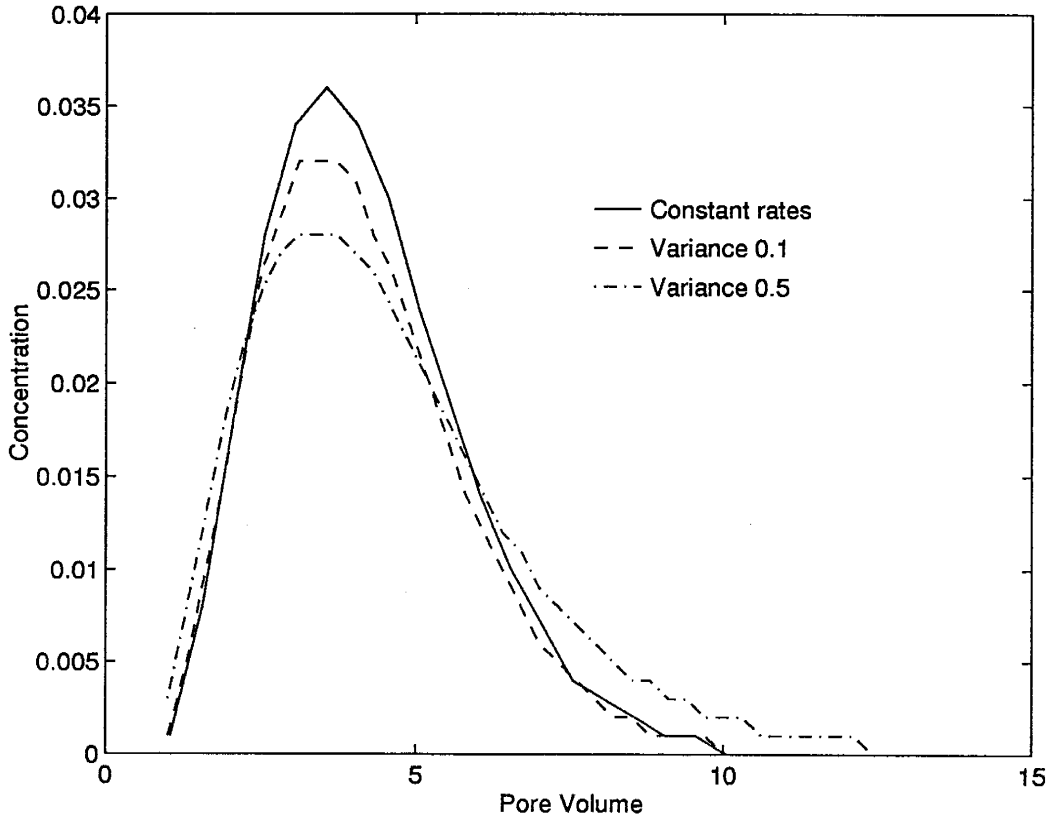

Figure 3.13: Breakthrough curves for spatially variable sorption, desorption and biodegradation rate. Two different variances of 0.1 and 0.5 for all the three parameters are shown.

kinetic sorption. Spatial variability of sorption kinetics is incorporated easily within the recursion formulation.

Application of the recursion formulation along numerically computed streamtubes or pathlines enables an extension of this formulation to multidimensional transport simulation. Unlike some previous streamtubes analyses [e.g. Simmons et. al., 1995], the computational advantages and analytical simplicity of the recursion formulation are not lost when the reaction rates and velocity are variable along the streamtubes. The extension to a two-dimensional flow field is developed in Chapter 5. One limitation of the recursion formulation is that it was derived ignoring the influence of local dispersion. This assumption is not likely to be very limiting in the context of transport in heterogeneous media, if the small-scale variations in the velocity field are resolved adequately.

The results of this study show that in the non-equilibrium case, the individual rate coefficients can have an important effect on the breakthrough curve. In particular, the slower rates of the sorption-desorption process for the case of a linear isotherm do control the behavior of the breakthrough curve, leading to a long tail.

We have also seen that spatial variability of the rates could have a significant effect on the breakthrough curve. Recent studies based on field observations also show that sorptive parameters are spatially variable [Robin et al., 1991]. The spatial variability of sorption rates has a potentially important influence on field-scale behavior.

The sensitivity studies presented here suggest that the desorption rate is the important parameter controlling the long tail seen in the breakthrough curve. There is a need for more field studies to assess the degree of variability of k_r.

A one-dimensional model of reactive transport was developed to model the sorption-desorption and decay of the solute, either in the aqueous phase or in the sorbed phase. The decay in sorbed phase is used to describe the biodegradation mechanism. Spatial variations of k_f and k_r are used to mimic the variability of the biofilm as regards the lateral extent and the thickness of the biofilm. We see that heterogeneity of k_f and k_r causes larger spread in the breakthrough curve. This study suggests that characterizing the shape and aggregation of the biofilm could be important in understanding transport of biodegradable solutes.

The one-dimensional recursion model, while appealing, is restricted to linear sorption-desorption reactions. The recursion formulation can also be extended to modeling multi-component transport involving linear reactions, by beginning from a multi-state Markov process model.

Another avenue of research is for the case where sorption and desorption rates are correlated. To handle these situations, cross- correlated k_f and k_r processes can be jointly generated using a Fast Fourier Transform algorithm developed by Bullard [1994] and Gutjahr et al. [1996] .

Chapter 4

Semi-Markov Models For Multple Sorption Sites

4.1 Overview

The important role of sorption processes in the transport of organic contaminants in subsurface systems is widely accepted. However, a consensus regarding mechanistic characterization of these processes is lacking. In this chapter we hypothesize that sorption processes are intrinsically heterogeneous in the sense that multiple sorption sites are available to a solute. Different regions of the rock matrix may contain different types, amounts and distributions of surfaces and of soil organic matter, even at the particle scale. The physical and chemical properties of an aquifer material can vary at scales ranging from microscopic (grains/pore scale) to macroscopic (field scale). The impact of variations in the sorbent microscopic properties (in particular the sorbent structure and composition) on the rate-limiting process can be significant [Weber et al., 1992]. We present two formulations, a hyperexponential model for sites which are accessed in parallel by the sorbing solute, and a gamma model for sites which are accessed in series. Alternatively the models presented here can be viewed as ways to study non-exponential residence times without the mechanistic interpretation given above.

4.2 Introduction

We developed a model for transport of a linearly sorbing solute in a porous medium subject to rate-limited reactions in the last chapter. Conventional approaches to model the kinetically limited behavior often assume an equivalent homogeneous medium with a deterministic description of the rates for one type of sorption sites. However, it is evident that this assumption is not valid, both at the column scale and at the field scale. Heterogeneity at the sorbent grain scale is a major research focus, motivated by the fact that single rate processes often fail to give a complete description of the sorption-desorption phenomenon in batch studies and the breakthrough curves in column experiments. We describe such a model as a single-site model. The recursion formulation developed in Chapter 3 is a single-site model.

A number of different models have been proposed to overcome the limitations imposed by the constraints of a model which assumes a single uniform equilibrium or rate process. A two-site model was found to be in better agreement with the experimental observations than a single site model by Gamerdinger et al. [1990] and Brusseau et al. [1989]. However, recent studies [Pignatello et al., 1993] have shown that a two-site approach often fails to predict concentration changes at long time scales. An extension of that two-site model has been proposed which includes a population of sorption sites to describe longer time-scale sorption behavior [Chen and Wagenet, 1995].

Different mechanisms have been proposed for slow desorption. One possible explanation is the molecular diffusion within the matrix. Wu and Gschwend [1986] developed a diffusion model for halogenated benzenes, and Steinberg et al. [1987] argued for a diffusion kinetics-based mechanism for desorption of 1,2-dibromomethane

(EDB) from fumigated soils. However the effect of the structural characteristics of the sorbent involved in slowly reversible desorption are yet to be fully understood. While there is a thermodynamic basis for proposing an entropy-driven hydrophobic partitioning of the sorbate into the organic phase [Chiou, 1989], others have put forth the importance of the sorbate-surface interactions [Mingelgrin and Gerstl, 1982]. Still another hypothesis is that sorbate molecules must diffuse through the interstitial pores of the aggregates and that migration is retarded by rapid, "micro-scale partitioning" between pore fluids and the pore walls [Wu and Gschwend, 1986].

Pignatello [1990] showed that residual concentrations of EDB and TCE are higher in the samples with larger organic carbon content. Furthermore the humic materials are heterogeneous at the microscopic level, the humic polymer being denser and more hydrophobic with distance from the aqueous-humic interface [Hayes and Himes, 1986]. Assuming that the sorbate molecule primarily interacts with the soil organic matter and that the penetration of the organic matter is diffusion limited [Bouchard et al, 1988] the kinetics can then be described by first-order rate coefficients.

Alternatively we can extend the recursion formulation for the single-site case to accommodate multiple sites of sorption and desorption, and to look at the heterogeneity in sorption sites. The term "site" does not refer to a distinct physical point but a portion of the sorbent surface having uniform local sorption properties. Once again, we do not distinguish among the different sorbing mechanisms, diffusion-controlled processes and sorption kinetics. Heterogeneity in soil physical and chemical properties that are related to rate limiting processes are variable at almost every microscopic scale [Weber et al., 1992]. In the proposed first-order approach, these variations are lumped into a characteristic rate for each site. In particular we use a

Markov-process-based recursion to account for multiple sites based on the accessibility of sites. The aim of this chapter is to focus on the processes occurring on a small scale, say at the level of grain surfaces and to be able to predict the lumped behavior that is observed for an entire column when transport experiments are conducted. We develop a modeling framework (the hyperexponential) to study multiple sites which are accessed in parallel by the solute present in the aqueous phase. The case of sorption sites which are accessed in series (the gamma model) is also briefly discussed. Finally we study the sensitivity of the breakthrough curves to the mean and variances of the hyperexponential model.

4.3 Hyperexponential Model

A conceptual model of the multiple sorption sites with different solid phases is shown in Figure 4.1. We visualize a surface with patches of different mineral compositions and other solid phase (organic carbon coating in our example) and with desorption rates (μ_i) different for each of the surfaces. We consider the formulation for a three-site process where we hypothesize that three different sorbing surfaces are present on which the solute can be sorbed. The choice of a three-site model is for illustrative purposes only. These sites are available in parallel and the solute can move from one sorbed surface to another only by going back into the aqueous phase. The time spent in each of the sorbed stages is still exponentially distributed while the desorption rate, μ_i varies from site to site and the solute can be sorbed on any of the three surfaces with a given probability, α_i. The resulting sorbed time will have a hyperexponential distribution and we term our model of sorption site heterogeneity as the hyperexponential model.

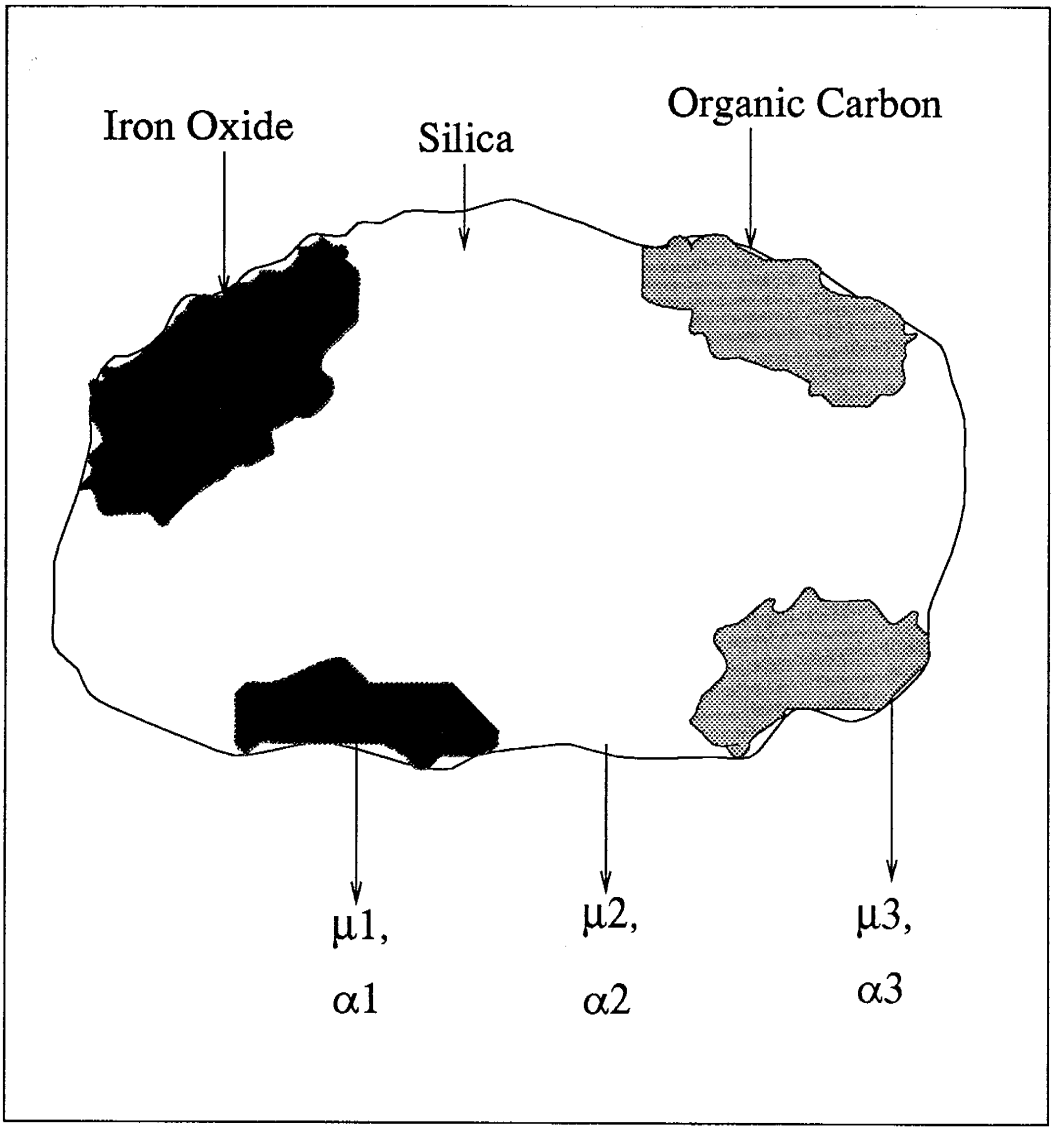

Figure 4.1: A conceptual model for a three-site hyperexponential model showing three sorption sites with desorption rates of μ_1, μ_2, and μ_3 and probabilities of sorption to each of the three sites given by α_i, $i = 1, 2, 3$.

The hyperexponential probability density function (pdf) is given by

$$f(t; m, \alpha, \mu) = \sum_{i=1}^{m} \alpha_i \, \mu_i \, e^{-t \, \mu_i} \tag{4.1}$$

$$\sum_{i=1}^{m} \alpha_i = 1 \tag{4.2}$$

The mean and variance of a m-parameter hyperexponential pdf are given by

$$\text{Mean} = \sum_{i=1}^{m} \frac{\alpha_i}{\mu_i} \tag{4.3}$$

$$\text{Variance} = \sum_{i=1}^{m} \frac{2 \, \alpha_i}{\mu_i^2} - \left(\sum_{i=1}^{m} \frac{\alpha_i}{\mu_i} \right)^2 \tag{4.4}$$

This represents a model for sorption-desorption onto site i with probability α_i where the time spent in the sorbed state at each site is an exponential with a site-dependent mean, $1/\mu_i$.

Consider again the case of linear sorption and desorption rates where the distribution coefficient K_d is defined by $K_d = k_f/k_r$ and where k_f and k_r are sorption and desorption rates for the one-site model. For the multi-sorption sites, we still have the same sorption rate, k_f but the desorption rates are now designated by μ_i, i=1 to m. To make valid comparisons with the constant rate case, we chose the different values of μ_i to be such that the mean of hyperexponential distribution (i.e. the mean time spent in the sorbed phase) is same as $1/k_r$ and these values are given in Table 4.1 for several cases. For linear kinetic models where the sorption-desorption process only depends on the forward and backward rate coefficients, recursive equations can be developed for the probability distribution of the number of time steps taken to

Distribution	Parameters	Mean	Variance
Exponential	k_f=1, k_r=0.2	5	25
Gamma	θ=0.4	5	12.5
Hyperexponential (Two-site)	α_1=0.3, μ_1=0.5 α_2=0.7, μ_2=0.159	5	35
Hyperexponential (Three-site)	α_1=0.3, μ_1=0.5 α_2=0.6, μ_2=0.8 α_3=0.1, μ_3=0.0274	5	255

Table 4.1: Parameters used for hyperexponential and gamma distribution. Means and variances are for the desorption time.

reach the effluent end. The probability distribution of the residence time can then be related to the concentration breakthrough curve.

We denote the status of solute as either mobile (j=1) or sorbed (j=2, 3, 4) and let $P_{n,k}^{(j)}$ denote the probability that it takes k time-steps for a solute particle to move n space steps, starting in state j. If the transition probability for solute to remain in the aqueous phase is denoted by r_{11}, then r_{12} is the transition probability for moving from the aqueous to sorbed phase 2. Similarly, if r_{22} is the transition probability that solute initially in the sorbed phase 2 remains the sorbed phase 2, then $r_{21} = 1 - r_{22}$ is the transition probability for moving from the sorbed phase 2 to the aqueous phase.

The transition probabilities for fixed Δt are given by

$$r_{12} = \alpha_1 \, k_f \, \Delta t + \mathcal{O}(\Delta t) \cong \alpha_1 \, k_f \, \Delta t \tag{4.5}$$

$$r_{21} = 1 - r_{22} = \mu_1 \, \Delta t + \mathcal{O}(\Delta t) \cong \mu_1 \, \Delta t \tag{4.6}$$

in the discrete approximation adopted here. The transition probability for moving from the aqueous state to sorbed state 1 is related to the sorption rate (k_f) and the probability that sorption is to site 1 (α_1). The transition probability of moving from sorbed state 1 to the aqueous state is the product of the desorption rate (μ_1) and the time step (Δt). Similar transition probabilities can be obtained for sorption and desorption to sites 2 and 3.

Using these transition probabilities the following recursions are true, for $k > n$,

$$P^{(1)}_{n,k} = r_{11} \, P^{(1)}_{n-1,k-1} + r_{12} \, P^{(2)}_{n,k-1} + r_{13} \, P^{(3)}_{n,k-1} + r_{14} \, P^{(4)}_{n,k-1} \tag{4.7}$$

$$P^{(2)}_{n,k} = r_{22} \, P^{(2)}_{n,k-1} + r_{21} \, P^{(1)}_{n-1,k-1} \tag{4.8}$$

$$P^{(3)}_{n,k} = r_{33} \, P^{(3)}_{n,k-1} + r_{31} \, P^{(1)}_{n-1,k-1} \tag{4.9}$$

$$P^{(4)}_{n,k} = r_{44} \, P^{(2)}_{n,k-1} + r_{41} \, P^{(1)}_{n-1,k-1} \tag{4.10}$$

These recursion formulas are solved with boundary conditions:

$$P^{(1)}_{n,n} = r_{11}^{n} \tag{4.11}$$

$$P^{(2)}_{n,n} = r_{11}^{n-1} \, (1 - r_{22}) \tag{4.12}$$

$$P^{(3)}_{n,n} = r_{11}^{n-1} \, (1 - r_{33}) \tag{4.13}$$

$$P^{(4)}_{n,n} = r_{11}^{n-1} \, (1 - r_{44}) \tag{4.14}$$

$$P_{1,k}^{(1)} = r_{12}\, r_{22}^{k-2}\, r_{21} + r_{13}\, r_{33}^{k-2}\, r_{31} + r_{14}\, r_{44}^{k-2}\, r_{41}, \quad k \geq 2 \tag{4.15}$$

$$P_{1,k}^{(2)} = r_{22}^{k-1}\,(1 - r_{22}), \quad k \geq 2 \tag{4.16}$$

$$P_{1,k}^{(3)} = r_{33}^{k-1}\,(1 - r_{33}), \quad k \geq 2 \tag{4.17}$$

$$P_{1,k}^{(4)} = r_{44}^{k-1}\,(1 - r_{44}), \quad k \geq 2 \tag{4.18}$$

$$P_{n,k}^{(j)} = 0, \quad k < n, j = 1, 2, 3, 4 \tag{4.19}$$

For example, the boundary condition in equation 4.15 represents the probability of moving one space step in k time steps, starting in the aqueous state. This probability can be obtained in three ways

1. The solute particle moves from the aqueous state to the sorbed state (2) which is given by r_{12} and remains in sorbed state 2 for k-2 time steps which is given by r_{22}^{k-2} and then comes back to aqueous state in the kth time step given by r_{21}; or

2. The solute particle moves from the aqueous state to the sorbed state (3) and remains in sorbed state 3 for k-2 time steps and then comes back to aqueous state in the kth time step; or

3. The solute particle moves from the aqueous state to the sorbed state (4) and remains in sorbed state 4 for k-2 time steps and then comes back to aqueous state in the kth time step.

As all of the above events are disjoint, the final result is obtained as a sum of the three probabilities.

The breakthrough curve for the case of three different sorption sites can be compared with the case of single sites for the same values of sorption and desorption rates. The parameters used are given in Table 4.1. The choice of the parameters (μ_i), i=1,3 are for the purposes of illustration only. The only restriction that we impose is that the mean of the hyperexponential distribution be the same as that of the one-site exponential model. We could have selected another set of parameters with the same mean and different variance which would have resulted in a different breakthrough curve. We postpone the discussion of the non-uniqueness issue to a later section.

The mean desorption time is 5 days for both the exponential (Markov) and the three-site hyperexponential model. The variance for the exponential model is 25 while it is 255 for the hyperexponential model. The example shown in Figure 4.2 illustrates the long tail seen in the case of the three-site model. This kind of behavior is typical of what has been termed to be non-equilibrium sorption phenomena (Figure 4.2).

By way of contrast, a case of two different sites is shown in Figure 4.3. In this case the breakthrough curve shows behavior similar to the one-site Markov model. In this case also, the mean desorption time is same (5 days) for the two models. The variance of the two-site hyperexponential model is 35 compared to 25 for the Markov model. The values of α_i, $i = 1,\ 2$ and the μ_i are given in Table 4.1. The choice of the values for the different parameters (μ_i, α_i's) were made so as to have the same mean desorption time in all the different cases.

The differences in the two breakthrough curves obtained using the hyperexponential model for two sites and three sites can possibly be explained on the basis of the variances of the desorption times which are given in Table 4.1. The variance

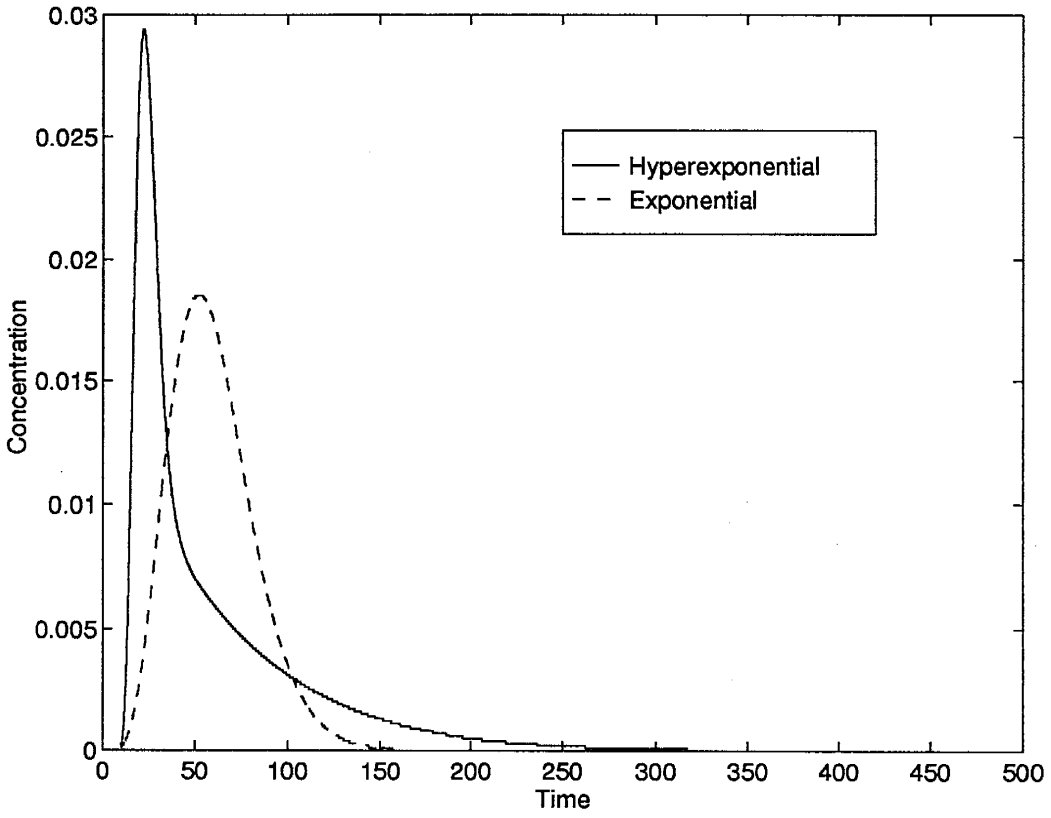

Figure 4.2: Breakthrough curves for a three-site hyperexponential model compared to a single-site model for same mean k_f, k_r values. The variance of the hyperexponential model is 255 compared to 25 for the exponential model.

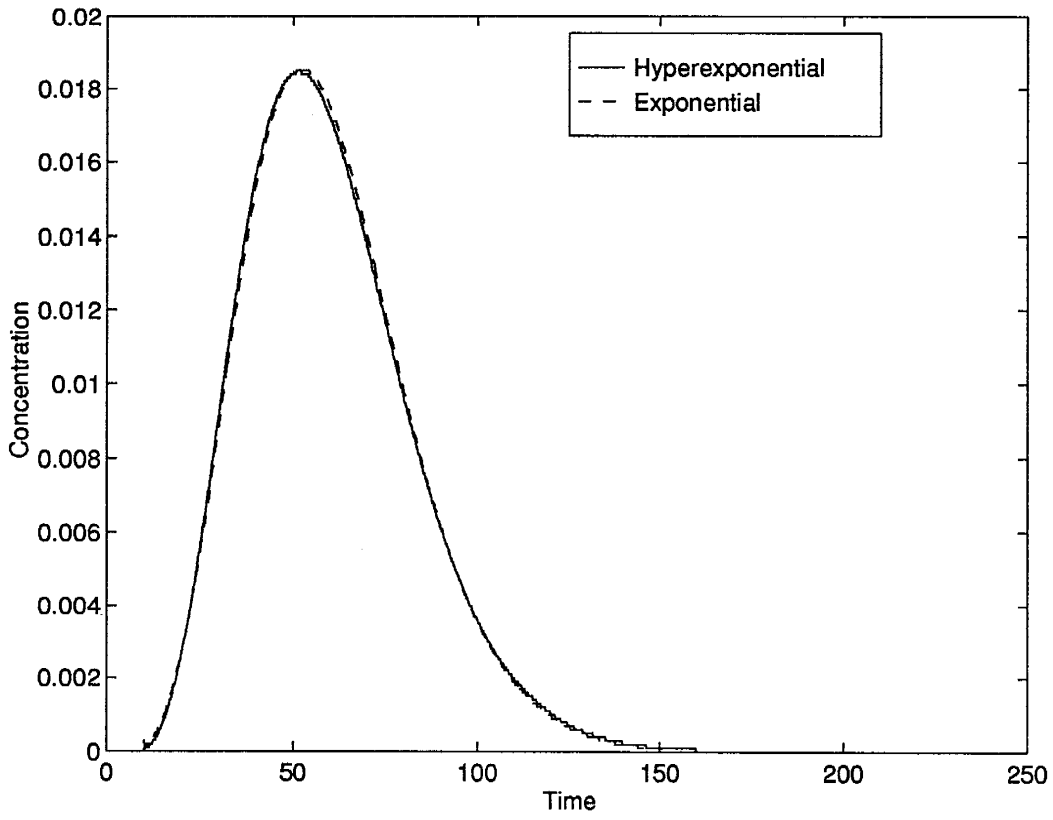

Figure 4.3: Breakthrough curves for a two-site hyperexponential model compared to a single-site model for same mean k_f, k_r values. The variance of the hyperexponential model is 35 compared to 25 for the exponential model.

of the desorption time for the three site model is an order of magnitude higher than the two site model and is the major factor influencing the shape of the breakthrough curve.

In our derivation of the results above, particular reference was made to a physical model with different sites. However the results also hold for single site models where the residence time has the hyperexponential density given by equation 4.1, and the "different sites" are essentially just mathematical devices to emulate the mixed probability density given in equation 4.1. Stating it differently, the model presented above describes the breakthrough curve for the case where the time spent in the sorbed phase has a hyperexponential distribution. We can make the distinction between the one-site and the multi-site model based on the assumption that the one-site model has an exponential distribution of the sorbed time while the multi-site has a hyperexponential distribution. If the exponential and hyperexponential can be chosen to have the same mean, the hyperexponential will have a larger variance. In the next section we examine a model with a variance smaller than that of the corresponding exponential.

4.4 Gamma Model

In the discussions above, the sorption to the surface, either one site or multiple sites was directly from the aqueous phase. However there could be situations where the solute may pass through intermediary steps before being sorbed onto the final surface. This process we term as phased sorption and we develop the recursion formulation for this below.

Here we hypothesize a phased sorption process - sorption onto the overlying

organic matter and then onto the mineral surface, for example. If the time spent in both the phases are two independent identically distributed exponentials, then the entire sorbed time has a gamma distribution.

Once again we restrict ourselves to linear sorption and desorption rates where the distribution coefficient K_d is defined by $K_d = k_f/k_r$ and where k_f and k_r are sorption and desorption rates, respectively. If the solute is sorbed, the time spent in the sorbed phase will have a gamma distribution with mean m/θ, where m is the number of possible states in the sorbing phase and θ is the rate parameter for the gamma distribution. Since we want the mean time in the sorbed state to be $1/k_r$, the parameter θ for the gamma distribution is $m\ k_r$. Below we assume that there are two states; namely m is 2.

The three possible states in which the solute can reside in are designated as 1 (the aqueous state); 2 (the first sorbed state) and 3 (the second sorbed state). The following transitions are considered: r_{12}, the transition from the aqueous to sorbed state 1 which is equal to $1 - r_{11}$; r_{23}, the transition from sorbed state 2 to 3 which is equal to $1 - r_{22}$ and r_{31}, the transition from sorbed state 3 to the aqueous state which is equal to $1 - r_{33}$. It should be noted that the solute can only go to sorbed phase 1 from the aqueous state and can enter the aqueous state from sorbed state 3 signifying a one-way street from $1 \rightarrow 2 \rightarrow 3 \rightarrow 1$.

The recursion formulation can be written as before with $k >^* n$,

$$P^{(1)}_{n,k} = r_{11}\ P^{(1)}_{n-1,k-1} + r_{12}\ P^{(2)}_{n,k-1} \tag{4.20}$$

$$P^{(2)}_{n,k} = r_{22}\ P^{(2)}_{n,k-1} + r_{23}\ P^{(3)}_{n,k-1} \tag{4.21}$$

$$P^{(3)}_{n,k} = r_{33}\ P^{(3)}_{n,k-1} + r_{31}\ P^{(1)}_{n-1,k-1} \tag{4.22}$$

These recursion formulas are solved with the following boundary conditions:

$$P_{n,n}^{(1)} = r_{11}^{n} \tag{4.23}$$

$$P_{n,n}^{(3)} = r_{11}^{n-1}\, r_{31} \tag{4.24}$$

$$P_{1,k}^{(1)} = r_{11}\, r_{12}, \quad k = 2 \tag{4.25}$$

$$P_{1,k}^{(1)} = r_{11}\, r_{12}\, (r_{22} + r_{23}), \quad k = 3 \tag{4.26}$$

$$P_{1,k}^{(1)} = r_{11}\, r_{12}\, (r_{22}^2 + r_{22}\, r_{23} + r_{23}\, r_{33}), \quad k = 4 \tag{4.27}$$

$$P_{1,k}^{(1)} = \sum_{l=0}^{k-3} r_{22}^{l}\, r_{33}^{k-3-l}\, (r_{12}\, r_{23}\, r_{31} + r_{11}\, r_{12}\, r_{23}), \quad k \geq 5, l = 0, k-3 \tag{4.28}$$

$$P_{1,k}^{(2)} = r_{23}\, r_{31}, \quad k = 2 \tag{4.29}$$

$$P_{1,k}^{(2)} = (r_{22} + r_{33})\, r_{23}\, r_{31}, \quad k = 3 \tag{4.30}$$

$$P_{1,k}^{(2)} = \sum_{l=0}^{2} r_{23}\, r_{31}\, (r_{22}^{l})\, (r_{33}^{2-l}), \quad k = 4 \tag{4.31}$$

$$P_{1,k}^{(2)} = \sum_{l=0}^{k-2} r_{23}\, r_{31} (r_{22}^{l})\, (r_{33}^{k-2-l}), \quad k \geq 5 \tag{4.32}$$

$$P_{1,k}^{(3)} = r_{33}\, r_{31} + r_{31}\, r_{12}, \quad k = 2 \tag{4.33}$$

$$P_{1,k}^{(3)} = r_{31}(r_{33}^2 + r_{22}\, r_{12} + r_{23}\, r_{12}), \quad k = 3 \tag{4.34}$$

$$P_{1,k}^{(3)} = r_{31}(r_{33}^3 + r_{22}^2\, r_{12} + r_{23}\, r_{12}\, r_{22} + r_{23}\, r_{12}\, r_{33}), \quad k = 4 \tag{4.35}$$

$$P_{1,k}^{(3)} = r_{31}(r_{33}^{k-1}) + r_{31} r_{22}^{k-2}\, r_{12} + r_{31}\, r_{23}\, r_{12}\, r_{22}^{k-3} + r_{31}\, r_{23}\, r_{12} r_{33}^{k-3}, \quad k \geq 5 \tag{4.36}$$

$$P_{1,k}^{(1)} = 0, \quad k < n, j = 1, 2, 3, 4 \tag{4.37}$$

The boundary conditions are slightly complicated to account for the transitions from sorbed state 2 to 3. As an example the boundary condition in equation 4.34

represents the probability that a solute particle starting in the second sorbed state (state 3) moves one space step in k=3 time steps. This can be done in the following three possible ways:

1. The solute particle remains in state 3 for 2 time steps given by r_{33}^2 and then moves from state 3 to 1 i.e. the aqueous state;

2. The solute particle moves from the state 3 to 1 i.e. the aqueous state given by $1 - r_{33}$ where it travels one space step in a given time step; it then makes the transition to state 2 given by $1 - r_{11}$ and then stays in state 2 given by r_{22}; and

3. The solute particle moves from the state 3 to 1 i.e. the aqueous state given by $1 - r_{33}$ where it travels one space step in a given time step; it then makes the transition to state 2 given by $1 - r_{11}$ and then makes one more transition from sate 2 to 3 given by $1 - r_{22}$.

The events are disjoint and the sum gives the final result.

The breakthrough curve for a gamma model is shown in Figure 4.4. The peak concentration is slightly increased when compared to the single-site model and the spread of the breakthrough curve is slightly decreased because the variance is smaller than the exponential model (Table 4.1).

It appears that the mean of the different distributions controls the peak position while the variances control the tailing of the breakthrough curves. In all the above cases the k_r value is 0.2/day giving a mean desorption time of 5 days, with an input velocity of 0.1 m/day; the peak is around 60 days (Figure 4.2) for a 1 m flow length. For the three-site hyperexponential model the peak shifts to about 20 days

which can be explained by the parameters in Table 4.1. A significant portion of the sites (60%) had a faster rate of 0.8/day which contributed to the peak position, while 10% of the sites with a very slow rate of 0.0274/day led to the very extended tailing seen on the breakthrough curve. This observation of the apparent non-equilibrium effect seen for the three-site hyperexponential model is examined further in the next section.

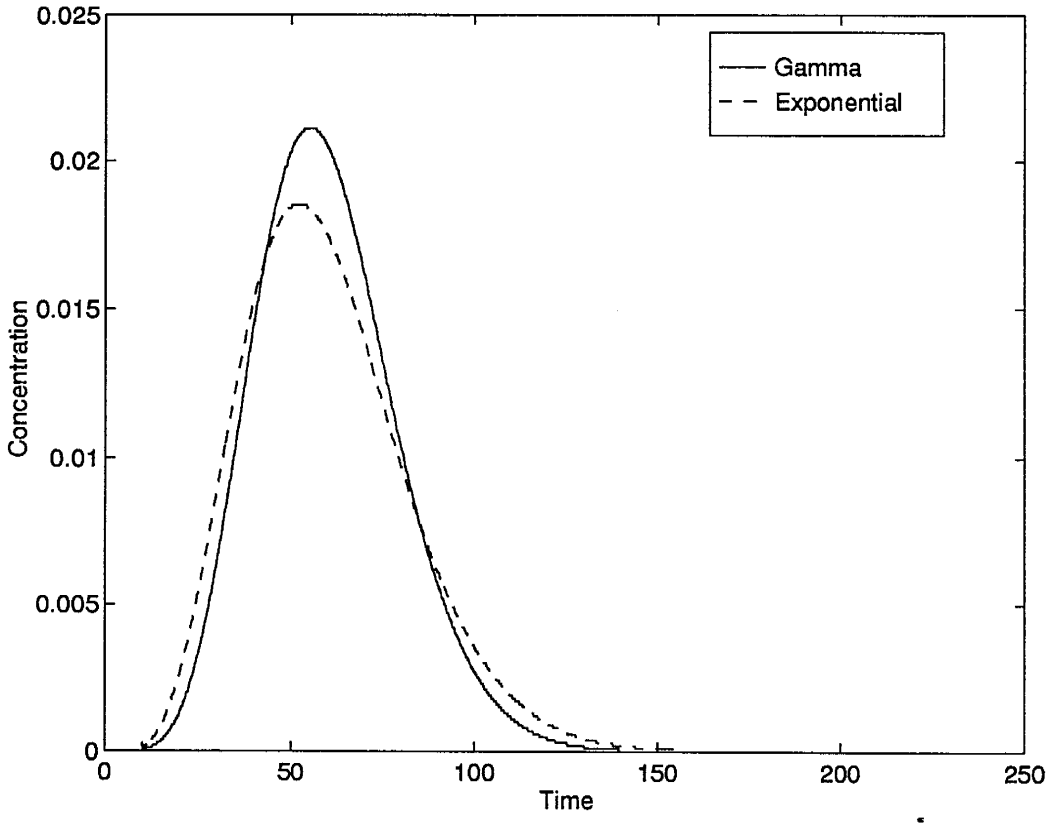

Figure 4.4: Breakthrough curves for a two-site gamma model compared to the single-site model for same mean k_f, k_r values. The variance of the gamma model is 12.5 compared to 25 for the exponential model.

4.5 Sensitivity Analysis

Our preliminary analysis shows that the the mean and the variance of the desorption time are the two parameters which effect the shape and the peak position. Both these parameters are lumped into one parameter, the coefficient of variation (CV) defined as

$$CV = \frac{(variance)^{1/2}}{mean} \tag{4.38}$$

For a hyperexponential random variable with the same mean as a corresponding exponential, the variance will exceed that of the exponential. For a gamma random variable with the same mean as an exponential the variance will be less than that of the exponential. Specifically the CV of a m stage gamma is given by

$$CV = \frac{1}{m^{1/2}} \tag{4.39}$$

The breakthrough curve for the hyperexponential model is sensitive to both the mean and the variance of the desorption time. However, in the cases above, the μ_i's for the desorption times for the individual sites were changing. In the next series of simulations, the values of μ_i are kept same and the α_i's are gradually changed to obtain different values of the CV (Table 4.2). The effect of the CV for the three-site hyperexponential model is clearly observed in Figure 4.5, when the CV is increased from 1.4 to 3.2 and the complete range of breakthrough curves is observed starting with a Gaussian shaped curve to one that shows a sharp peak followed by an extended tail. In the four simulation runs made (R1-R4) an increase in CV leads to non-equilibrium behavior as seen in the breakthrough curves.

Description	μ_1	μ_2	μ_3	α_1	α_2	α_3	Mean	Variance	C.V.
R1	5	0.1	0.5	0.3	0.6	0.1	6.26	81.64	1.44
R2	5	0.1	0.5	0.5	0.4	0.1	4.30	62.35	1.84
R3	5	0.1	0.5	0.6	0.3	0.1	3.32	49.83	2.13
R4	5	0.1	0.5	0.7	0.2	0.1	2.34	35.38	2.54

Table 4.2: Parameters to study the effect of varying CV for a three-site hyperexponential model.

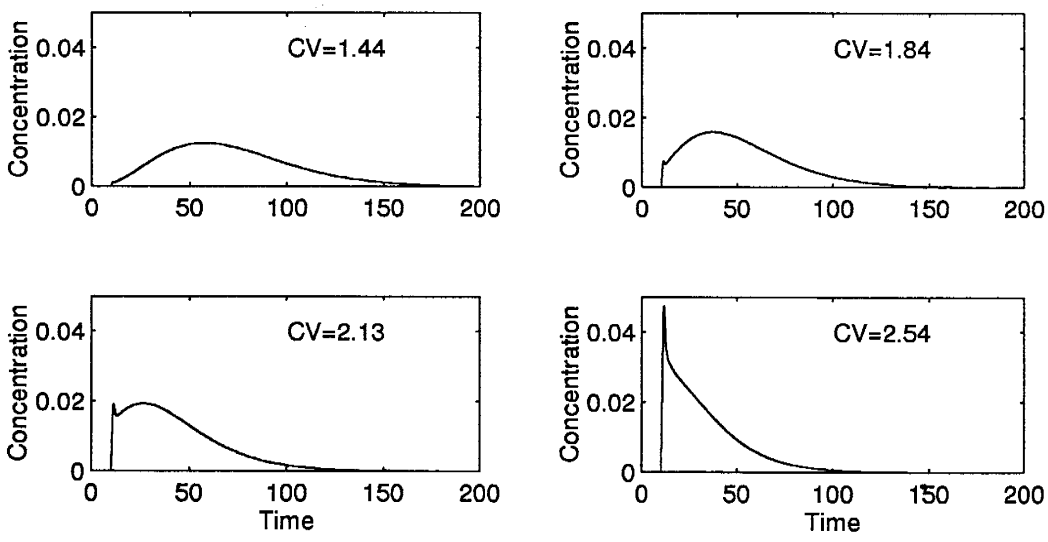

Figure 4.5: Breakthrough curves for the three-site hyperexponential model for CV ranging from 1.44 to 2.54.

4.6 Non-uniqueness Issue

We used the CV for the hyperexponential distribution to characterize the breakthrough curves. The three-site model has five independent parameters (three μ_i's and the two α_i's). There are various combinations of these parameters which would give same mean and variances and hence the same CV. However, the breakthrough curves may differ significantly between the various cases with the same CV as we show below.

First, we show the case where the mean desorption time is kept constant (a value of 6) but the variances differ to see whether different combinations of μ_i and α_i lead to significant differences in the breakthrough curve (Table 4.3). For a mean desorption time of 6 days, the curves in Figure 4.6 show that the individual rates are important. Three runs (CM1, CM2, and CM3) are presented with variances of 122, 79 and 78 respectively. Run CM1 which has the highest variance shows extended tailing. Also noticeable is the bimodal peak with the contribution of the fastest site (rate=5) and with the largest fraction of sites present (0.51).

Description	Rates	α_i	Mean	Variance	C.V.
CM1	5, .1, .05	.51, .39	6.002	122.02	1.84
CM2	5, .1, .5	.33, .57	5.996	79.23	1.49
CM3	5, .1, 1.0	.1, .57	6.05	78.06	1.46

Table 4.3: Parameters used to study the sensitivity of the breakthrough curves for a constant mean of a three-site hyperexponential model.

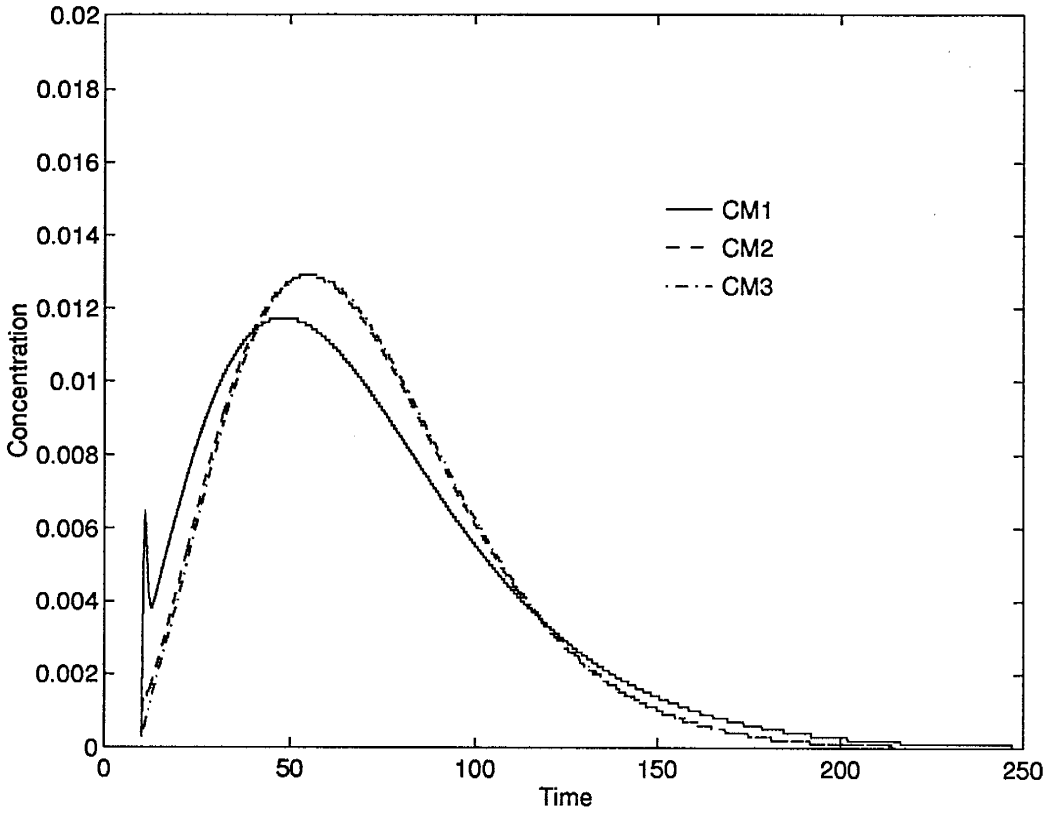

Figure 4.6: Breakthrough curves for the three-site hyperexponential model for same mean but different variances.

Cases CM2 and CM3 have very similar means (5.996 and 6.05) and similar variances (79 and 78) and show very similar breakthrough curves. The specific values of the μ_i's and α_i's are different in these two runs. One observation to be noted is that the rates in the two runs (CM2 and CM3) are varying over just one order of magnitude unlike case CM1 where the difference in the rates between the fastest and the slowest sites is two orders of magnitude.

The last case studied was one where both the means and variances were

constant to see if a large contrast in rates still contributes to significant differences in the breakthrough curves. Two runs (CONS1 and CONS2) are presented in Figure 4.7. The parameters for these two runs are given in Table 4.4. Both the runs have the same mean of 6 days and variances of around 122. However run CONS1 which has rates varying over two orders of magnitude (5 and 0.05) shows a bimodal behavior while the other run (CONS2) which has a maximum rate difference of a factor of 5 does not show the same behavior. This signifies that we need to consider the heterogeneity of sites explicitly in our models to be able to predict the breakthrough behavior.

Description	Rates	α_i	Mean	Variance	C.V.
CONS1	5, 0.1, 0.05	0.51, 0.39	6.002	122.02	1.84
CONS2	0.29, 0.04, 0.05	0.87, 0.08	6.001	124.69	1.86

Table 4.4: Parameters used to study the sensitivity of the breakthrough curves for constant mean and variance of a three-site hyperexponential model.

4.7 Discussion and Conclusions

Partitioning of nonionic organic compounds due to sorption between the aqueous and the solid phases has been observed to be incompletely reversible and to exhibit non-equilibrium behavior. Slow desorption behavior has been noted for several types of compounds, e.g. pesticides, phenols, halogenated aliphatic hydrocarbons, chlorinated benzenes, and polynuclear aromatic hydrocarbons [Pignatello, 1989, 1990].

We have shown that, for the case of sorbing molecules exhibiting a wide

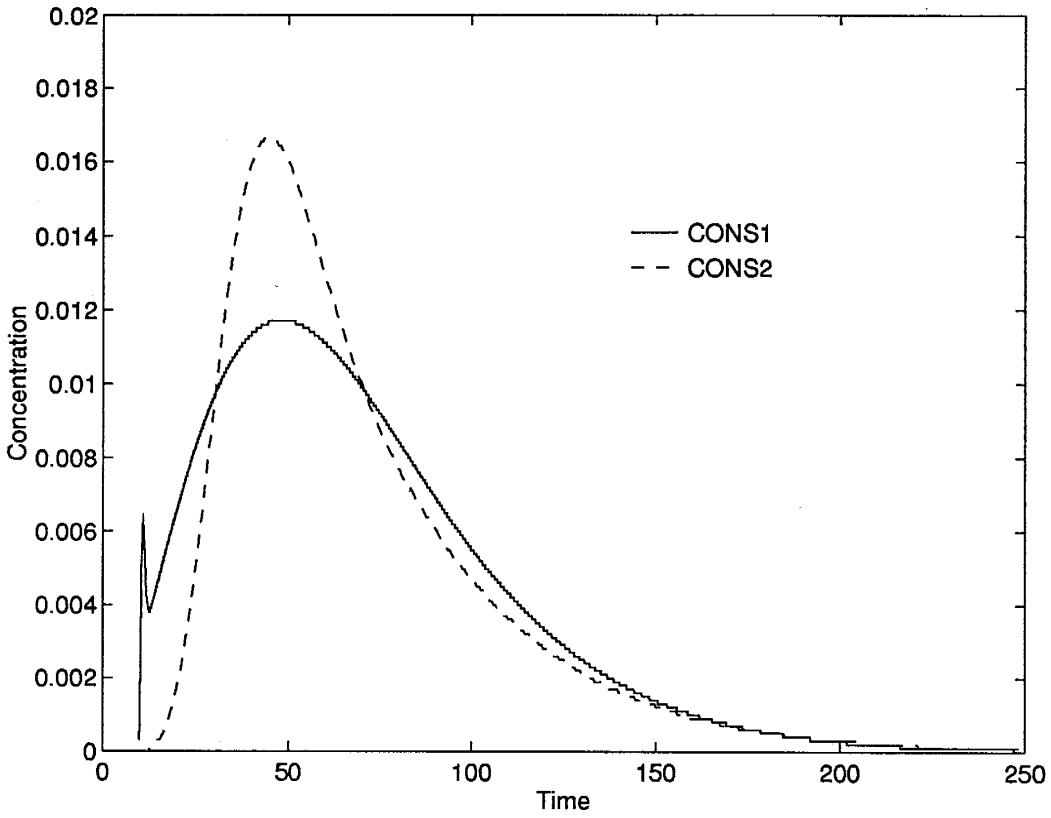

Figure 4.7: Breakthrough curves for the three-site hyperexponential model for same mean and variance.

range of desorption rates, that a semi-Markov model can be used to predict the breakthrough curves. The hyperexponential model presented for two and three sites shows that explicitly modeling the presence of different types of sorption sites can lead to a breakthrough curve which shows behavior similar to kinetically limited sorption models. This may also provide a model to account for heterogeneity of sites that are available for sorption. In addition, the effect of aging of the soils can be modeled by varying the proportion of different surfaces which are participating in the sorption processes. This model thus provides a very elementary but a mechanistically-based approach to study and model some of the time-dependent sorption phenomena observed for pesticides in soils.

We have studied the sensitivity of the breakthrough curves to the means and variances of the three-site hyperexponential model. While we were able to show the effect of CV on the breakthrough curve, the non-uniqueness of the parameters remained an issue. Our results indicate that a complete evaluation of all the specific sorption sites are required to be able to use the semi-Markov models, specifically when the multiple sorption sites have rates that vary over two to three orders of magnitude. For porus medium with similar rates of desorption, modeling in terms of CV may suffice.

Chapter 5

A Streamline Simulator For Field-Scale Transport

5.1 Overview

We present a two-dimensional field scale simulator for modeling transport of sorbing solutes characterized by linear kinetic rates of sorption and desorption. Our method involves applying a one-dimensional semi-analytical reactive transport solution along each streamline to account for a varying velocity field as well as spatially varying rates. This approach captures the tails on the breakthrough curve which is a major advantage when compared to other numerical methods used for modeling non-equilibrium transport. An application of the method to transport of PCE at a field similar to the Borden site experiment [Roberts et al., 1986] illustrates several important features about plume shape, particularly the highly heterogeneous and irregular pattern of the aqueous concentration distribution. We study (1) the effect of spatially varying sorption-desorption rates (k_f and k_r) and the mean rates (sensitivity of aqueous concentration distribution to mean rates varied over two orders of magnitude); (2) the effect of varying correlation between ln K_d and ln K; and (3) the effect of initial plume size. Sensitivity to the various parameters is studied by analyzing the first three spatial moments.

5.2 Introduction

In Chapter 1 we discussed the complexity of modeling the wide variety of interactions that occur at the rock-water interface. However, we are often interested in studying a particular process, e.g. transport of a sorbing solute under natural gradient conditions. We develop a simpler conceptual model of the problem and define the problem in a more precise mathematical form which (under various assumptions of the initial and boundary conditions) can be solved analytically or numerically. Groundwater flow and transport simulations are used for a number of purposes: as a modeling tool to study the various processes affecting the solute movement, as a calibration tool to obtain estimates of parameters such as dispersion coefficients, retardation factors, etc., in an inverse modeling sense, and perhaps most widely as a predictive tool for assessing alternative remediation designs.

These simulators involve discretization of the spatial domain of the study area and use finite-difference, finite elements, mixed boundary element, and other numerical schemes with the appropriate boundary and initial conditions (Anderson and Woessner [1992] and Zheng and Bennet [1996]). The starting point for all these models is the advection-dispersion equation defined for a representative elementary volume (REV) which is then solved numerically. We present an alternative scheme for modeling solute transport in a two-dimensional flow field based on the recursion formulation developed for one-dimensional flow presented in Chapter 3. In particular the focus is on developing a fast and efficient algorithm for modeling transport of a linearly sorbing solute undergoing kinetic sorption. The rates of adsorption and desorption, denoted by k_f and k_r, are spatially variable. We will use the Lagrangian approach in order to develop a field-scale simulator to study the interactions of a

linearly sorbing solute along a streamline.

5.3 Reactive Transport for a Linearly Sorbing Solute

The transport of organic solutes at the field scale has been investigated for several decades. Understanding the role of the various mechanisms and verification of the analytical results developed for a linearly sorbing solute at equilibrium conditions has been a major focus of these experiments. The results of a field experiment [Roberts et al., 1986] conducted at the Canadian Air Forces Base, Borden, Ontario, Canada (henceforth referred to as the Borden site) show that the retardation factor (R) for nonpolar organic solute increases with time (or displacement). The field results further indicate that the solute may incur enhanced spreading. The increase in the bulk retardation factor seen at the Borden site field is not observed in simple laboratory column experiments for solutes exhibiting linear equilibrium sorption.

The increase in the observed R with time has led to several diverse theories to explain this anamolous behavior. These can be briefly categorized as follows:

1. several types of rate-limited sorption may be the primary controlling mechanism including intra-particle mass transfer limitations [Goltz and Roberts, 1988, and Burr et al., 1994]; soil surface reaction kinetics [Burr et. al., 1994, Cvetkovic and Dagan, 1994, Ptacek and Gilham, 1992]; and a combination of the two above [Brusseau, 1992];

2. spatial variability of the soil sorption distribution coefficient (K_d) correlated with variations of the hydraulic conductivity [Burr et al., 1994] may lead to an increase in R with time.

Using the concept of immobile water, which is present in the microscopic fractures and dead ends of the solid phase, it has been postulated that intra-particle diffusion will be the controlling mechanism for a rate-limited sorption process [Roberts et al., 1986; Goltz and Roberts, 1986, 1988; Ball et al., 1990; Wood et al., 1990; Ball and Roberts, 1991]. Theoretical analyses by Kabala and Sposito [1991] showed that an increasingly negative cross correlation between spatially varying K and K_d can lead to an R increasing with time. However Dagan [1989] suggests that if the cross correlation between the two parameters is constant with time, then the bulk R is also a constant and its value is a function of the degree and type of cross correlation. Kabala and Sposito [1991] and Dagan [1989] showed that for a decaying solute undergoing first-order decay with spatially varying decay coefficient, the retardation factor can show a time-dependent behavior. Thus a number of possible mechanisms can contribute to the temporal behavior of R.

Increased dispersion, especially in the direction of the mean groundwater flow for a reactive solute, based on another field experiment conducted at Cape Cod Site [LeBlanc et al., 1991], was larger than that of a non-reactive solute after the plumes in both the cases have traveled an equivalent distance [Garabedian, 1987]. The cause of this enhanced dispersion is attributed to the spatial variability of the solute velocity and the interaction with the heterogeneous sorption parameter fields [Hu et al., 1995]. A number of results based on stochastic-analytic techniques have been developed to relate macrodispersion to field scale flow, based on simple linear correlation between the spatially variable hydraulic conductivity and retardation factor (R) or distribution coefficient (K_d). Numerical evaluation of these theories have been done in studies conducted by Graham and McLaughlin [1989a], Quinodoz and Valocchi [1990], and Bellin et al. [1992] in two-dimensions and by Robin [1991] and

Burr et al. [1994] in three dimensions.

In the previous chapters we developed a recursion formulation for the transport of a sorbing solute with spatially varying rates. This formulation is used to extend the semi-analytical solution developed in one-dimension to a two-dimensional problem.

5.4 Development of a Streamline Simulator

We present a streamline-based algorithm to model reactive transport where the spatial heterogeneity of both the hydraulic conductivity field and the sorption parameters are incorporated. This work extends the results of Burr et al., [1994] where the kinetic sorption rates were constant. The use of streamlines to model areal flow has been quite prevalent in hydrology [Daus and Frind, 1985; Burnett and Frind, 1987; Matanga, 1988, 1993, 1996] and petroleum engineering [Martin and Wegner, 1979; Lake et al., 1981; Hewett and Behrens, 1991]. These models have been applied to water-flooding and miscible displacements in two and three dimensions [Thiele et al., 1996].

The advantages of using the streamline approach are

1. there is no restriction on the time-step size as is the case with finite-difference simulators which must be dictated by Courant number; and

2. grid orientation effects are minimized.

The governing flow equations used to define the streamfunctions are first developed. The procedure for defining streamlines based on the streamfunction is

then described. The recursion formulation which describes the transport of kinetically limited sorbing solute is presented after that and is used to obtain the plume position at different times for a setting similar to the Borden site. The different spatial moment estimators are obtained from the concentration field and these moments are used for comparisons with the field data, other theoretical results and for studying field-scale migration of the sorbing plume.

5.4.1 Flow Problem

The governing flow equation for steady-state fluid flow in a saturated, rigid two-dimensional porous media is given by

$$\sum_{i=1}^{2} \frac{\partial}{\partial x_i} q_i(x) = 0 \tag{5.1}$$

where $\mathbf{x}$ is the spatial coordinate vector $\mathbf{x}=(x_1,\ x_2)$. The flow field considered is a two dimensional system with prescribed heads on the two sides and no-flux on the other two sides.

For a two-dimensional field with steady-state conditions, we can define a streamline to be the curve everywhere tangent to the velocity field. This can be expressed using the cross product of the specific discharge ($\mathbf{q}$) and an incremental distance ($\mathbf{dr}$) as

$$\mathbf{q} \times d\mathbf{r} = 0 \tag{5.2}$$

In two dimensions this implies

$$q_y dx - q_x dy = 0 \tag{5.3}$$

The streamlines can be computed directly by means of streamfunctions. Plots of streamlines and equipotential lines are called flownets and are used in calculating flux through the system. This method assumes no distributed sources or sinks. Two adjacent streamlines form a streamtube; for steady-state flow, the flux through the streamtube is constant. Flownets for anisotropic and heterogeneous media may be constructed more easily by generating equipotential lines and streamlines numerically. We briefly outline the numerical procedure used to generate these two functions.

The streamfunction is analogous to the equipotential function and is obtained from equation 5.3 by noting that

$$d\psi = \frac{\partial \psi}{\partial x} dx + \frac{\partial \psi}{\partial y} dy \tag{5.4}$$

$$q_x = -\frac{\partial \psi}{\partial y} \tag{5.5}$$

$$q_y = \frac{\partial \psi}{\partial x} \tag{5.6}$$

The units of the streamfunction are L^2/T. A streamtube is the region between two adjacent streamlines with streamfunction values ψ and $\psi + \Delta\psi$ (the flux through the streamtube is equal to $\Delta\psi$). We can solve for the streamfunctions directly by writing [Bear, 1972]

$$\nabla \times \mathbf{q}/\mathbf{K} = 0 \tag{5.7}$$

and substituting for $\mathbf{q}$ from equation 5.3 to give

$$\frac{\partial}{\partial x}\left(\frac{1}{K_y}\frac{\partial \psi}{\partial x}\right) + \frac{\partial}{\partial y}\left(\frac{1}{K_x}\frac{\partial \psi}{\partial y}\right) = 0 \tag{5.8}$$

The above equation is similar in form to the governing equation for two- dimensional steady-state flow with hydraulic head as the dependent variable:

$$\frac{\partial}{\partial x}(K_x\frac{\partial h}{\partial x}) + \frac{\partial}{\partial y}(K_y\frac{\partial h}{\partial y}) = 0 \tag{5.9}$$

The similar forms of equation 5.8 and equation 5.9 allows us to use standard finite-difference flow codes to solve for h to calculate streamfunctions by replacing K_x with $1/K_y$ and K_y with $1/K_x$ and some modifications to the boundary conditions [see Bramlet and Borden, 1990 and Fogg and Senger, 1985 for details].

The streamfunction field is contoured to give the position of the paths along which a solute particle injected at the upstream end will move through the field. Fluxes in streamtubes are calculated directly from the streamfunction solution. The linear velocity can also be calculated from the streamfunction solution as follows:

$$v = \frac{\Delta\psi}{n_e \Delta s} \tag{5.10}$$

where n_e is the effective porosity and Δs is the distance between two streamlines. These velocities are the inputs for the solute transport model, in which the recursion formulation is applied along different streamlines.

5.4.2 Outline of the Algorithm

For the cases examined here the conductivity, $\mathbf{K(x)}$ and the rates $k_f(\mathbf{x})$ and $k_r(\mathbf{x})$ are considered to be random fields. In the simulations these are generated as log-normal random fields with a prescribed mean and a given covariance structure with a Fast Fourier Transform method [Gutjahr, 1989].

A brief description of the different steps of the simulation follow.

1. We generate a hydraulic conductivity or transmissivity field using a random field generator.

2. We solve equation 5.8 using a finite-difference formulation as outlined above.

3. The next step is to model the transport of solutes that undergo kinetically limited linear sorption. We solve the recursion formulation along each streamline to get the breakthrough curves.

$$P^{(1)}_{n,k} = r_{11}(n)\, P^{(1)}_{n-1,k-1} + (1 - r_{11}(n))\, P^{(2)}_{n,k-1} \tag{5.11}$$

$$P^{(2)}_{n,k} = r_{22}(n)\, P^{(2)}_{n,k-1} + (1 - r_{22}(n))\, P^{(1)}_{n-1,k-1} \tag{5.12}$$

   The symbols have the same meaning as discussed in Chapter 3. The one-dimensional transport solution for the adsorbing solute is applied to each of the streamlines to obtain the concentration distribution at any given time for each of the streamlines.

4. Each streamtube is bounded by two adjacent streamlines. The flux of water through any streamtube section is determined by the difference in the values of the two streamfunctions difference in the two values of the streamfunctions. The streamtube velocity is calculated at each position where the the concentration is to be evaluated by the recursion formulation. The recursion formulation gives a variable velocity simulation in each tube, assuming a uniform cross-sectional area. The variation in the cross-sectional area along a streamtube is shown schematically in Figure 5.1. The concentration obtained from the recursion formulation is weighted by the product of velocity and cross-sectional area at each location. This weighting takes into account the variable cross-sectional area.

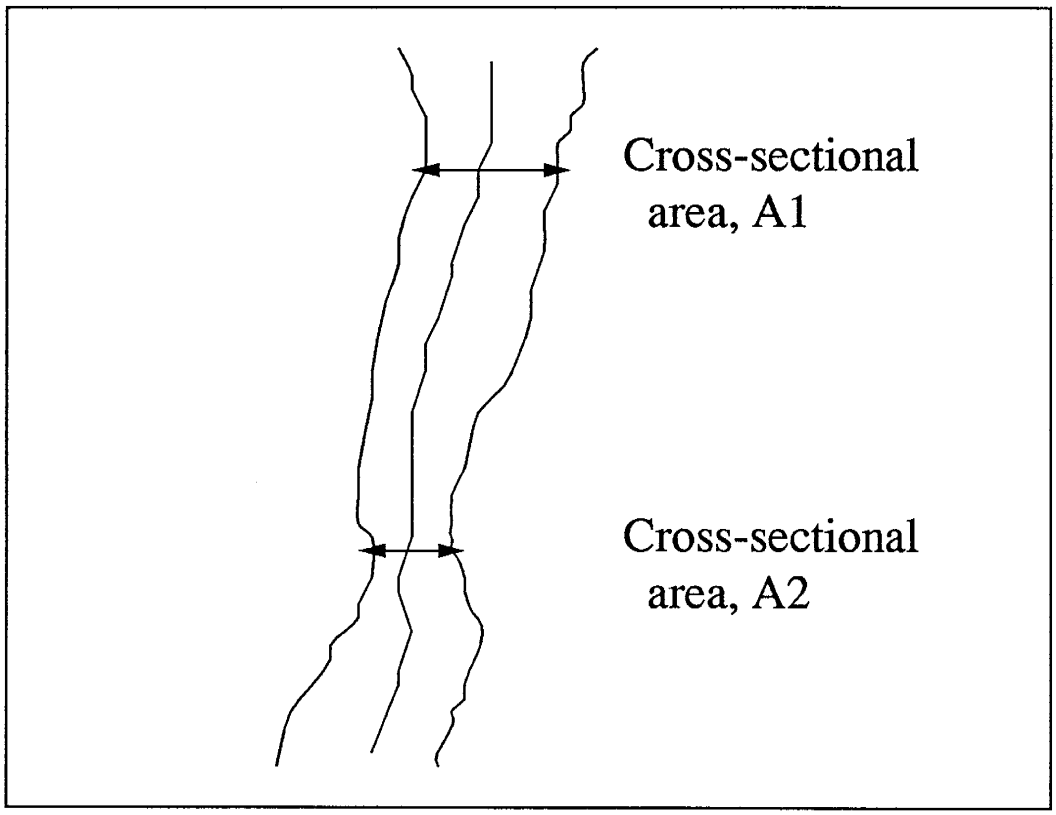

Figure 5.1: Schematic representation of a streamline within a streamtube.

5. The concentration distribution is contoured across the flow domain to give the plume position at the given time.

6. The various spatial moments are evaluated as discussed in a later section.

This algorithm is applied to a field-scale test conducted at the Borden site [Mackay et al, 1986; Freyberg, 1986; Roberts et al., 1986; Curtis et al, 1986; Sudicky, 1986] where detailed spatial monitoring of reactive and non-reactive solutes was conducted over a period of more than two years as mentioned above. One of the main features evident in the field data is the increase of the bulk retardation factor (R) with time.

5.4.3 Description of the Flow Field

We consider a steady state two-dimensional flow field governed by the flow equation 5.1. The hydraulic conductivity field is assumed to be a heterogeneous field with a prescribed covariance structure. We use an exponential covariance function given by

$$C_f(\mathbf{h}) = \sigma_f^2 \, exp[-(\frac{h_1^2}{\lambda_1^2} + \frac{h_2^2}{\lambda_2^2})^{1/2}] \tag{5.13}$$

where h_1, h_2 are the lags in the x_1, x_2 directions, λ_1, λ_2 are the correlation length scales of ln[K(**x**)], and σ_f^2 is the variance of ln[K(**x**)]. We assume that the field is isotropic with $\lambda_1 = \lambda_2 = 5.2$ m, $\sigma_f^2 = 0.29$ and a geometric mean of **K** equal to 6.182 m/d. These values are similar to those reported by Woodbury and Sudicky [1991] and were used by Burr et al. [1994] in their three-dimensional simulations.

Five realizations of spatially correlated random log hydraulic conductivity fields using the FFT algorithm [Gutjahr, 1989] were generated (Table 5.1). The field

generated has 128x128 nodes with a grid spacing of 56 cm in both the directions and approximately 10 points per correlation length for a square field of 14 correlation lengths. One such realization of the ln[K(x)] field is shown in Figure 5.2. The x_1 axis is aligned with the mean flow direction while x_2 is horizontally transverse to it. A fixed hydraulic head of 30.8224 cm on one end and 0 at the other end was imposed to produce an average hydraulic gradient of 0.0043 in the x_1 direction while the other two boundaries were no-flow boundaries.

Description	Value	Remarks
Covariance	Exponential	Isotropic
Variance	0.29	σ_f^2
Mean K	6.182 m/day	Geometric Mean
Corr. Length	5.2 m	$\lambda_1 = \lambda_2$
Field Size	128 x 128	approx. 14 corr. lengths
Grid Spacing	56 cm	$\Delta x = \Delta y$
Fixed Head	30.8224 and 0 cm	Hydraulic Gradient=0.0043
Mean velocity	0.089 m/day	Orientation y direction

Table 5.1: Flow Field Simulation Parameters

The random field generated was used as the input to a finite-difference flow simulator that calculated the head field as well as the streamfunctions solution. Figure 5.3 shows the streamfunctions solution corresponding to the hydraulic conductivity field shown in Figure 5.2.

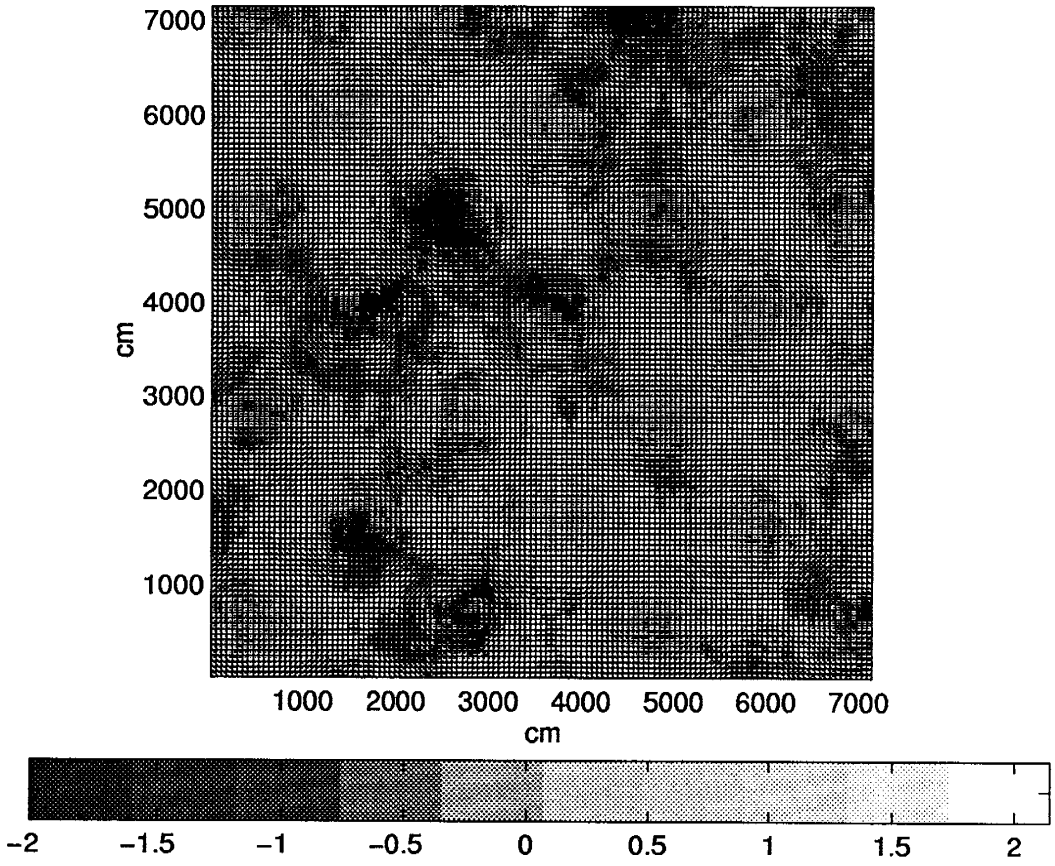

Figure 5.2: Perturbations of the hydraulic conductivity field (f) generated as a log-normal field with E(f)=0 by FFT method (Table 5.1).

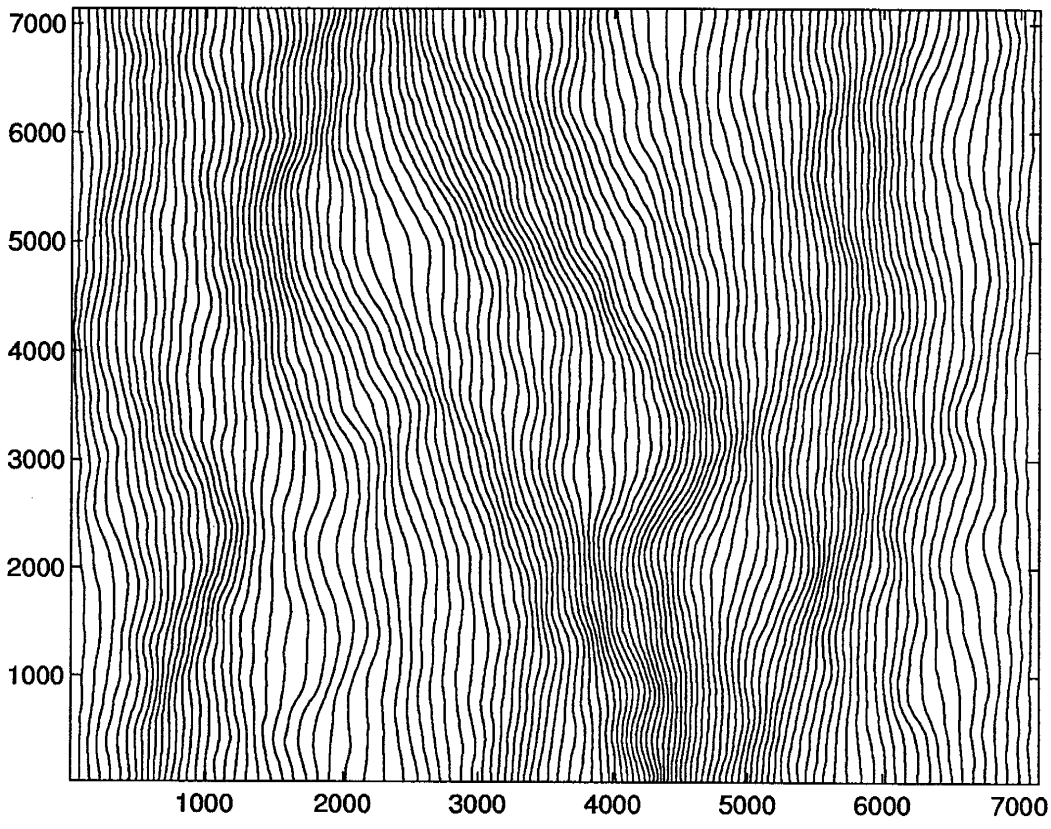

Figure 5.3: Streamlines corresponding to the K field given in Figure 5.2. The spacing between the streamlines= 0.0279 m^2/day.

5.4.4 Modeling Reactive Transport

The streamlines obtained from the steady-state solution to the flow problem determine the paths taken by the solute particles through the flow domain. Our approach is to use these streamlines to obtain the concentration distribution at any given time. The one-dimensional solution for kinetically limited sorption-desorption where the rates are spatially varying was developed in Chapter 3.

The concentration profile along each streamline is obtained for a given time using the algorithm outlined above. If we look at the streamline positions in Figure 5.3, we see that the streamlines converge in regions of high conductivity and diverge in areas where the conductivity is low. We take into account the varying fluxes across different regions by assuming the boundaries of two adjacent streamlines form a streamtube with varying cross-section and the flux is calculated by the product of velocity and the cross-sectional area, both of which vary with position. Accounting for this varying flux allows the model to preserve mass.

For the example considered here, we investigate the movement of a PCE plume as it is advected by the groundwater. In particular we focus our attention on the following:

1. The effect of rates of sorption and desorption;
2. The effect of different correlation between ln K and ln K_d, e.g. perfect correlation, either positive or negative, or partial correlation.
3. The effect of initial plume size.

The tools that we employ for studying these various factors and parameters are the spatial moments of concentrations. The first, second and third spatial moments of

the plume concentration are examined as they change temporally and compared with results based on field observations.

5.4.5 Transport Simulation Parameters

In the initial set of runs, ln K and ln K_d are independent of each other, although both vary spatially with prescribed covariance functions. Spatial variability of K_d has been observed in the field; however, the nature of correlation between K and K_d is still a matter of debate. In later runs the ln K_d's are generated with various degrees of correlation with ln K; the kinetically limited case where K_d is considered to be split up into two independent processes k_f and k_r with either equal or unequal variances is also treated. The input variance of ln $[K_d]$ was chosen to be 0.52, the input geometric mean of K_d was 0.526 mL/g, and the correlation length scale for spatially varying K_d was 5.2 m, equal to that of the ln K field. Tables 5.2 and 5.3 give details of all the various simulation runs with the values of the different parameters used.

For the non-equilibrium case, the desorption rate, k_r was obtained by using the empirical relationship between K_d and k_r developed by Brusseau and Rao [1989b] for a broad spectrum of nonpolar hydrophobic organic chemicals exhibiting non-equilibrium sorption on various natural sorbents:

$$log\ k_r \;=\; 0.301 - 0.668\ log\ K_d \tag{5.14}$$

These values are similar to those used by Burr et al. [1994] in their simulation of the Borden aquifer. However, unlike their simulations which are based on a constant value of kinetic rate parameter, we allow for spatial variability of the k_f

and k_r. We include one case in which the rates are kept constant [case CONS in Table 5.2]. The simulations were run for 650 days, the time period during which field observations were made, so that the results could be compared to data from the tracer test. For each realization, the spatial moments (Appendix D) are obtained from numerically simulated aqueous concentration. The plume dispersion is calculated for each realization with respect to the centroid of the plume for that realization.

Case	Mean k_f 1/day	Mean k_r 1/day	Variance k_f, k_r	Source Size (m)
CONS	2.412	0.67	-	6.0
FAST	2.412	0.67	0.26, 0.26	6.0
SLOW	0.2412	0.067	0.26, 0.26	6.0
DVAR	2.412	0.67	0.13, 0.39	6.0
LRGS	2.412	0.67	0.26, 0.26	10.5
SMLS	2.412	0.67	0.26, 0.26	2.5

Table 5.2: Parameters for (a) varying rates and (b) varying source sizes. The rates are generated as log-normal random variables with an exponential correlation structure, and correlation length of 5.2 m. The spatially varying rates are two individual SRFs, each independent of ln K and of each other.

The k_f and k_r fields were generated as a log-normal field with an exponential correlation structure of correlation length 5.2 m. For the case where ln K and ln K_d

Case	Mean K_d	Variance	Corr. ρ	Source Size (m)
KDSRF	-0.6425	0.52	0	6.0
NCOR1	-0.6425	0.52	-1	6.0
NCRP5	-0.6425	0.52	-0.5	6.0
PCOR1	-0.6425	0.52	1	6.0
PCRP5	-0.6425	0.52	0.5	6.0

Table 5.3: Parameters for varying correlation between ln K and ln K_d.

are correlated, the model used is

$$ln\, K_d \;=\; a\, lnK + b \tag{5.15}$$

The values of a and b are obtained by using the appropriate means and variances of ln K and ln K_d. The mean of ln K used is -4.83 and variance of ln K is 0.29. The mean of ln K_d used is -0.6425 and a variance of ln K_d of 0.52 (Table 5.3). These are the values also used by Burr et al. [1994] in their simulations.

5.5 Modeling PCE Plume Migration

We would like to emphasize that all the parameters used for the simulation runs are obtained from previous studies [Roberts et al., 1986; Woobury and Sudicky, 1991; Burr et al., 1994]. The only difference (which we will show is significant) is the spatial variability of the sorption-desorption rates.

The base case for all simulations is the case where the k_f and k_r fields are generated as two separate parameters and is referred to as case FAST in Table 5.2. The rates are fast enough so that equilibrium conditions are approached. In this case the sorption and desorption rates are generated as two independent processes with an exponential correlation structure of correlation length 5.2 m each with a variance of 0.26. By independence the variance of ln K_d is then 0.52 [Burr et al., 1994].

For each realization of the K field, the flow field was solved and the plume position evaluated at 15, 30, 85, 250, 400, and 650 days. The plume position at 250 days is given in Figure 5.4. The model parameters for this simulation correspond to case FAST. The following are some interesting features of the aqueous concentration distribution observed in Figure 5.4:

1. The aqueous concentration distribution shows an irregular pattern.

2. The peak concentration does not correspond to the center of the plume. The centroid co-ordinates at time equal to 250 days are 5.36 m along the flow direction and 3.71 m in the transverse direction.

3. The highly irregular pattern of concentration distribution with a number of local maxima or "hot spots" is similar to the spatial distribution observed in the Borden field and elsewhere [Roberts et al., 1986; LeBlanc et al., 1991].

4. The simulation results which represent individual realizations are a better representation of the subsurface concentration than other methods which predict the mean concentration [Hu et al., 1997].

While a study of the individual realizations provides information about the interactions between the spatially varying rates and the velocity field, we can also

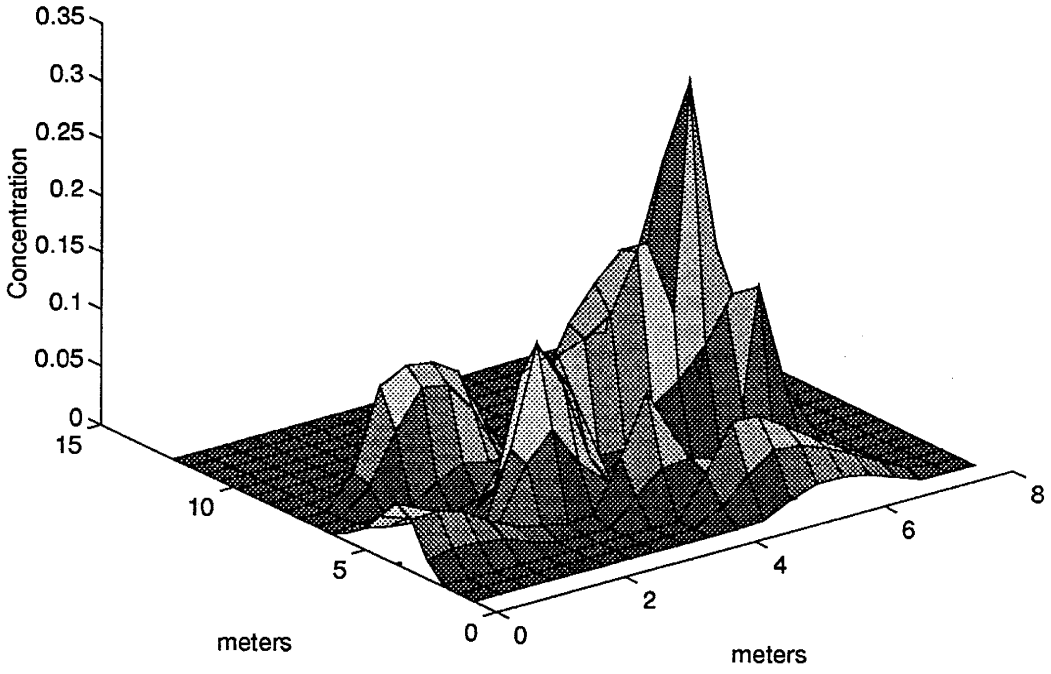

Figure 5.4: Aqueous concentration distribution for the PCE plume for case FAST after 250 days, realization number 5.

study the various spatial moments that provide summary statistics for the plume. The spatial moments are also a useful bulk measure of transport phenomena. Another motivation for calculating the various spatial moments is that most of the stochastic analysis results are in the form of expressions for the various moments and a comparison of the spatial moments computed from the numerical simulations with the analytical results provides a means to test the assumptions and the simplifications used in the stochastic analysis. It should be noted that in the discussions below, the spatial moment results are the averages of five realizations.

Details of the spatial moments analysis developed by Dagan and Cvetkovic [1993] using a Lagrangian approach are presented in Appendix F. Their analysis assumed a constant K_d. An alternative derivation for the first three spatial moments is presented in Appendix F. We note the equivalence in the definition of γ from Dagan and Cvetkovic [1993] with $P_{n,k}^{(1)}$ of our recursion formulation. Both of these terms give the spatial distribution of a linearly sorbing solute along a streamline at a given time. While the expression for γ is evaluated for constant rates, we can generalize the results for the spatially varying rates by replacing γ with $P_{n,k}^{(1)}$ and evaluating the Γ_i, $i = 0, 1, 2$ (see Appendix F for an explanation of the term) to obtain the various moments.

In this work we evaluated the first three spatial moments and used the results to study

1. The displacement of the centroid with time. The first moment results are also used to calculate the retardation factor of the bulk plume.

2. The second moment or the spread of the plume. In particular we look at the longitudinal second moment.

3. The third moment which is used to evaluate the skewness coefficient of the plume.

5.6 Analysis of Centroid Displacement

The bulk velocity of a reactive plume and hence its displacement, is less than that for a non-reactive solute because the solute partitions onto the solid phase of the aquifer material. This reduction of the reactive solute plume displacement is referred to as retardation. Much interest has focused on the apparent time dependence of the retardation factor of the reactive solutes as seen in the field-scale experiment performed at the Borden site [Roberts et al., 1986]. We will examine some of the scenarios discussed earlier and study the temporal behavior of R.

The simulated plume centroid, X_1 is plotted in Figure 5.5 and compared to the first moment estimated by Roberts et al. [1986] from the field data. The fit is remarkable, especially since the parameters used for the simulation (case FAST) were based on previous studies and not adjusted. In this and some of the following plots we also show the predicted behavior for the case of constant rates (CONST, see Table 5.2), as a control.

An interesting feature observed for PCE simulation is an overall slowing down of the bulk plume displacement with time, due to a slight decrease in the bulk solute velocity. In contrast, some analytical results based on Eulerian and Lagrangian analyses that assume constant K_d but spatially varying velocities are not able to predict the field-scale based time-dependent behavior [Dagan and Cvetkovic, 1993, Hu et al., 1995]. It may be noted that recently some work done by Miralles-Wilhelm and Gelhar [1996] and Rajaram [1997] showed time-dependent behavior for R. The ana-

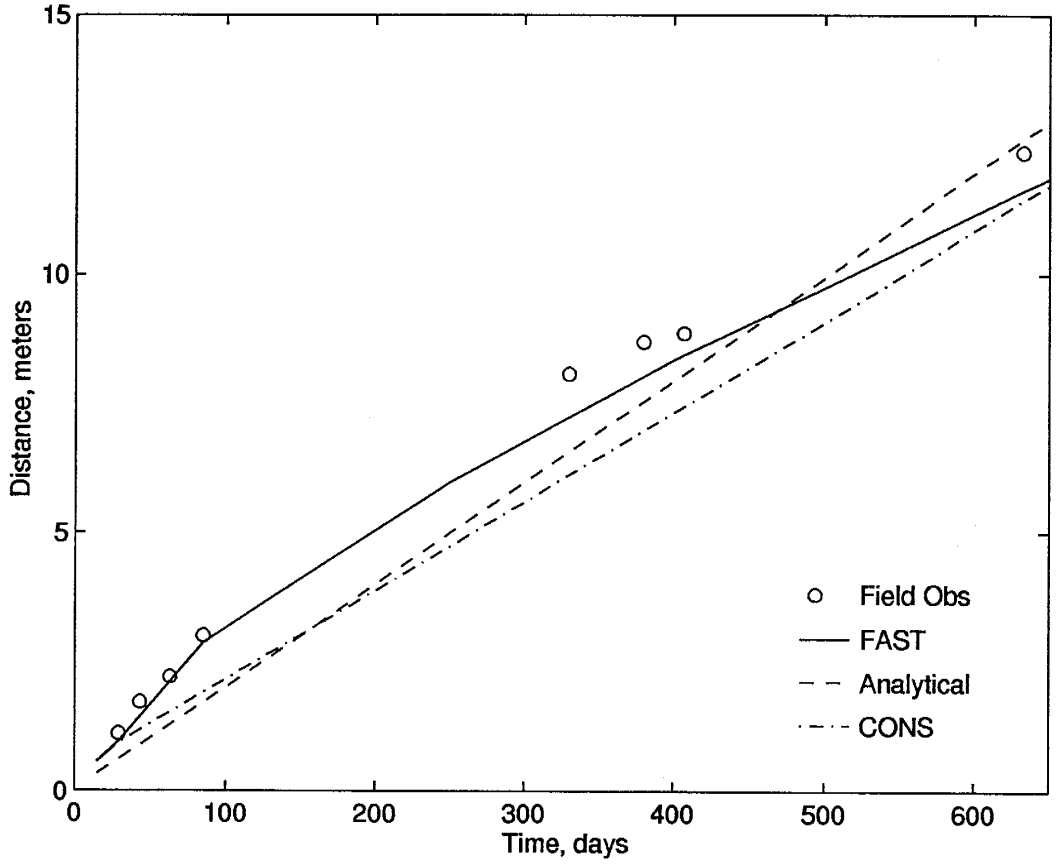

Figure 5.5: Position of the centroid of the plume. The analytical solution corresponds to results of Dagan and Cvetkovic [1993]. The field-based estimates of the first moment are obtained from Roberts et al. [1986].

lytical results [Dagan and Cvetkovic, 1993] for the same parameters are also shown in Figure 5.5 and show that the assumption of constant K_d does not accurately capture all the subtleties of the time-dependent behavior of the centroid displacement. Burr et al. [1994] and Hu et al. [1995] both have postulated the presence of an "undefined nonlinear time dependency" and "possible non-linear interactions between the spatially varying velocity field and the kinetically limited rates" to explain the time dependency observed in the field. Explicit modeling of the sorption and desorption rates would appear to provide a very good description of the phenomena controlling the contaminant transport. This is a relatively simple explanation in contrast to the postulation of the more complex non-linear time dependence discussed above.

It should be noted that Burr et al. [1994] performed a series of simulations based upon a three-dimensional form of the advection dispersion equation incorporating the multiprocess nonequilibrium (MPNE) model [Bruesseau et al., 1989; Therrien et al., 1990]. They studied two different forms of first-order mass transfer reactions:

1. Inclusion of a mass transfer coefficient representing solute diffusion between the mobile and immobile fluid zones, and

2. A first-order kinetic reaction reaction rate.

In above studies [Burr et al., 1994], both these parameters were kept constant. For their studies the results for centroid displacement showed that the process of intra-particle diffusion caused very little change to the time displacement curve for the duration of the simulation experiment.

5.7 Analysis of Retardation Factor

The study of time-varying R was motivated by the conclusions reached by Burr et al. [1994] who found that the early time R is the harmonic mean of the spatially varying R into which the initial plume is injected. At later time, after the plume has grown in size to encompass several horizontal length scales, the ensemble mean R is closer to the arithmetic mean R. This is the bulk estimate suggested by Garabedian [1987] based on his stochastic-analytic treatment of the linear equilibrium sorptive transport problem. However, Dagan [1989] found that the bulk R can differ from arithmetic mean if linear cross correlation between the local R and ln K is included.

The centroid displacement is a measure of the bulk plume movement and is used to calculate the retardation factor (see Burr et al., 1994 for an alternative definition of R in terms of the mean velocity of the reactive and non-reactive solutes). In our simulations, the nonreactive tracer is assumed to be moving at a constant velocity of 0.089 m/day based on observation of the chloride and bromide plumes [Roberts et al., 1986]. We next report R values for the various runs discussed in Table 5.2 and 5.3.

Varying Rates

As discussed above, the simple equilibrium model with spatially varying k_f and k_r gives a good description of the centroid position and the resulting retardation factor. In Figure 5.6 we present additional results showing the sensitivity of R to hypotheses about the k_f and k_r processes:

1. Case FAST : Equilibrium conditions (shown above).

2. Case DVAR: The variance of k_r is higher than that of k_f. The total variance of ln K_d was split into one-third and two-thirds for ln k_f and ln k_r, respectively. This simulation was motivated by our one-dimensional simulation studies where the BTC was shown to be sensitive to the variance of k_r.

3. Case SLOW : In order to study the effect of kinetically limited sorption, mean k_f and k_r were reduced below the values used in case FAST. For slow sorption the mean rates were 0.246/day and 0.067/day with variances of 0.26 each.

All three cases (Figure 5.6), show the retardation factor R increasing with time. The FAST case most closely matches the retardation estimates based on field observations. The plots in the figure are for averages of the retardation calculated for each of five realizations and are based on travel distances. The same behavior was observed in each of the individual realizations. This result stands in contrast of Burr et al.'s [1994] results, which show erratic behavior from realization to realization. Even their ensemble behavior showed only a very mild increase in R unlike the field observations where R increased from about 3 to 6 over a 650 day period.

The case of spatially varying rates with unequal variance (DVAR) shows that R changes with time and is similar to the trend of the field observations. The slower rates of sorption-desorption (SLOW) lead to R changing much more slowly. Similar results were also observed by Burr et al. [1994] but they only reported centroid displacement with time for a case where k_r=0.001/day. A fourth simulation where the rates were reduced still further (k_r=0.0067 /day) was also studied. However the results of this run were similar to SLOW and so are not reported here. Both slow rate cases showed a much smaller change in R. It did not reach an asymptote even after 650 days (Figure 5.6).

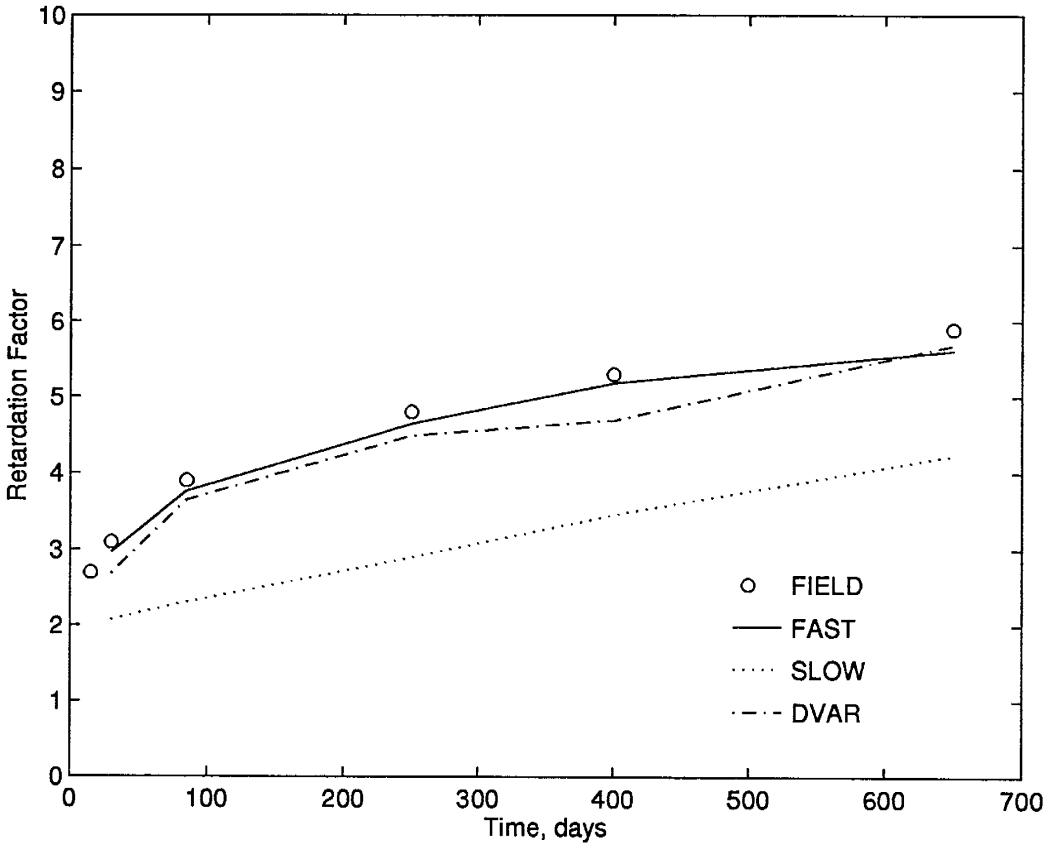

Figure 5.6: Retardation factor for the case of spatially varying rates.

Varying Correlation Between K and K_d

Cross-correlation of K and K_d has been invoked in a number of studies involving reactive transport of a sorbing solute [Kabala and Sposito, 1991, Dagan, 1989]. Burr et al. [1994] used a perfect negative cross-correlation between ln K and ln K_d for their detailed three-dimensional simulations of PCE plume. We also ran a series of simulations where different cross-correlations were assumed between ln K and ln K_d (Table 5.3). These cases are

1. Case KDSRF: ρ(Ln K_d, Ln K) = 0.
2. Case NCOR1: ρ(Ln K_d, Ln K) = -1.0.
3. Case NCRP5: ρ(Ln K_d, Ln K) = -0.5.
4. Case PCOR1: ρ(Ln K_d, Ln K) = 1.0.
5. Case PCRP5: ρ(Ln K_d, Ln K) = 0.5.

The case KDSRF assumes that the ln K and ln K_d fields are not correlated with each other. However, we would like to point out that this case is different from case FAST, SLOW or DVAR with respect to the procedure for obtaining the sorption and desorption rates. In the case of KDSRF, the K_d field is generated as a log-normal field with a given mean and an exponential correlation structure from which the rates are obtained using the relationship given in equation 5.14. This is slightly different from the other cases where the two rates are generated independently of each other (see Chapter 3 for additional discussion). In the case of KDSRF, the rates are negatively correlated as shown below.

$$log\ K_d \;=\; log\ k_f - log\ k_r \tag{5.16}$$

$$log\ K_d = -1.409\ log\ k_r + 0.4506 \quad (5.17)$$

$$log\ k_f = log\ K_d + log\ k_r \quad (5.18)$$

$$= -1.409\ log\ k_r + 0.4506 + log\ k_r \quad (5.19)$$

$$= -0.409\ log\ k_r + 0.45 \quad (5.20)$$

Sorption parameters that are spatially varying but not strongly correlated to hydraulic conductivity have been independently confirmed in the field study of Robin et al. [1991] who found either a weak negative correlation or no correlation between ln K and ln K_d for strontium for the Borden site. Comparison of R from the runs where different correlations between ln K and ln K_d were postulated showed that the perfectly negative correlation (NCOR) and negative correlation of 0.5 (NCRP5) provided a bound to the time varying R (Figure 5.7). The case where ln K_d was generated as an independent random field (KDSRF) is also presented. These observations based on matching R with time show that modeling K_d as an independent process uncorrelated with K is an adequate assumption for these simulations. However, none of these simulations provided as good a fit to the observed field data as the FAST case where the rates were generated as two independent spatially varying fields. The positive correlation cases (PCOR1 and PCRP5) both did not show a good match with the data and are presented in Appendix E.

Effect of Source Size

The next series of simulations were run to study the effect of the source size on the bulk retardation factor. Three different runs are discussed below:

1. Case FAST where the source size is 6 m, the same as used in the Borden field site study, and about the same correlation length used for ln K, ln k_f and ln k_r.

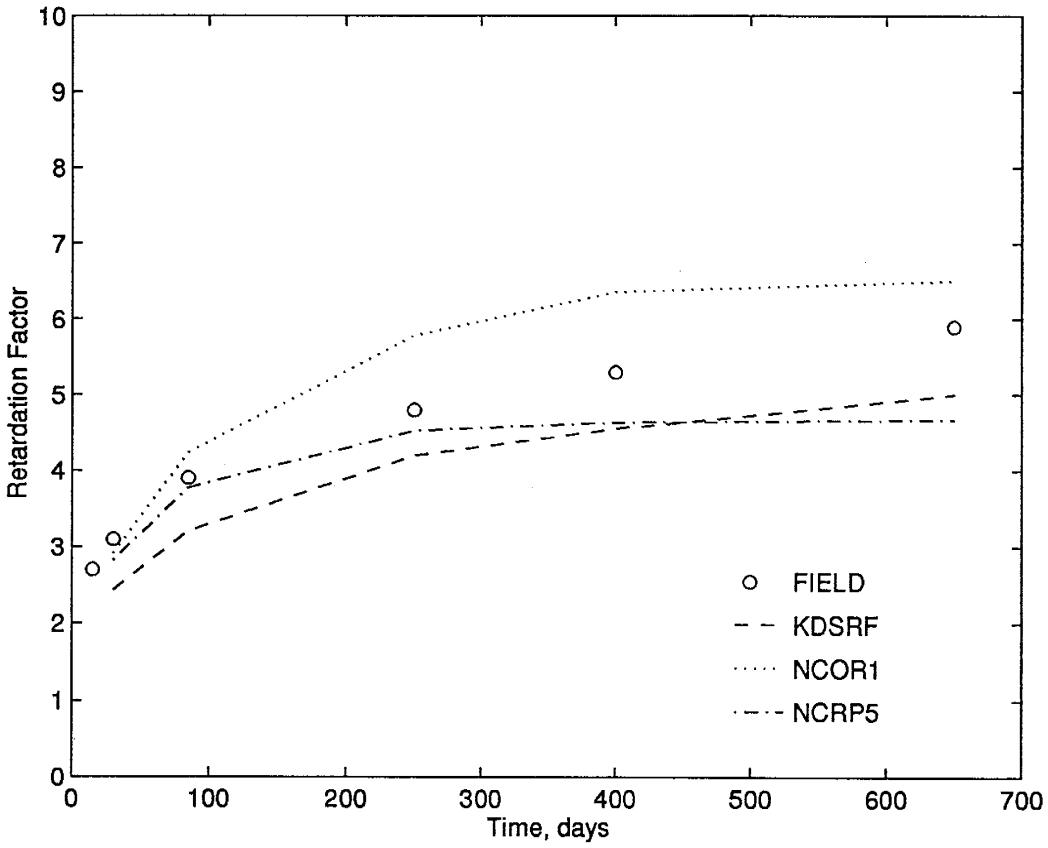

Figure 5.7: Retardation factor for the case of correlated K and K_d.

2. Case LRGS, where the source size is 10.5 m which is about twice the correlation length of the ln K field; and

3. Case SMLS, where the source size is 2.5 m, about half the correlation length of the ln K field.

The individual parameters for the three cases are given in Table 5.2 and R as a function of time is shown in Figure 5.8. The two largest source (FAST and LRGS) show a trend like that observed in the field. Retardation for the smaller source (SMLS) grows significantly faster, perhaps because of insufficient sampling of the heterogeneities by the initial plume.

Using theoretical results of Dagan [1989], Burr et al. [1994] calculated a mean R of 4.55 which differs from their value of 4.48 for the equilibrium case. We have shown that bulk R temporal behavior can be easily explained by modeling the sorption and desorption rates as two independent processes. A review of the various runs discussed above also shows that in all the cases R increases from about 2.5 to 6. While the field observations are closely matched by case FAST, the other cases, DVAR, NCOR1 and KDSRF, show the same general trend. Unlike Burr et al. [1994] we did not see any case where R first decreases and then increases. The mean R calculated for the case of NCOR1, which corresponds to the simulation study of Burr et al. [1994], shows a very distinct increasing trend unlike their results where the ensemble mean R did not show any trend at all. We believe the temporal behavior of R is the result of the heterogeneities in the sorption-desorption parameters. We next look at the spreading of the plume about its centroid.

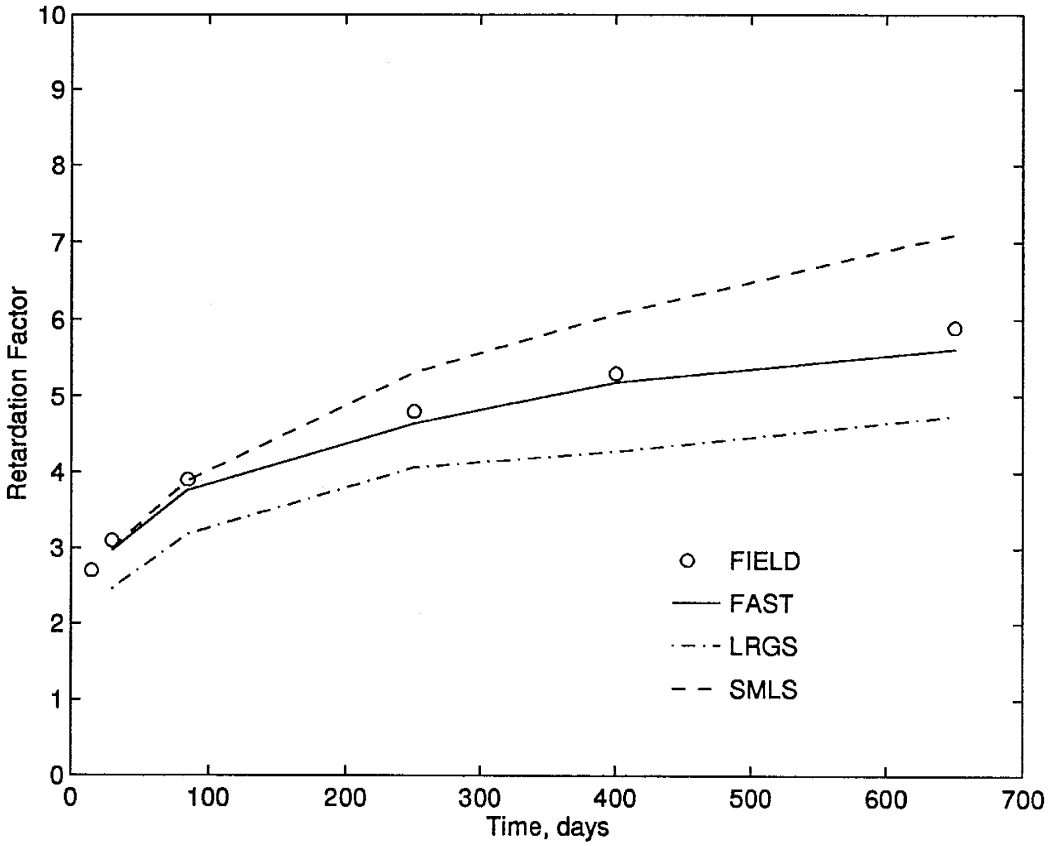

Figure 5.8: Retardation factor for varying initial plume sizes.

5.8 Analysis of Longitudinal Second Moment

One of the striking observations of the field-scale experiments is the enhanced dispersion of the plume relative to the predictions based on column experiments [Sudicky et al., 1983; Freyberg, 1986; Garabedian, 1987]. One possible explanation suggested for this phenomenon has been the heterogeneity of the aquifer materials, in particular that of K. The increase in the plume's spreading rate is attributed to the variability in the direction and magnitude of the solute velocity field at the field scale. As discussed in Chapter 2 previous studies have assumed that K_d is constant or correlated with K field. We will use our computational algorithm, which incorporates spatially variable kinetic sorption to study the effects of those assumptions. The goal of this investigation is to examine the specific features of plume spreading resulting from non-equilibrium behavior of the sorbing solute. Once again we will study the effect of rates, of varying cross-correlation between ln K and ln K_d and of the source size.

We report the second moment results for spreading about the centroid position of each realization, rather than the ensemble mean centroid location. These individual results are again averaged. It has been shown [Rajaram and Gelhar, 1993] that using the bulk displacement of each individual plume realization as a basis for plume spreading produces less dispersion in a mean sense than if second moment values were obtained with respect to the ensemble mean displacement.

Varying Rates

Centroid-based longitudinal second moment values are calculated for each of the five realizations and the mean result at various time is depicted in Figure 5.9 for cases FAST, DVAR and SLOW. Roberts and Mackay [1986] computed the second spatial

moments of the PCE plume based on the site data. A comparison of the modeling results for the case where k_f and k_r are modeled as two independent random processes (case FAST) shows a good match with the data, especially at later time. The second moment is very sensitive to low to low rates of sorption and desorption, which cause large plume spreading. The higher rates, FAST and DVAR, provide a better match than the SLOW rate case.

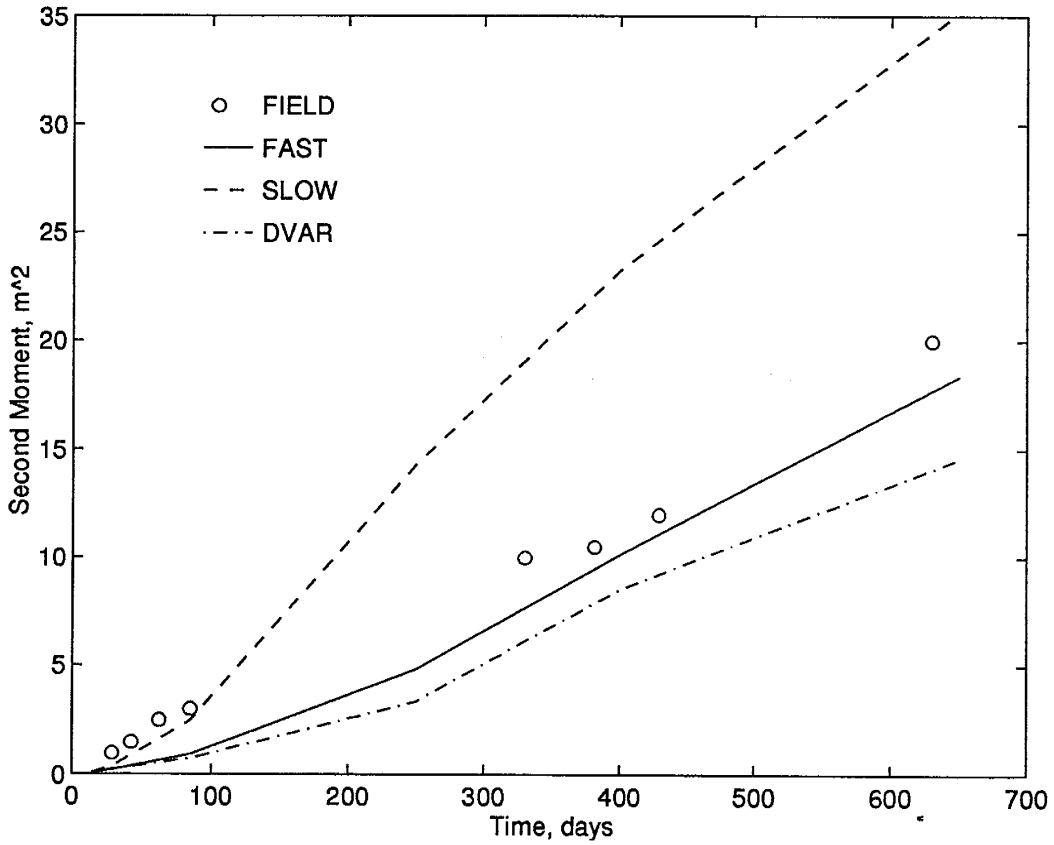

Figure 5.9: Longitudinal second moment for varying rates.

Varying Correlation Between K and K_d

We present the result of longitudinal second moment for the three cases of KDSRF,

NCOR1, NCRP5 (Table 5.3). We have indicated earlier that several recent studies assumed some cross-correlation between K and K_d. The second moment for the three cases, NCOR1, NCRP5, and KDSRF, are shown in Figure 5.10. All have similar behavior. NCOR1, which assumes perfect negative correlation between ln K and ln K_d fields, gives the highest dispersion, although it is still below field observation. The positively correlated cases, PCOR1 and PCRP5 have even smaller values than these three and are shown in Appendix E.

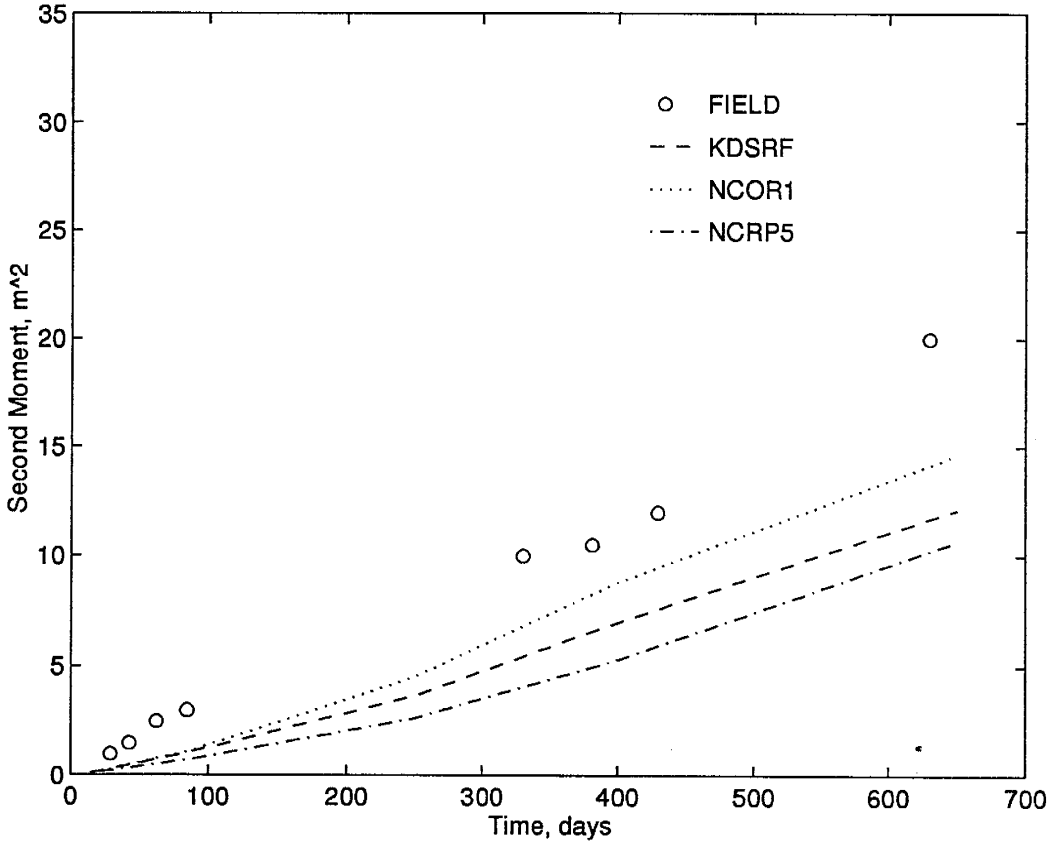

Figure 5.10: Longitudinal second moment results for the correlated K and K_d case compared with field results.

Varying Initial Plume Size

One of the issues of interest is the influence of the plume size on the various spatial moments. This is of importance because classical stochastic theory assumes that the plume size is sufficiently large so that it has sampled all the heterogeneities of the velocity field. This requires that the plume size be about 10-20 times the correlation length of the ln K field. The base case (FAST) assumed that the initial plume source was about a correlation length. As discussed above we examined two other source sizes, one smaller (SMLS) and one larger (LRGS) than the actual experiment (Table 5.2). The plots in Figure 5.11 show very similar second moments for the two larger sources, and a much smaller plume dispersion for the small source. Presumably the small source has a larger drift, a feature that would be reflected in a much larger ensemble average second moment.

Comparison of Analytical Solutions

Analytical results based on Lagrangian analysis neglecting local dispersion [Dagan and Cvetkovic, 1993] and also an Eulerian framework which includes local dispersion [Cushman et al., 1996] have been discussed by these researchers. Their second moments based on constant K_d are discussed in Appendix F.

The second moment results based on the analytical solution of Dagan and Cvetkovic [1993] are plotted in Figure 5.12 and compared to the FAST simulation. It is very clear that the best match to the field data is obtained for the case where the rates are assumed to be two independent spatially varying processes. Neglecting the variability of the sorption-desorption parameters underpredicts the spreading of the reactive plume.

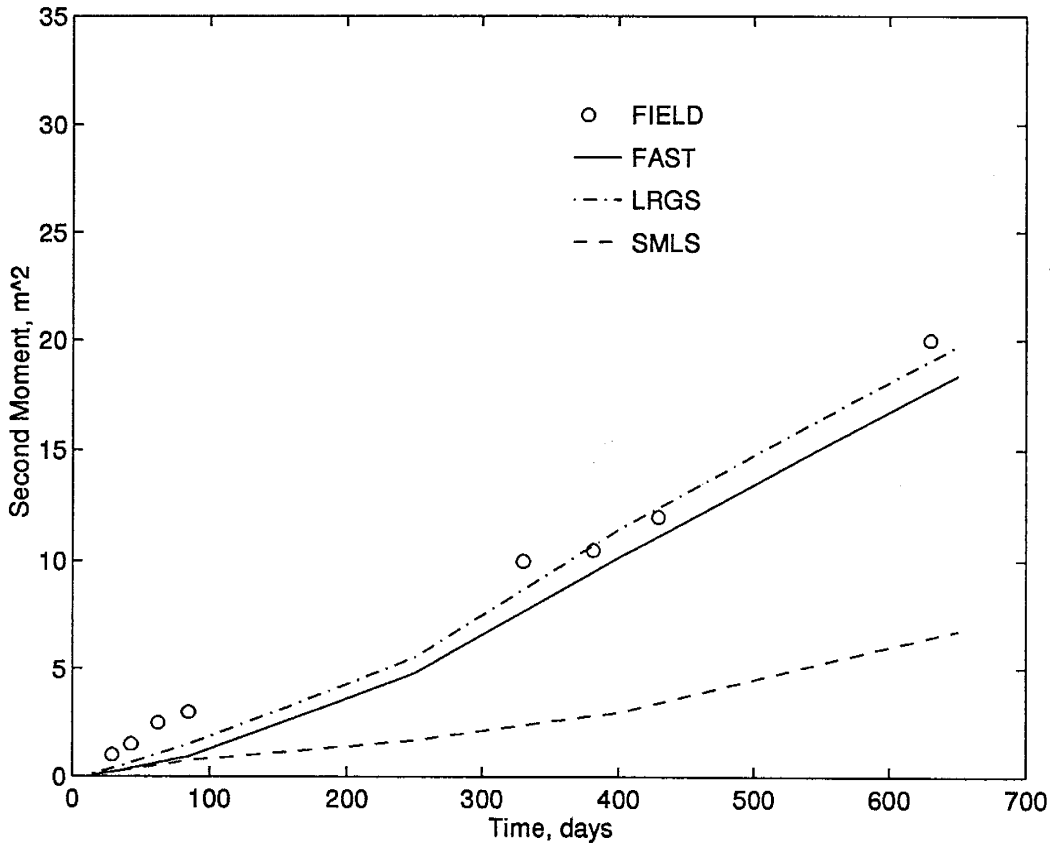

Figure 5.11: Longitudinal second moment for different initial plume sizes.

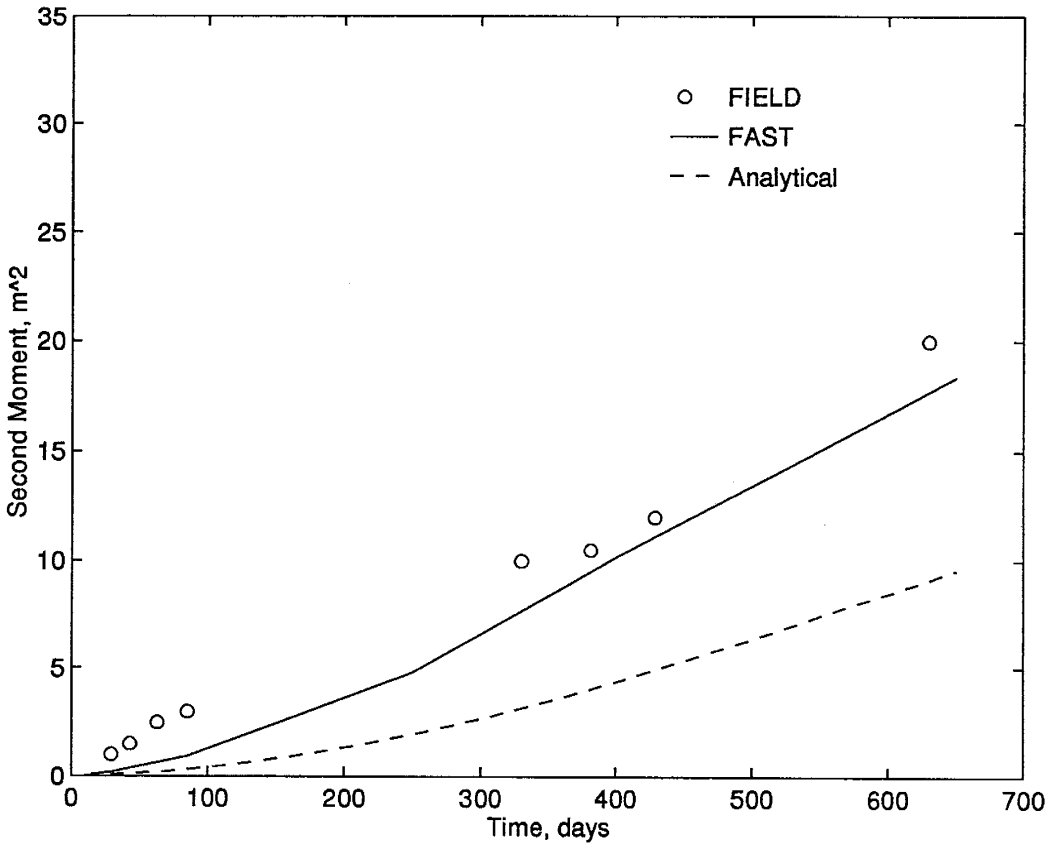

Figure 5.12: Longitudinal second moment results (case FAST) compared with analytical results of Dagan and Cvetkovic [1993].

5.9 Analysis of Macrodispersivities

The field-scale hydrodynamic dispersion tensor D_{ii} can be expressed as (Robin, 1991)

$$D_{ii} = \frac{< R >}{2} \frac{d < S_{11} >}{dt} \tag{5.21}$$

where $< S_{11} >$ is the ensemble longitudinal second moment, and $< R >$ is the bulk retardation factor. The principal macrodispersivity components, $< A_{ii} >$, can be evaluated by assuming that $D_{ii} =< A_{ii} > v$.

Theoretical macrodispersivities for the PCE plume can be obtained from the formulation developed by Garabedian [1987] and Dagan [1989]. They assume a linear relationship between the ln K_d and ln K fields. The reactive solute macrodispersivity in the longitudinal direction is given by [Garabedian, 1987]

$$A_{11} = \frac{\sigma_f^2 \lambda_1}{\eta^2}(1 - \frac{\eta b}{\theta_m R_A})^2 \tag{5.22}$$

where b is the slope of the linear relationship between ρ_b K_d and ln K and R_A is the arithmetic mean retardation factor. The expression derived by Dagan [1989] is the same as that above with $\eta^2 = 1$. For negatively cross-correlated ln K and ln K_d, evaluation of the above equation suggests that the theoretical longitudinal macrodispersivity for PCE should be 5.2 m. Burr et al. [1994] obtained a value of 2.1 m based on a much longer simulation time of 2000-2500 days when the second-moment showed a linear trend with time. However his mean value of the dispersivity, based on five realizations, was 1.565 m (equilibrium case) and 1.025 m for the kinetic sorption case (rates constant).

Varying Rates

The dispersivity values calculated from our simulated second moments show a contin-

uously increasing trend with time which ranges from 0.25 m to a maximum of about 1 m for the FAST case and about 1.5 m for SLOW case (Figure 5.13). Unlike the non-reactive tracer results of Burr et al. [1994] where the longitudinal dispersivity approaches an asymptotic limit, we do not see any such limiting behavior for the linearly sorbing solute when the rates vary. A possible reason a constant value of dispersivity is not attained is that the simulations were only run for 650 days. Further studies with a longer simulation time extending to 2000-2500 days is warranted to study this aspect.

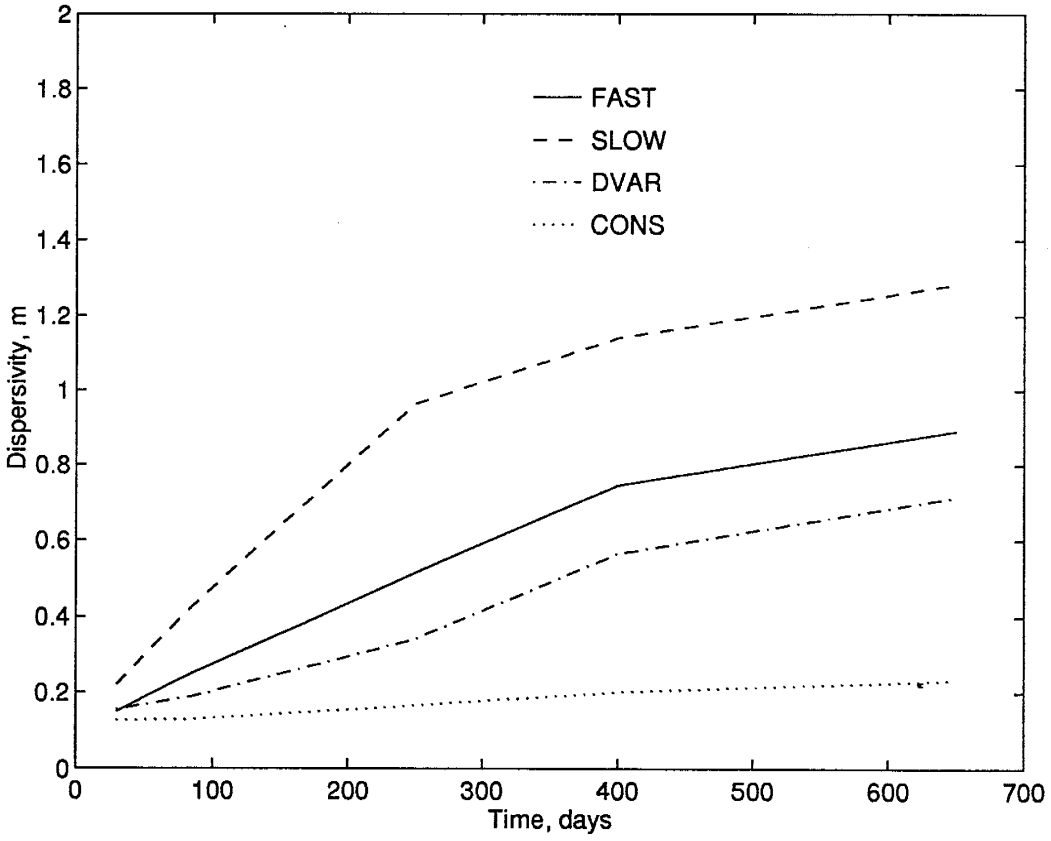

Figure 5.13: Longitudinal macrodispersivities for varying rates

Varying Correlation between ln K and ln K_d

Similar trends of increasing macrodispersivity with time are obtained as the cross-correlation between ln K and ln K_d is varied, with maximum dispersivity values less than 1 m (Figure 5.14). These values are substantially smaller than 5.2, the theoretical asymptotic macro-dispersivity calculated from the stochastic analyses of Dagan [1989] or Garabedian [1987]. One possible explanation is that the asymptotic regime has not yet been reached since the plume has traveled only about 2 correlation lengths (I_{yh}) while the theoretical results would be applicable only for travel distances on the order of 10 or more correlation lengths. The simulations suggest that there is a long period of preasymptotic plume development with a time-dependent macrodispersivity. The asymptotic analytical results overpredict the dispersion and hence would underpredict the resulting concentration of the contaminant.

Varying Initial Plume Sizes

The longitudinal macrodispersivities for the three different souce cases, FAST, LRGS, and SMLS show a continuous increase in the macrodispersivity with time and do not reach any sort of a limiting value over the period of simulation of 650 days (Figure 5.15). The larger initial size plumes have dispersivities that grow at a faster rate initially but this growth rate of dispersivity decreases at around 400 days. The smaller size plume initially has a slow growth rate but this growth continues to show an increase of dispersivity even at 650 days. This result can be explained by realizing that the smaller plume has not yet sampled all the heterogeneities and is still growing in size with time at a rate which keeps increasing with time.

The concept of macrodispersion has been helpful in characterizing the plume shape, assuming it is Gaussian. We have seen that for reactive plumes undergoing

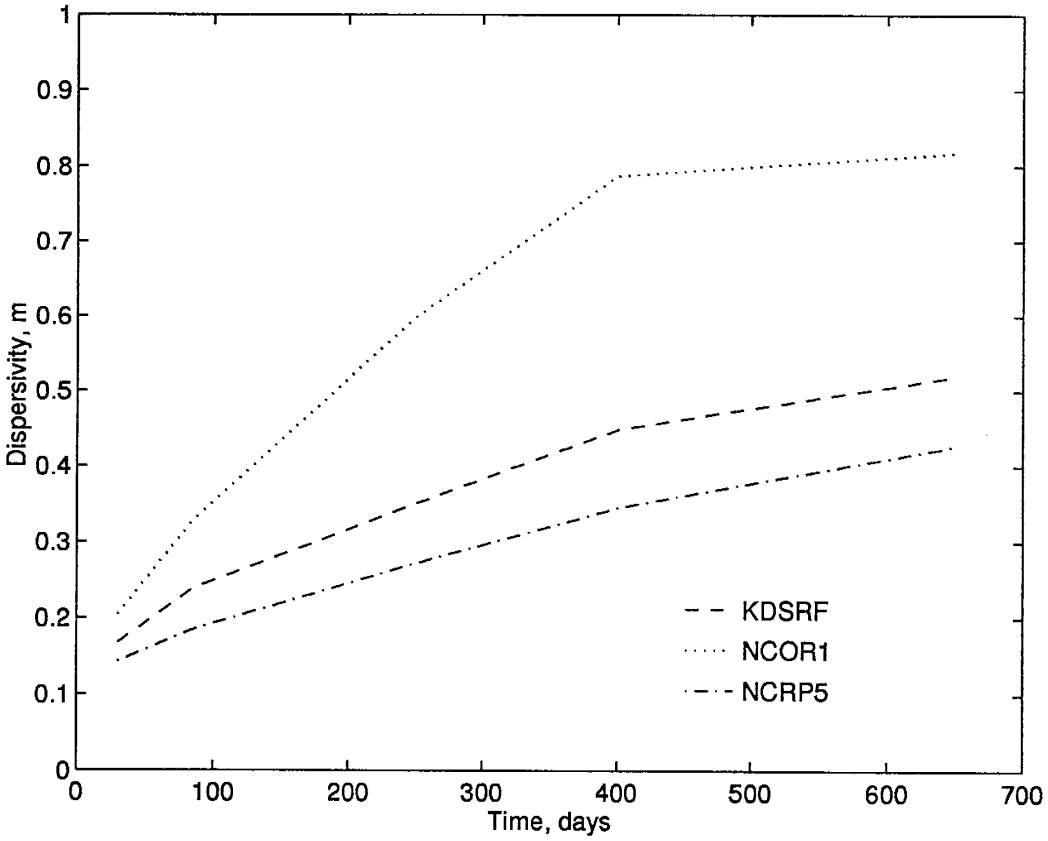

Figure 5.14: Longitudinal macrodispersivities for ln K and K_d correlated.

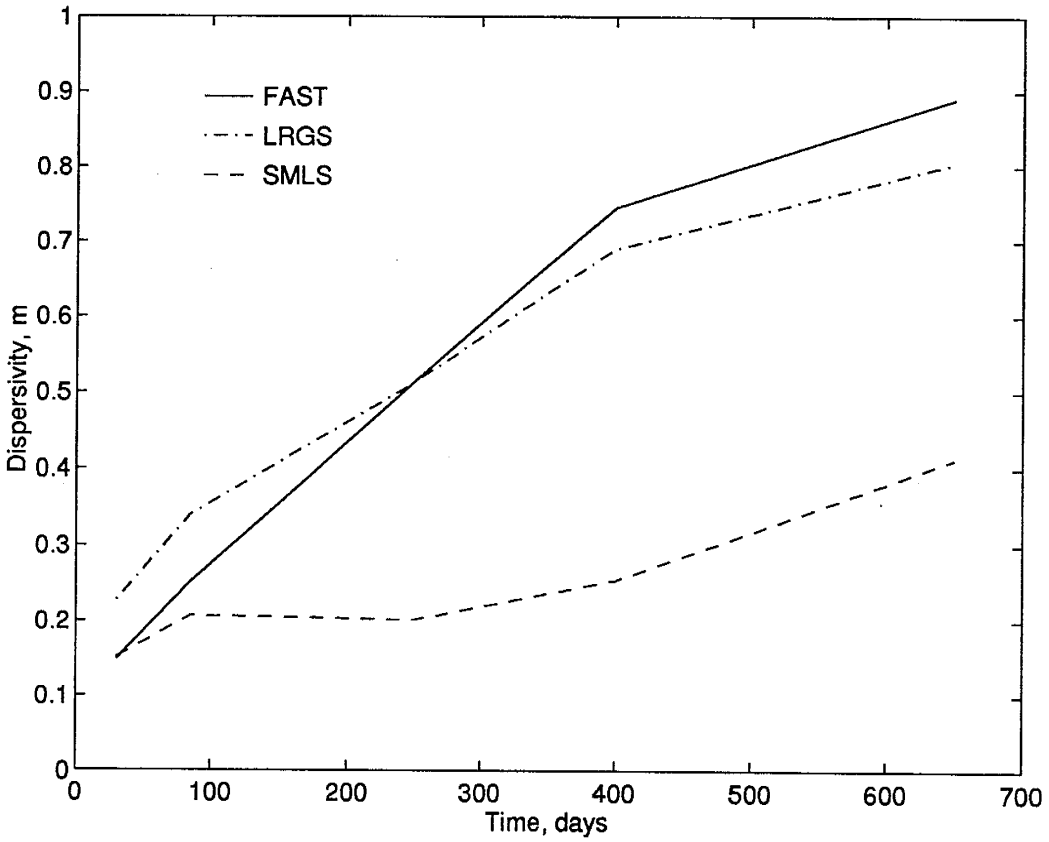

Figure 5.15: Longitudinal macrodispersivities for different initial plume sizes.

sorption, the asymptotic results may not be applicable for the times considered here. The plume-scale transport is a complicated interaction of the spatially varying velocity field with the sorption-desorption rates. In the next section we briefly examine the shape of the plume in terms of its skewness coefficient.

5.10 Analysis of Skewness Coefficient

The Lagrangian formulation [Dagan and Cvetkovic, 1993] and Eulerian formulation based on the non-local theory of transport [Cushman et al., 1995] show that the third moment is linear in time for large time. Since the first moment $X_1(t)$ increases linearly with time, the skewness decreases at the rate of $1/\sqrt{t}$. Once again we studied the sensitivity of the skewness coefficient of the plume to various sorption-desorption parameters: (a) varying rates, (b) varying correlation between ln K and ln K_d and (c) initial plume sizes.

Varying Rates

Simulations FAST and DVAR show a gradual approach to zero skewness, as predicted by stochastic analyses (Figure 5.16). However SLOW shows an anamolous behavior, with a continuously increasing skewness coefficient.

Varying Correlation Between ln K and ln K_d

For the case where ln K and ln K_d are cross-correlated, all the various cases show a gradual approach to zero skewness, with KDSRF and NCOR1 reaching it very rapidly, within about 400 days, while NCRP5 shows a very gradual approach to zero (Figure 5.17).

Effect of Plume Size

The skewness coefficient for the smaller size plume shows a very erratic behavior. It

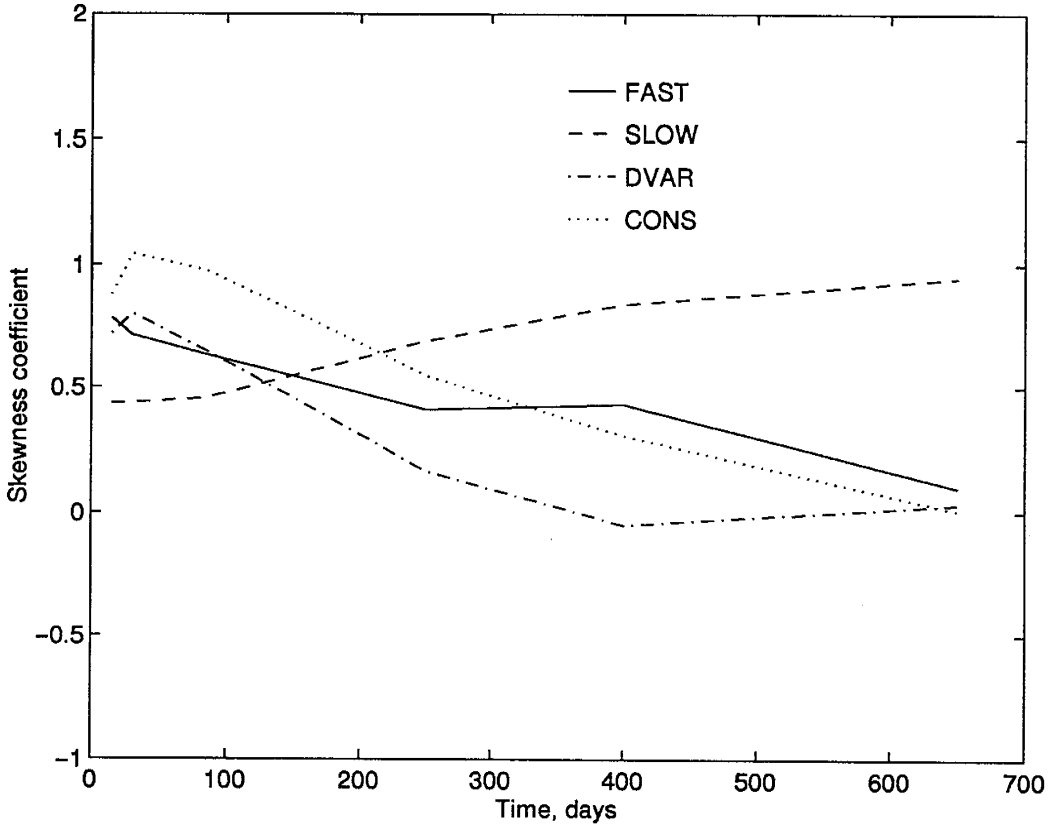

Figure 5.16: Skewness coefficient for the varying rates.

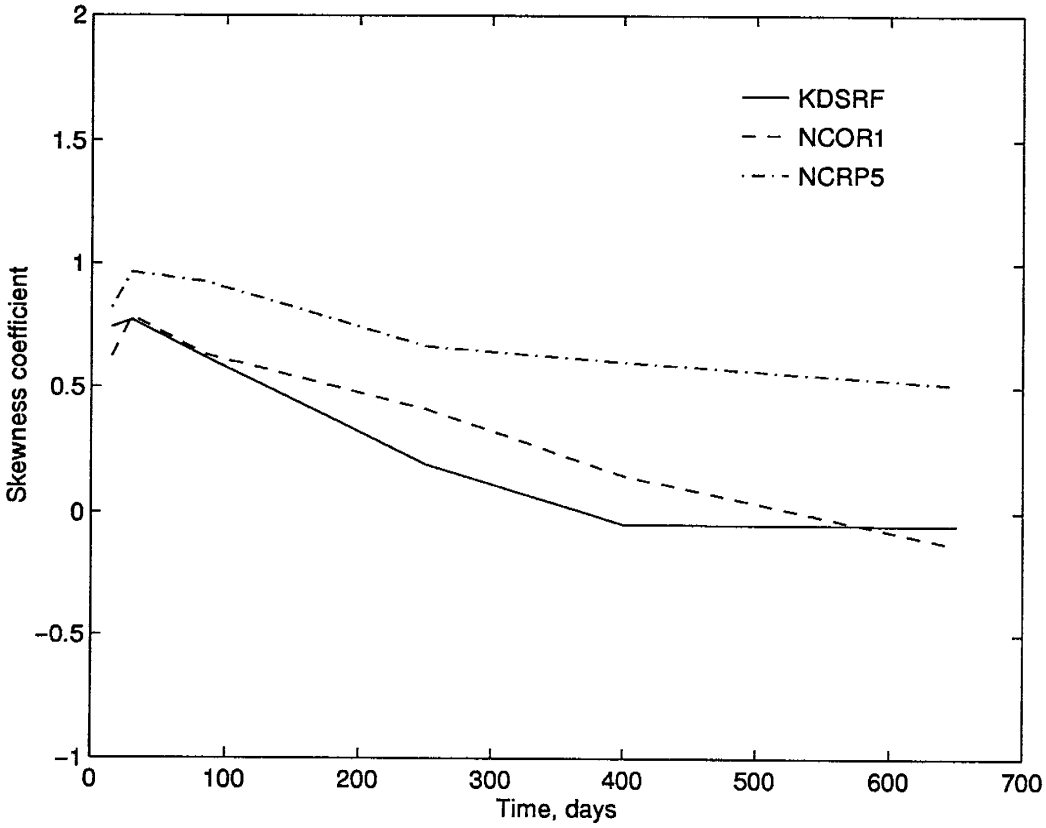

Figure 5.17: Skewness coefficient for the case of cross-correlated ln K and ln K_d.

increases during the first 100 days, then starts decreasing, goes negative and then finally starts increasing again after 400 days (Figure 5.18). The other two plumes show a gradual approach to zero skewness with time.

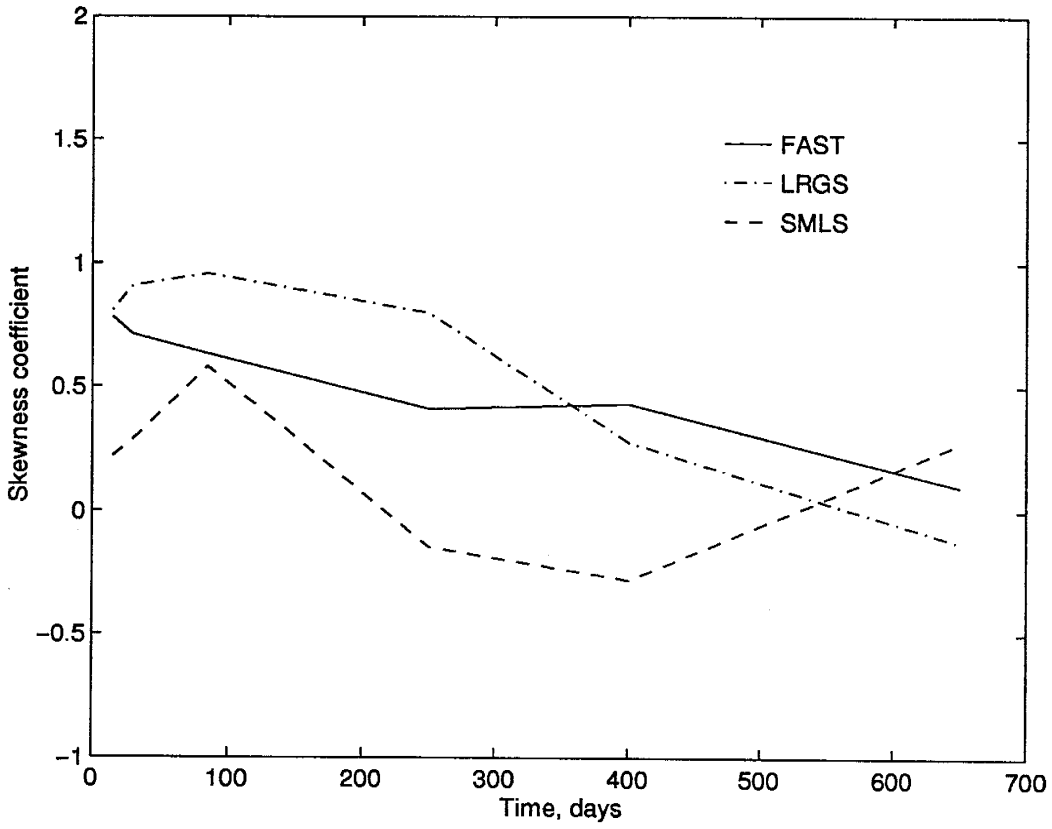

Figure 5.18: Skewness coefficient for different initial plume sizes.

5.11 Discussion and Conclusions

The transport of a sorbing solute dissolved in groundwater was simulated based on the detailed geostatistical parameters obtained at the Borden site from previous studies. The goal of this study was to use the transport simulator based

on a recursion formulation to study contaminant transport in a heterogeneous media by means of Monte-Carlo simulation. The focus was on field-scale displacement and dispersive behavior of PCE migrating in a aquifer with characteristics similar to Borden aquifer. Previous studies have assumed equilibrium conditions for sorption and concluded that the effect of local-scale transport processes such as intra-particle diffusion and kinetic sorption do not contribute to the field-scale plume behavior [Burr et al., 1994].

The results of our simulation have shown that sorption-desorption heterogeneities can explain the observed behavior of increasing R with time seen in the field. A number of possible mechanisms can explain the temporal growth of R with time; interestingly the simplest case when sorption-desorption processes are modeled as two independent processes with different variances for k_f and k_r gave very good agreement with field data (see Figures 5.6, 5.12). This conclusion contradicts that of Burr et al., [1994] who did not see any effect of kinetic sorption on the reactive solute displacement process and hence the bulk retardation factor. They used a spatially varying ln K_d negatively correlated with ln K in their simulations which is similar to our case NCOR1. The results of the different cases show that NCOR1 is just one particular case of the various possible correlations. Simulation of the plume transport and the resulting plume position at a given time illustrates the complex characteristics of the concentration field. The shape of the plume is highly irregular and the shape is distorted relative to the initial well-defined injection profile. The resulting concentration field is an outcome of the interactions of the spatially varying velocity field and the kinetically limited sorption and desorption rates. Cushman et al. [1995] postulated a non-linear interaction which is not amenable to straightforward analyses [Hu et al., 1997]. However we consider only linear interactions and can easily simulate

the complexity of the varying rates along with the velocity field, obtaining a better understanding of the plume scale transport.

The semi-analytical method is fast and robust while accurately capturing the extended tailing due to non-equilibrium sorption phenomena. The plot of the plume position (Figure 5.4) shows a very complicated pattern of the aqueous concentration distribution very similar to the pattern seen in the field experiment including distributed areas of high concentrations or local "hot spots" which are non-continuous.

Using our simulations, particularly FAST (sorption and desorption rates are two independent SRFs) and NCOR1 (ln K and ln K_d negatively correlated) the need for modeling k_f and k_r as two independent spatially varying processes can be examined. Does the negative correlation between K and K_d (equilibrium conditions) give a different spreading behavior compared to uncorrelated rates (kinetically limited sorption)? Burr et al. [1994] used a cross-correlation between ln K and ln K_d to simulate PCE migration and compared the dispersive behavior of a solute undergoing equilibrium linear sorption with that of a non-reactive solute. They concluded that the dispersion in the longitudinal direction is the largest for the reactive solute (for an equivalent centroid displacement) compared to a non-reactive solute, and the transverse spreading is of the same magnitude in both the vertical and horizontal transverse directions. The assumed negative cross-correlation between the ln K and ln K_d fields presumably leads to an increase in the variability of the solute velocity, which in turn causes larger spreading [Garabedian, 1987; Dagan, 1989; Valocchi, 1989; Robin, 1991]. The effects of the local-scale processes of kinetic sorption and intra-particle diffusion on the longitudinal second moment of the PCE plume were found to be weak and the results differed from those of equilibrium conditions by only

a few percent [Burr et al., 1994].

The results of the simulations with spatially varying rates that are uncorrelated with K show a larger spreading in comparison to the spatially varying K_d case, where ln K_d is either independent of ln K or negatively correlated with ln K. The difference in the second moment in the longitudinal direction increases with time and would be significant for longer time period. The kinetically limited non-equilibrium sorption case (case FAST) has a second moment temporal behavior similar to the field observations. Modeling the sorption-desorption rates as random processes provides a good match with both the first and second moment results for the Borden site data.

During the course of the simulation we were able to see a distinct change in the shape of the plume which was related to the rates. The slower rates corresponding to non-equilibrium sorption-desorption showed that the skewness kept increasing with time, while for the equilibrium cases, the plume approached a Gaussian shape. We find that for kinetically limited conditions which may exist in the field, the skewness coefficient is an additional feature for characterizing the plume.

Chapter 6

Transverse Dispersion Of A Sorbing Solute

6.1 Overview

In transport theory one goal is to study plume evolution with time as the initial plume mass is advected by groundwater flow. The movement of the solute mass is affected by spreading and dilution. For a sorbing solute we studied the evolution of a plume due to a spatially varying velocity field and sorption and desorption rates. We focussed our attention in the previous chapter on the longitudinal second moment which provided a measure of spreading of the plume in the direction of the mean flow field. For a multi - dimensional flow field, the plume will also spread in the transverse directions. In this chapter we study transverse dispersion of a linearly sorbing solute in order to address the asymptotic behavior of a plume.

We will first outline past results of two different existing approaches (Eulerian and Lagrangian) to predict spatial moments, with particular attention on the transverse second moment. The second moments in the transverse direction obtained using the two approaches are significantly different. We briefly review these published approaches, outline the reasons for the difference, and then present our formulation for transverse dispersion in a stratified aquifer for both non-reactive and linearly sorbing solutes.

6.2 Spatial Moments Results

Using a first-order perturbation analysis within an Eulerian framework, non-local models of flow and transport have been developed for non-reactive solutes [Koch and Brady, 1987; Cushman, 1991; Cushman and Ginn, 1993; Deng et al., 1993; Neuman, 1993], and for reactive solutes undergoing linear sorption with deterministic K_d [Hu et al., 1995]. Analytical methods have been used to analyze the various spatial moments for reactive transport with kinetically limited linear sorption assumptions. In the previous chapter we outlined the results of spatial moments obtained from Lagrangian analyses [Dagan and Cvetkovic, 1993]. Here we present the expressions for the spatial moments obtained from Eulerian analysis [Hu and Cushman, 1997].

$$X_1(t) = U\frac{H_1(t)}{H_0(t)} \tag{6.1}$$

$$X_{11}(t) = 2d_1\frac{H_1(t)}{H_0(t)} + U^2\frac{H_2(t)}{H_0(t)} - U^2\left(\frac{H_1(t)}{H_0(t)}\right)^2 + \frac{A_2^1(t)}{H_0(t)} \tag{6.2}$$

$$X_{jj}(t) = 2d_j\frac{H_1(t)}{H_0(t)} + \frac{A_2^j(t)}{H_0(t)},\ j = 2,3 \tag{6.3}$$

$$H_0(t) = \frac{1}{R}(1 + K_d e^{-k_r R t}) \tag{6.4}$$

$$H_1(t) = \frac{1}{R^2}(1 + K_d^2 e^{-k_r R t})t + \frac{2K_d}{k_r R^3}(1 - e^{-k_r R t}) \tag{6.5}$$

$$H_2(t) = \frac{1}{R^3}(1 + K_d^3 e^{-k_r R t})t^2 + \frac{6K_d}{k_r R^4}(1 - K_d e^{-k_r R t})t + \frac{6K_d(K_d - 1)}{k_r^2 R^5}(1 - e^{-k_r R t}) \tag{6.6}$$

where $X_1(t)$ is the first moment, $X_{ii},\ i = 1,2,3$ are the second moments. These spatial moments are obtained as functions of U, the mean velocity along the flow direction, $d_i,\ i = 1,2,3$, the local dispersivities, and other terms like $H_0,\ H_1,\ H_2$

given above. The expression $A_2^j(t)$ is given by

$$A_2^j(t) = \frac{2}{(2\pi)^3}\int_{R^3} \hat{Y}(\mathbf{k},t) < v_j\hat{v}_j > (\mathbf{k})d\mathbf{k} \tag{6.7}$$

where $< v_j\hat{v}_j >$ is the Fourier transform of the velocity covariance function in j direction. A detailed evaluation of the different quantities (like $\hat{Y}(\mathbf{k},\mathbf{t})$) is given in Hu and Cushman [1997].

For the Lagrangian analysis, the zeroth and the first moment are identical to the Eulerian results (see Appendix F). The second moment differs from the Eulerian case by the presence of the d_i terms that account for the local dispersion. For example, in equation 6.2, d_1 is the local longitudinal dispersitvity and the remaining parameters are as defined before. Hu and Cushman [1997] compared the first three central moments for the case of an exponential correlation of the ln K field. Their comparisons showed that both the Eulerian and Lagrangian approaches yield the same values if local dispersivity is neglected.

While it is a common assumption in Lagrangian analysis to neglect the local dispersivity, Hu and Cushman [1997] illustrated the errors that can occur when this is done. For a mean velocity of 1 m/day, σ_f^2=1, a correlation length of 1 m and an anisotropy ratio of 1, the second longitudinal moments are only slightly affected by the local dispersion. However, the transverse second moments are significantly affected by the presence of local dispersion. Their comparisons indicate that if local dispersion is included, the second transverse moment will increase linearly with time in contrast to the second transverse moment reaching a constant asymptotic value if local dispersion is zero.

For the case of an isotropic medium at large time, the longitudinal and

transverse second moment Eulerian results obtained by Hu and Cushman [1997] are

$$X_{11}(t) = \frac{2d_1}{R}t + \frac{2V^2K_d}{k_rR^3}t + \frac{2\sigma_f^2 lV}{R}t \tag{6.8}$$

$$X_{jj}(t) = \frac{2d_j}{R}t + \frac{4d_jK_d}{k_rR^2} + \frac{2\sigma_f^2 l}{3}, \quad j = 2,3 \tag{6.9}$$

where R is the retardation factor, V the mean velocity, l the correlation length, σ_f^2 the variance of ln K field. Thus, for the Eulerian analysis, the asymptotic values of the second spatial moments in both the longitudinal and transverse directions are linear in time. In equations 6.8 and 6.9 the first term represents the contribution of local-scale dispersion to spreading in both the longitudinal or transverse directions. Only for d_i equal to zero, do Eulerian and Lagrangian results agree. At large time this first term will dominate, indicating a linear increase with time of the second transverse moment. Hu and Cushman [1997] have hypothesized "that inclusion of a Brownian local-scale dispersive displacement in the Lagrangian analysis would result in moments consistent with the Eulerian moments (with local dispersivity)".

In this chapter we present an approach for transverse dispersion using a Lagrangian framework where local dispersion is included to verify the above hypothesis. To illustrate this we restrict our attention to a simplified two-dimensional stratified flow system. Again we use a recursion formulation for the transverse motion with an added recursion used for the the horizontal motion.

6.3 Transverse Dispersion in a Stratified Aquifer

In this section, we study the effect of local dispersion on the transverse spreading of a contaminant source injected at a point in a stratified aquifer. An idealized stratified system is used to understand and develop the algorithm in a simplified

setting. The ultimate goal is to use it in a real-world situation of anisotropic flow regime in three dimensions. In a stratified system which is oriented in the horizontal direction, the velocity variations depend only on the transverse direction.

Consider a stratified aquifer in which flow is at steady state. The K field and the resulting velocity field vary only in the transverse directions (Figure 6.1). Here we define v_j=velocity in the jth streamline or layer; Δz= distance between two adjacent streamlines; and Δt= one time step.

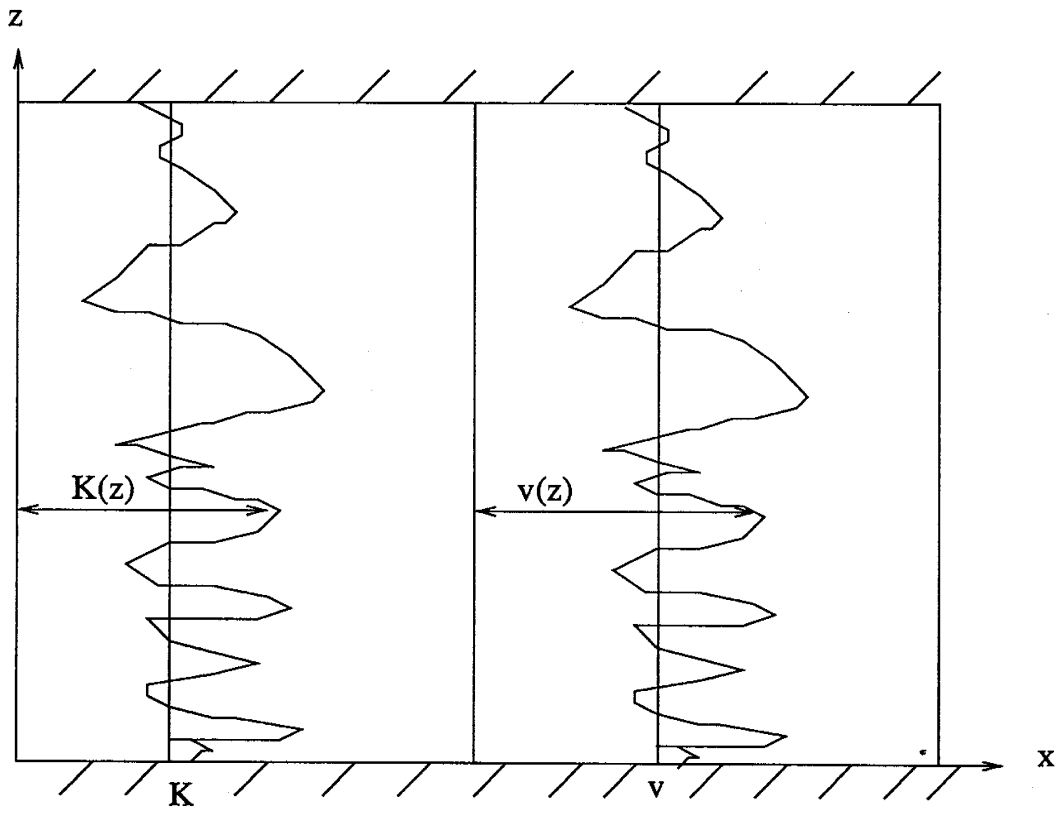

Figure 6.1: Schematic representation of hydraulic conductivity and velocity variations in a stratified aquifer based on Gelhar et al. [1989].

Our primary interest is in the transverse spreading of the injected contaminant source. Thus let q_j= probability that a solute particle in layer j moves to an adjacent layer (streamline) in time Δt. The random variable Z denotes a particle's transverse position indexed by the the streamline number. We allow a particle to either remain in the streamline or move from streamline j to an adjacent streamline with the following probabilities

$$P(Z = j + \Delta z) = q_j \tag{6.10}$$

$$P(Z = j - \Delta z) = q_j \tag{6.11}$$

$$P(Z = j) = 1 - 2q_j \tag{6.12}$$

$$\text{Then } E(Z) = j \tag{6.13}$$

$$Var(Z) = 2\,(\Delta\, z)^2\, q_j \tag{6.14}$$

We further define α_T= local transverse dispersivity. For a time interval, Δt, the variance of the particle displacement is also given by

$$Var(Z) = 2\,\alpha_T\, v_j\, \Delta t \tag{6.15}$$

Equating the two variance expressions (equations 6.14 and 6.15) gives a relationship between q_j, Δz, Δt and α_T:

$$q_j = \frac{\alpha_T\, v_j\, \Delta t}{(\Delta\, z)^2} \tag{6.16}$$

This relates the probability that a solute particle will move from a given streamline to an adjacent one to the local transverse dispersivity, (α_T), the velocity (v_j), the spacing between the streamlines (Δz) and the discretization in the time domain (Δt). Note one could also let Δz depend on j but for simplicity we take it to be constant. Varying

Δz may be useful for cases where large changes in velocity occur over short vertical distances.

For a reactive solute undergoing sorption-desorption under linear sorption conditions, we can envisage a particle injected at a given location moving along the mean flow direction. The process of transverse dispersion will shift the particle to an adjacent streamline with a given probability, q_j and the particle then moves along the new streamline until it is shifted to another adjacent streamline. A particle can undergo many such transverse displacements as it moves in the longitudinal direction. The resulting position of all the particles after a given time then will give a measure of the spread in the transverse direction. We are interested in evaluating this expression for the variance of a particle position, which is then related to the transverse dispersion.

Let $\beta_j^m(s)$ be the probability that a solute particle leaves layer j for the first time at time step s (or time $s\ \Delta t$) starting from state m, where m=1 again indicates the aqueous state; m=2 sorbed state. As before, r_{12} is the probability of moving from the aqueous to the sorbed phase in time Δt. The transition probabilities given by r_{12} are related to the sorption and desorption rates for a linearly sorbing solute as discussed in Chapter 3. The formulation given below considers constant r_{12} and r_{21} but we will later generalize the results to the spatially varying case. We then have the following expressions

$$\beta_j^1(1) = 2\, q_j\, (1 - r_{12}) \tag{6.17}$$

$$\beta_j^2(1) = 2\, q_j\, r_{21} \tag{6.18}$$

$$\beta_j^1(s) = r_{12}\, \beta_j^2(s-1) + r_{11}\, (1 - 2\, q_j)\, \beta_j^1(s-1) \tag{6.19}$$

$$\beta_j^1(s) = r_{21}\, (1 - 2\, q_j)\, \beta_j^1(s-1) + (1 - r_{21})\beta_j^2(s-1) \tag{6.20}$$

Once again we have a set of recursion equations for the β's. Equation 6.17 refers to the probability that the solute particle leaves the jth streamline at time Δt; this is the probability that the particle remains in the aqueous phase (given by $1-r_{12}$) times the probability that the solute particle leaves the jth streamline or (2 q_j).

Using the $\beta_j^m(s)$ values we next develop the recursion for the transverse particle position: namely the probability that a particle will be in layer j at time t. Since the particle can only move when in the aqueous phase, we will henceforth be working only with m=1 and so we drop the superscript to simplify the notation.

Let $Q_{n,\,j}(k)$=Probability that a solute particle is in layer n at time $k\Delta t$ starting in the aqueous phase from layer j at time 0. The recursion formulation for $Q_{n,\,j}(k)$ is given by

$$Q_{n,\,j}(k) \;=\; \frac{1}{2}\sum_{s=1}^{k}[Q_{n,\,j-1}(k-s)+Q_{n,\,j+1}(k-s)]\;\beta_j^1(s) \qquad (6.21)$$

Equation 6.21 gives the probability that a particle is in layer n starting from layer j. This is obtained as follows:

1. $\beta_j^1(s)$ = probability that a particle leaves the layer j for the first time on time step s;

2. When the particle leaves layer j, it will go to either layer j-1 or j+1, each with probability 1/2.

3. The first expression in the bracket sum gives the probability of moving to layer n from layer (j-1) in time (k-s);

4. The second expression in the bracket sum gives the probability of moving to layer n from layer (j+1) in time (k-s);

5. We then multiply by $\beta_j^1(s)$ and sum over all possible values of s=1 to k time steps.

The boundary conditions are

$$Q_{1,1}(k) = (1-2q_1)^k + \sum_{s=1}^{k-1} \beta_1^1(s) Q_{1,2}(k-s) \tag{6.22}$$

$$Q_{N,N}(k) = (1-2q_N)^k + \sum_{s=1}^{k-1} \beta_N^1(s) Q_{N,N-1}(k-s) \tag{6.23}$$

Since the boundaries are closed, the particles are reflected back from the boundary streamlines. We further assume all mass is injected in the aqueous state at time 0. Here the initial condition is given by

$$Q_{j_0,j_0}(0) = 1; \tag{6.24}$$

$$Q_{i,j}(0) = 0; i = j \neq j_0 \tag{6.25}$$

The initial condition specified by equations 6.24 and 6.25 indicate that all the mass is injected into a specified layer, j_0 at time zero and there is no solute present in the aqueous state in any other layer before time zero.

We look at the growth of the transverse dispersion in a stratified model by instantaneously injecting solute in the aqueous phase in layer N/2. The steady state velocity field and local dispersion will lead to the solute particles being distributed across the various layers until after a sufficiently long time the particles occupy all the layers from j=1 to N where N is the maximum number of layers. The variance of the particles in the transverse direction at time $k\Delta t$ is a measure of the second transverse spatial moments. It is given by

$$S_{22}(k) = \sum_{i=1}^{i=N} (i-j)^2 \, Q_{i,j}(k), \; j = N/2 \tag{6.26}$$

6.4 Outline of the Algorithm

In our simulations we used a system with 128 layers. Table 6.1 summarizes the various system and numerical model parameters. Spatially varying parameters (V, k_f and k_r) are independent log normally distributed Gaussian random variables, with an exponential spatial covariance function. The parameters of variance and correlation length for generating the three different fields (V, k_f and k_r) are the same. We simulated 100 days of transport using 1000 timesteps. The simulations were designed so that the transverse boundaries should not play a role.

Description	Value
Δz, spacing between streamlines	0.04 m
Δt	0.1 day
α_T, local transverse dispersivity	0.001 m
E(V), Mean Velocity	1.0 m/day
$\sigma^2_{ln\ v}$, Variance of ln v	0.1
λ_v, vertical Corr. Length	0.4 m

Table 6.1: Parameters for Transverse Dispersion Simulations

The simulation steps consist of the following

1. Compute q_j, r_{12}, r_{21} from the input parameters of $v_j, k_f(j), k_r(j), \Delta t, \Delta z$.

2. Calculate $\beta_j^m(s)$ terms.

3. Calculate $Q_{n,j}(k)$ from the recursion formulations and the boundary conditions at different time steps, k ranging from 1 to 1000 in our example.

4. Calculate the variance of the particle positions at each time.

6.5 Non-reactive Solute

The recursion formulation given above for a linearly sorbing solute can also be applied to nonreactive solutes by setting k_f and k_r equal to zero. For a non-reactive solute the transition probability r_{11} is always equal to unity (and $r_{12} = r_{22} = r_{21} = 0$) since the solute remains in the aqueous phase at all times. We first illustrate the second spatial moment for a non-reacting solute (Figure 6.2) where a constant velocity of 1 m/day in all the layers is used.

The variance of the particles initially injected in the middle layer is shown at various times in Figure 6.2. The two individual lines are for 128 and 64 layers. The increase in transverse variance is found to be linear with time. This result is in accordance with the theory where the variance of the particles is given by

$$\text{Variance} \;=\; 2\,\alpha_T\,U\,t \tag{6.27}$$

For the parameters chosen for the simulations, the variance at time = 100 days should be 0.2 which is indeed the value obtained from our simulation results. These simulations show that even for the 64 layer case the boundary conditions should not influence the result.

We next include the effect of spatially varying velocity field that varies with the stratification. A mean velocity of 1 m/day with an exponential covariance, a correlation length of 0.4 m and a variance of 0.1 is input for a 128 layer model.

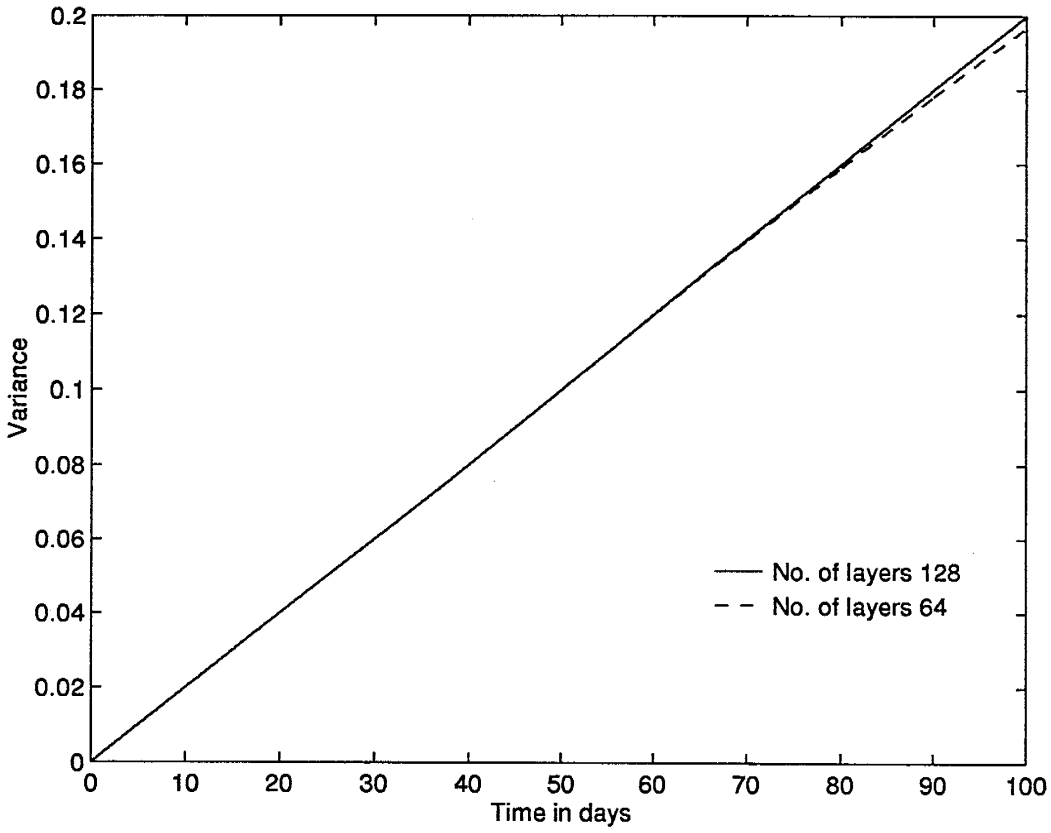

Figure 6.2: Second transverse spatial moment for a non-reacting solute.

The effect of velocity variations along the individual streamtubes leads to a higher spreading in the transverse direction, as shown in Figure 6.3. The salient feature is a linear trend of the transverse variance with time, very similar to the earlier case of constant velocity.

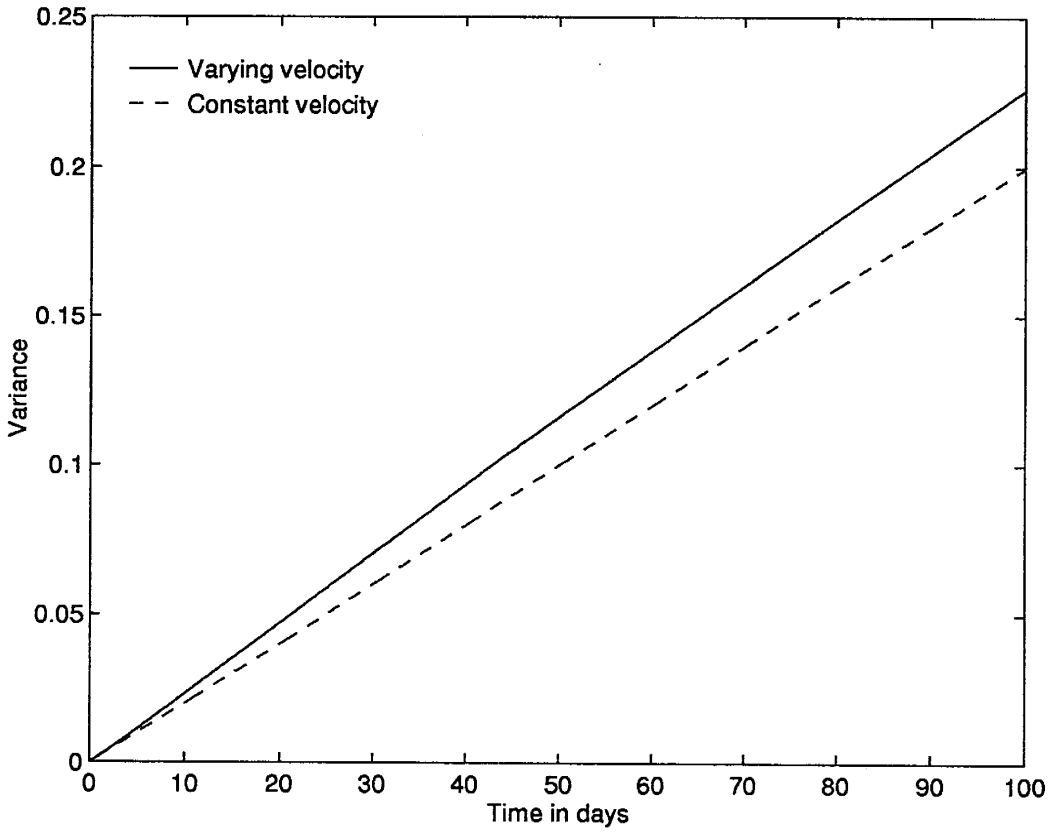

Figure 6.3: Second transverse spatial moment for a non-reacting solute for spatially varying velocity compared to constant velocity. N= 128

6.6 Reactive Solute Transverse Spreading

For linearly sorbing solutes, the k_f and k_r values are input to calculate the transition rates and hence the β_j^m's. Once again we will first evaluate the case of constant rates using k_f and k_r values of 1.0 and 0.2/day.

6.6.1 Constant Rates and Velocity

The base case of constant velocity for a linearly sorbing solute in a homogeneous medium is compared to the non-reactive solute in Figure 6.4. The transverse spreading of a sorbing solute is much smaller than the corresponding spreading of a nonreactive solute. The reactive solute curve follows the non-reactive curve for about a time period of 5 days which corresponds to the mean time of sorption and then the reactive curve follows a different curve with a much smaller slope due to the retardation of transverse motion by sorption. However the variance increases linearly with time and does not show an asymptotic limit even after a time period of 100 days unlike previous results of Dagan and Cvetkovic [1993]. These results show that inclusion of local dispersion does contribute to a different behavior for transverse dispersion, especially for large time in a Lagrangian framework and is consistent with the Eulerian analysis [Hu and Cushman, 1997] where local dispersion was included.

6.6.2 Constant Rates and Spatially Varying Velocity

If the velocity is spatially varying in the different streamlines, the resulting transverse spreading is increased compared to the case where the velocity is constant (Figure 6.5). We still see the same linear trend of variance with time. In this case

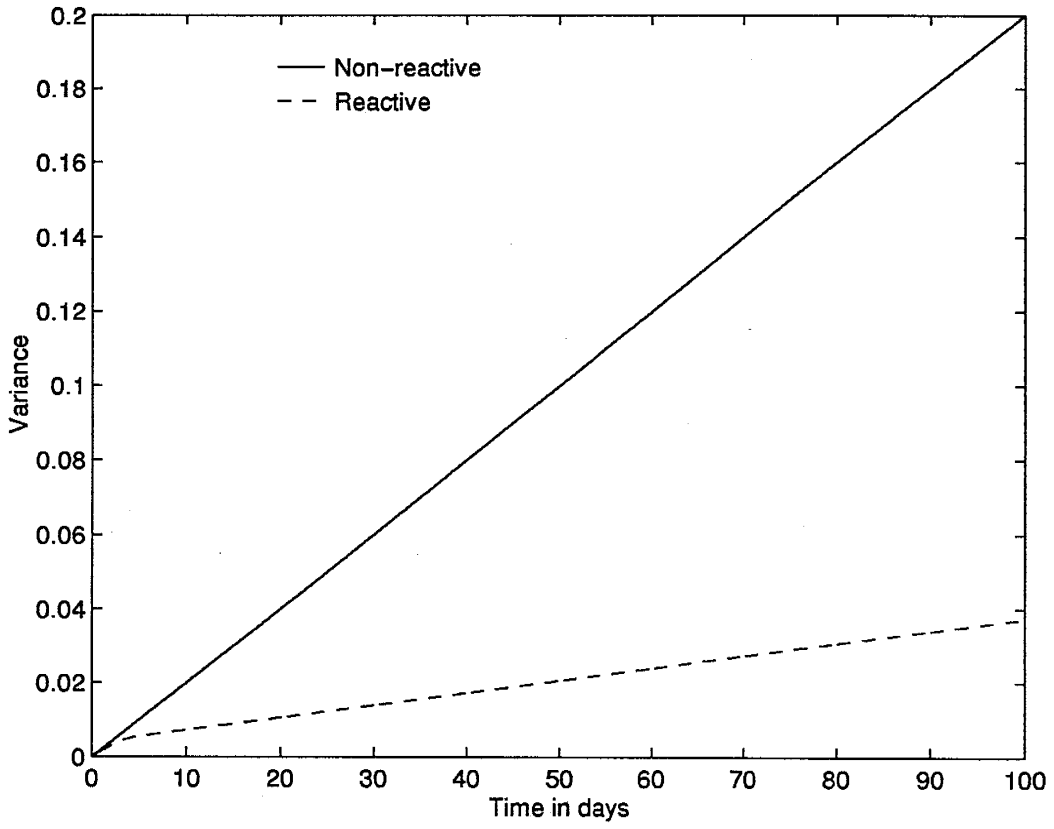

Figure 6.4: Second transverse spatial moment for a non-reacting solute compared to that of a reacting solute. The velocity and the reaction rates are constant in all the layers.

the solute dispersion follows that of a non-sorbing solute for a time corresponding to $1/k_r$ which in our example is 5 days (k_r=0.2/day). Only after this period does the bulk plume experience the effect of kinetic sorption-desorption.

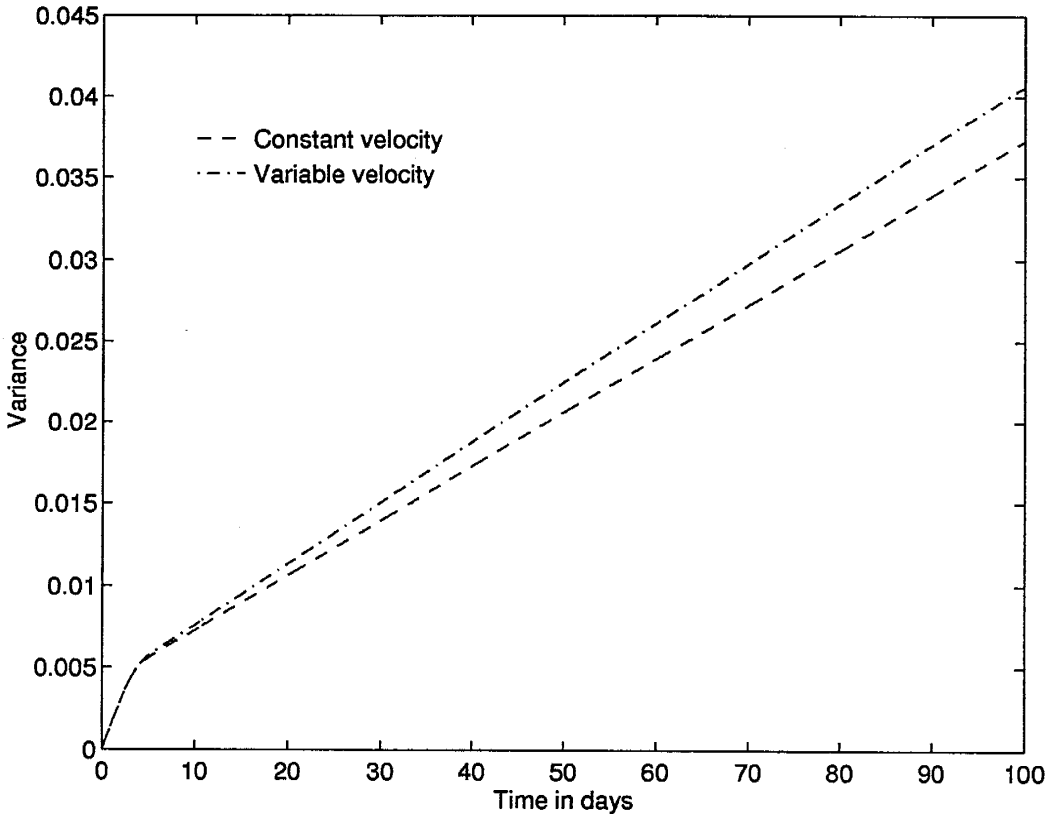

Figure 6.5: Second transverse spatial moment for a reacting solute. The case of constant velocity of 1 m/day is compared to the case where velocity is log-normally distributed with a mean of 1 m/day and a variance of 0.1.

6.6.3 Spatially Varying Rates and Velocity

The most general case where all three fields (V, k_f, and k_r) are spatially varying is considered next. The k_f and k_r fields are assumed to be log-normally distributed with a mean of 1/day and 0.2/day, respectively. The velocity field is generated as a log-normal distribution with a mean velocity of 1 m/day. The covariance structure of all the three random fields are kept the same: an exponential covariance with a variance of 0.1 and a correlation length of 0.4 m. The variance is plotted in Figure 6.6. Although it initially grows at a faster rate than before, after 5 days the rate becomes significantly smaller. The variability in the rates has a greater effect on the transverse dispersion behavior than the velocity fluctuations alone, and it is in the opposite direction. It lowers transverse dispersion.

In Figure 6.7 we examine the sensitivity to the mean values of k_f and k_r: for slower rates the transverse variance results show an approach to the non-reacting case. The figure shows two different cases – Case 1, rates of 1 and 0.2/day and Case 2, rates of 0.1 and 0.02/day. For case 2 (i.e. non-equilibrium conditions), the plume continues to grow in the transverse direction like a non-reactive solute and after a time equal to 50 days which corresponds to the mean time of sorption, follows a different trajectory. Case 1 (i.e. equilibrium conditions) shows a very different time behavior of the growth of the transverse second moment. For a kinetically limited sorption behavior, the equilibrium conditions will underpredict the transverse spreading. We have illustrated in this example that an accurate prediction of transverse dispersion is greatly affected by the rates.

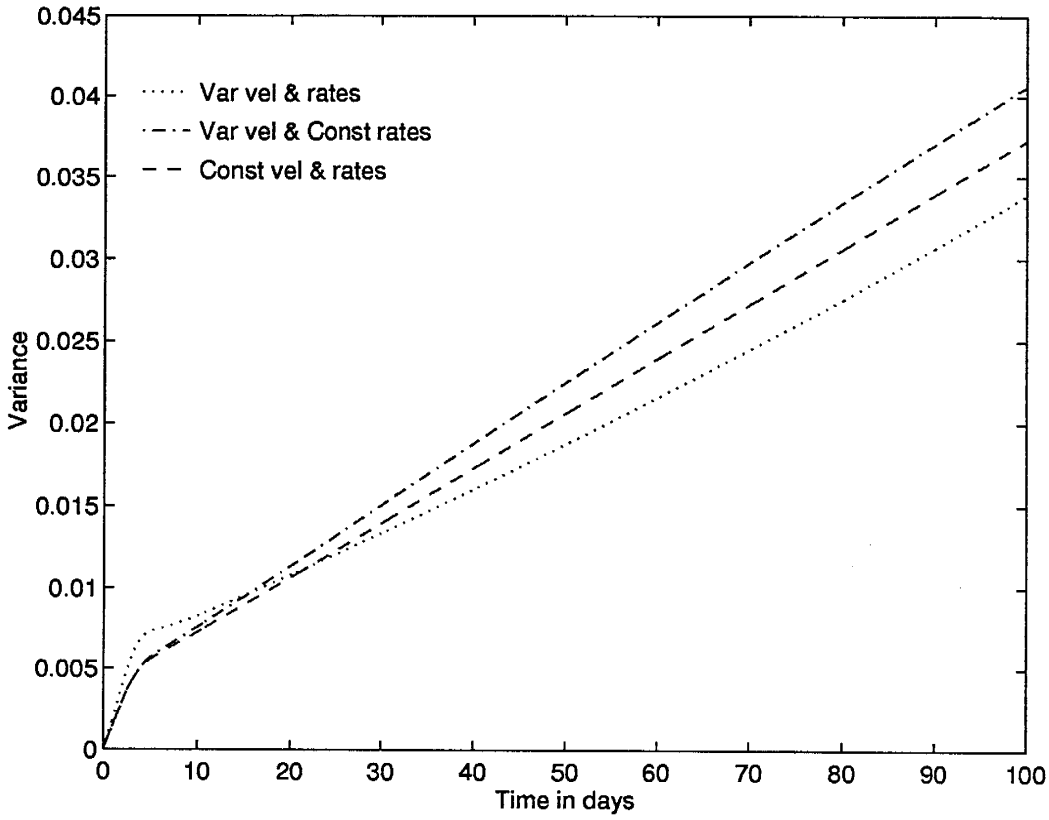

Figure 6.6: Second transverse spatial moment for a sorbing solute in a spatially varying velocity field. The two cases (1) Constant rates and (2) Spatially varying rates are compared with the case of constant velocity and constant rates in all the layers.

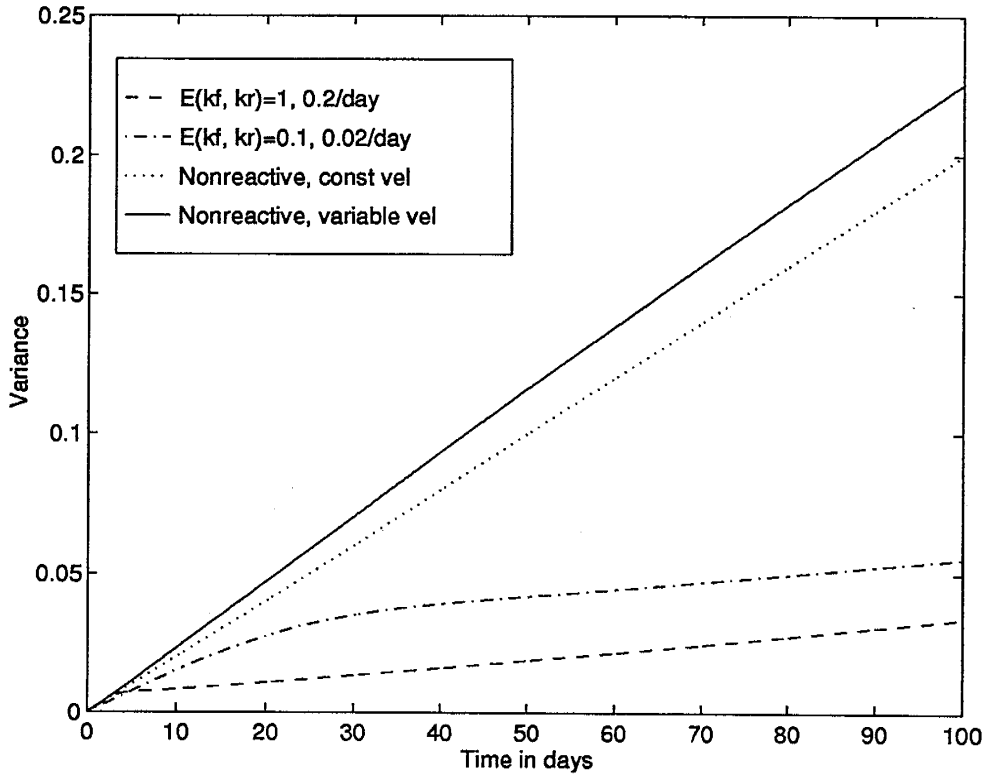

Figure 6.7: Second transverse spatial moment for a reacting solute in a spatially varying velocity field for spatially varying rates. The effect of two different means of k_f, k_r are contrasted with a non-reactive solute.

6.7 Discussion and Conclusions

We have developed a Lagrangian formulation for transverse spreading which incorporates local dispersion. The formulation is very general and can be used to model both nonreactive and reactive transport. Both the velocity field and the rates could be constant or spatially varying. Our simulations indicate that including the local dispersion in transverse spreading leads to an increase of transverse variance with time unlike results where local dispersivity is neglected [Dagan and Cvetkovic, 1993]. Our results agree with Hu and Cushman [1997] who show that if local dispersivity is not included, the asymptotic transverse second moment will reach a constant value.

The second transverse moment for a linearly sorbing solute is an order of magnitude smaller than that of a non-reactive solute. The linearly sorbing solute however follows the same trend as the non-reactive solute for a time equivalent to $1/\mathrm{E}(k_r)$ before the effect of the sorption is felt. At this time the slope of the line changes and after a period of transition attains the smaller slope corresponding to the reactive solute. The transition zone is a function of the rates and for slow rates we see a much longer zone relative to the case when the rates are high.

Chapter 7

Summary And Recommendations For Future Work

We studied transport of linearly sorbing solutes under non-equilibrium conditions. The main focus was to study the transport of solute at the field scale where physical and chemical heterogeneity characterizes the natural variability of the different parameters like hydraulic conductivity, sorption and desorption rates. We developed an efficient approach to simulate the breakthrough curves accounting for the heterogeneity of the rates. The recursion formulations both for the constant and spatially varying cases are one of the main contributions of this work.

For the case of constant rates, the results for the breakthrough curves are similar to results presented previously [Giddings and Eyring, 1955]. Extension to the more general case of spatially varying rates is easily accomplished within our recursion formulation.

7.1 Important Results

7.1.1 One-dimensional Flow System

1. We formulate a recursion formulation for the transport of linearly sorbing solutes undergoing non-equilibrium sorption. The sorption and desorption rates are

specified in terms of k_f and k_r. Constant or spatially varying sorption kinetics are modeled using the recursion formulation.

2. We investigate the influence of spatial variability in sorption-desorption rates on solute breakthrough by computational studies on one-dimensional systems. The sorption and desorption rates are modeled as two independent random processes with a prescribed mean and covariance structure. Incorporation of spatial variability in the rate parameters is the main feature of this work. The recursion solution, given in terms of the probability density function for solute travel times, is derived by specifying transition probabilities for moving between the aqueous and sorbed phases.

3. The recursion formulation effectively mimics particle tracking involving an infinite number of particles and hence enables accurate modeling of long-tailed breakthrough curves. Variability in sorption-desorption rates typically leads to longer tailed breakthrough curves. The influence of increased variance in sorption-desorption rates is seen for small as well as large Damkohler numbers.

4. Sensitivity studies of the relative influence of variability in sorption and desorption rates reveal that variability in the desorption rate influences solute breakthrough most significantly.

5. We can model the combined processes of sorption and decay by specifying a linear decay rate either in the aqueous and/or the sorbed phases.

7.1.2 Semi-Markov Models of Recursion Formulation

The recursion formulation developed for the simple case of sorption to a single type of site is extended to model more complex processes such as sorption to heterogeneous sites.

1. We model sorption to two or three different sites accessed in parallel by the solute in the aqueous phase. In this hyperexponential model the dissolved solute has a finite probability of accessing each different site with its individual k_r values.

2. We propose a gamma model for sites which are accessed in series and we develop a recursion formulation for two sites.

3. We study the sensitivity of the coefficient of variation (C.V.) for the hyperexponential model and note the influence of the variance which controls the extended tailing on the breakthrough curve. A higher C.V. leads to a sharp peak followed by a long tail of the breakthrough curve. The simulations, however, show that characterization of the problem in terms of C. V. does not provide unique identification of the breakthrough curve. We thus need to know the rates for the different sites explicitly to determine the breakthrough curve.

7.1.3 Streamline Simulator for Field-scale Transport

The recursion formulation obtained for a one-dimensional flow system provides a very efficient method for application to multi-dimensional transport of linearly sorbing solutes. For many non-polar organic solutes, which constitute the contamination at a significant number of facilities in the industrial world, the assumption of

linear sorption is adequate for the ranges of concentration in which these solutes are usually encountered. We address the problem of developing a fast and an efficient transport simulator for kinetically-limited conditions.

1. We develop a two-dimensional algorithm for simulating the transport of a linearly sorbing solute. The simulator is presently applicable to a steady-state flow field. We examined the case of prescribed heads on two sides of a flow domain and no-flow boundaries on the other two sides.

2. We apply the algorithm to model transport of PCE at Borden-like site. We obtain plume characteristics similar to those observed in the field, with areas of high concentrations irregularly distributed and not connected to one another.

3. We evaluate the first three moments for a number of scenarios that represent various combinations of the rates and possible correlations with ln K. These are denoted as FAST, DVAR, SLOW, KDSRF, NCOR1, NCRP5, SMLS, and LRGS.

4. We find that a very simple and general description of the chemical heterogeneity, in terms of spatially varying k_f and k_r uncorrelated with K, provides an adequate description of the plume migration. The centroid displacement, the retardation factor and the longitudinal second moment for the PCE plume at the Borden site are fairly well matched with the FAST case of our simulation runs.

5. We derive an alternate formulation of the one-dimensional breakthrough curve solution obtained by Dagan and Cvetkovic [1993]. The direct probabilistic formulation gives more insight to the mechanistic aspects of transport of a linearly

sorbing solute. We use our result to obtain the first three moments for the constant k_f and k_r case and show that results identical to that of Dagan and Cvetkovic [1993] are obtained. Using the equivalence of the γ and recursion formulation, $P_{n,k}$ we then propose to use our formulation for the case of spatially varying rates to obtain the spatial moment results for this case.

7.1.4 Transverse Dispersion

We next study the transverse dispersion of a sorbing solute in a stratified aquifer.

1. We develop a recursion formulation for computing the transverse dispersion of a non-sorbing solute and a linearly sorbing solute in a spatially varying velocity field. The sorbing solute has sorption and desorption rates which can be constant or spatially varying.

2. The Lagrangian formulation developed above includes local transverse dispersion. The second transverse moment is shown to continuously increase with time, unlike the moment computed by other Lagrangian analyses which do not include local dispersion. Our results, for the non-reactive and reactive solutes, are consistent with similar Eulerian analysis about the large time behavior of the second transverse moment.

7.2 Future Work

Starting from the very simple concept of Markov-process description of linear sorption phenomena, we have obtained a model of the transport behavior of

sorbing solutes exhibiting kinetically-limited rate conditions. However the major question of identifying the rates remain an open question. The identification of these parameters requires significant field and laboratory investigations where carefully designed experiments are run to get the data. The other big issue is the scaling of the rates determined from the small-scale or laboratory experiments to those required for studying field-scale migration. A preliminary attempt to address this issue has been discussed by Cvetkovic [1995]. The discrepancy between laboratory and field reaction parameters may be due to their spatial variability so that data from laboratory experiments do not provide representative values. In addition, due to heterogeneity, mixing will be different in the laboratory and the field, having significant impact on modeled reactions [Kent et al., 1994]. A straightforward approach to this problem is to derive an upscaled, effective value such that the rates are constant along a given flow path [Cvetkovic and Dagan, 1996]. By way of contrast we have tried to apply a simple conceptual model which is very general and allows the examination of the spatially varying interactions of a linearly sorbing solute with the porous media.

Within the framework that we have developed, there are a number of possible extensions that could be made:

1. The one-dimensional recursion model, while appealing, is restricted to linear sorption-desorption reactions for a solute. The recursion formulation can also be extended to modeling multi-component transport involving linear reactions, by beginning from a multi-state Markov process model.

2. We have discussed the combined processes of decay (e.g. radionuclide decay) in the aqueous or the sorbed phase along with sorption. This approach can also be used to study complex processes associated with biodegradation.

3. The semi-Markov model developed for the sorption site heterogeneities can be extended to model colloidal transport where the colloidal phase provides an additional site for sorption.

4. Another avenue of research is the case where sorption and desorption rates are correlated. To handle these situations, cross- correlated k_f and k_r processes can be jointly generated using a Fast Fourier Transform algorithm developed by Bullard, [1994], and Gutjahr et al., [1996].

5. The two-dimensional algorithm could be extended to a three-dimensional flow and transport code.

6. The method could be extended to apply to fields where the velocity field can be changing with time and to a remediation scenario where some initial solute concentration already exists in the aquifer which is then being removed by a pump-and-treat method or by the use of enhanced remediation methods.

7. Similarly, the effect of conditioning of the concentration to observed field data has not been considered. Joint conditioning on transmissivity, head and concentration along the lines of the work by Hughson [1997] could be coupled with the recursion approach.

The main emphasis of this work has been to study the effect of spatially varying sorption and desorption rates on the transport of a linearly sorbing solute. We have found that the interaction between the sorbing solute and the spatially varying velocity field even for the case of steady-state flow in a heterogeneous media results in distinct features of the breakthrough curve which are related to the kinetics

of the sorption processes. In a two-dimensional flow field, these complex interactions produce a plume characterized by a highly irregular pattern of concentration distribution, very similar to those observed in the field experiments.

Analysis of the resulting plumes based on the behavior of the spatial moments supports the hypothesis that the kinetically limited sorption and desorption rates interact in non-linear fashion with velocity field. The numerical scheme with its streamline-based recursion formulation, provides a very attractive option for studying the transport of a reactive solute. Further developments to the model should lead to a very general purpose algorithm suitable for a wide variety of applications in groundwater studies.

Appendix A

List Of Notation

A Macrodispersion, $[L^2/T]$

c Local concentration fluctuation, $[M/L^3]$

C Aqueous Concentration, $[M/L^3]$

$C(\xi)$ Covariance function at a lag ξ

D Hydrodynamic Dispersion, $[L^2/T]$

d First-order decay rate, [1/T]

DaI Damkohler Number I

DaII Damkohler Number II

D_T Diffusion Coefficient, $[L^2/T]$

E Expectation operator

F Mean of ln k_f process

g Freundlich exponent

h Hydraulic head, [L]

J Mean head gradient aligned along the flow direction

$\mathbf{K}$	Hydraulic Conductivity, [L/T]
K_d	Distribution coefficient, $[L^3/M]$
K_F	Freundlich coefficient
K_G	Geometric mean of hydraulic conductivity, [L/T]
k_f	Sorption rate coefficient, [1/day]
k_r	Desorption rate coefficient, [1/day]
L	Length of the column [L]
n	Porosity
$P^j_{n,k}$	Probability that a solute particle takes n space steps to move k time steps starting from state j, j=1 is aqueous state, j=2 is sorbed state
$Q^k_{n,j}$	Probability that a solute particle is in layer n at time k starting from layer j at time 0 (stratified aquifer)
$\mathbf{q}$	Specific discharge, [L/T]
q_j	Probability of moving from layer j to an adjacent layer (stratified aquifer)
r_{11}	Probability of remaining in the aqueous phase
r_{22}	Probability of remaining in the sorbed phase

r_{12} Transition probability to move from the aqueous to the sorbed phase

r_{21} Transition probability to move from the sorbed to the aqueous phase

R Retardation factor

S Mass of solute sorbed per dry unit weigth of solid, [mg/g]

S' Mass of solute sorbed per formation solid volume, [mg/cc]

S_{max} Maximum amount of solute sorbed on a solid, Langmuir model, [mg/g]

U Mean velocity, [L/T]

u Local fluctutaions in velocity, [L/T]

v Random velocity, [L/T]

v_j Velocity in layer j (stratified aquifer), [L/T]

var Variance

v Constant fluid velocity, [L/T]

α Mass transfer coefficient [1/T]

α_L Constant related to Langmuir isotherm

α_i Probability of sorption to site i in hyperexponential model

α_t Local transverse dispesivity

$\beta_j^m(s)$ Probability to leave layer j at time s

starting from state m (stratified aquifer)

Δt Time step [T]

Δx Space step [L]

Δz Distance between two adjacent streamlines (stratified aquifer), [L]

ρ Bulk density of the porous medium, $[M/L^3]$

μ_{kf} Mean of k_f, [1/T]

μ_i Desorption rate of site i in hyperexponential model, [1/T]

ψ Streamfunction, $[L^2/T]$

σ^2 Variance of ln k_f or ln k_r

σ_Y^2, σ_f^2 Variance of ln K

λ, l, I Correlation length of ln K(x), [L]

θ Desorption rate for the gamma model, [1/T]

Appendix B

Modified Covariance Function

A modified form of the covariance function for the retardation factor, R is developed where the two processes k_f and k_r are considered to be two independent processes.

Assume that k_f and k_r are log-normal processes with means given by K_f and K_r, respectively. Further, f_1 and f_2 are mean zero perturbations of the $ln\ k_f$ and $ln\ k_r$ random processes, with variances σ_1^2 and σ_2^2 respectively. The two processes k_f and k_r can then be denoted by

$$k_f = e^{K_f}\, e^{f_1} \tag{B.1}$$

$$k_r = e^{K_r}\, e^{f_2} \tag{B.2}$$

$$K_d = \frac{e^{K_f}}{e^{K_r}}\, e^{f_1 - f_2} \tag{B.3}$$

$$E(K_d) = \frac{e^{K_f}}{e^{K_r}}\, E(e^{f_1 - f_2}) \tag{B.4}$$

$$var(f_1 - f_2) = var(f_1) + var(f_2) \tag{B.5}$$

$$E(e^{f_1 - f_2}) = e^{\frac{\sigma_1^2 + \sigma_2^2}{2}} \tag{B.6}$$

$$R' = R - E(R) = \frac{e^{K_f}}{e^{K_r}} \left(e^{f_1 - f_2} - e^{\frac{\sigma_1^2 + \sigma_2^2}{2}} \right) \tag{B.7}$$

$$cov(R'(x), R'(x+y)) = e^{2\,(K_f - K_r)} e^{\sigma_1^2 + \sigma_2^2} \left(e^{C_1(y) + C_2(y)} - 1 \right) \tag{B.8}$$

where $C_j(y) = cov[f_j(x+y), f_j(x)], j = 1, 2$ represent the covariance function for the two second-order stationary processes f_1 and f_2. For our example we use an exponential covariance function with a variance of 0.1 and correlation length of 4.8 m to match with Chrysikopoulos et al., [1990] results.

Appendix C

Particle Tracking Algorithm For A Linearly Sorbing Solute

A brief description of the particle tracking code used for modeling transport of a linearly sorbing solute in a one-dimensional flow column is given in this appendix.

Describing the sorption process as a Markov process with two states, a sorbed state and an aqueous state, the number of transitions between the two states is given by a Poisson process with the time spent in each state being an exponential distribution.

Using our notation of k_f for the rate of sorption, and k_r for the rate of desorption, the mean time spent in the aqueous state is given by $1/k_f$ and in the sorbed state by $1/k_r$.

The algorithm for the reactive transport is

```
% input parameters

N= number of particles

L= length of column

v=velocity

dt=time step
```

```
D=dispersion coefficient

r12=transition probability for moving from aqueous to sorbed phase

r11=1-r12


for each particle

%start in aqueous phase at 0

%dis=distance moved in one time step

tot=total time spend in the column

dis=0

tot=0

while dis < L

dis= dis+ v*dt + \((2*D*dt)^{0.5}\)

tot=tot+dt

%at end of each time step check probability of moving to sorbed phase

tp=ran % generate a random number from uniform distribution

if tp > r12

move to sorbed phase

% spend  time  in sorbed phase given by an

% exponential distribution with mean 1/kr
```

```
st= time spent in sorbed state

tot=tot+st

else

remain in aqueous state

and check if dis > L

if not go back to beginning of loop

else

check if all particles traversed.

if not go back to next particle

else

quit
```

From the distribution of time taken for all N particles, the breakthrough curve is generated.

A matlab code is available from the author.

Appendix D

Calculation Of Spatial Moments

Spatial moments of the concentration distributions up to third order are calculated to facilitate comparison of the field data with the simulation results and to study how the different physical processes might impact movement of the solute. These spatial moments have been calculated on the basis of the aqueous phase resident concentration [Dagan, 1989]. The zeroth to third spatial moments are given below:

The zeroth moment, which gives the mass of the solute in the aqueous phase

$$M(t) = \int_{R^2} n\, C(\mathbf{x}, t)\, d\mathbf{x} \tag{D.1}$$

where n is the porosity and C(**x**,t) the aqueous concentration.

The first moment about the origin, which defines the location of the center of the mass of the plume

$$X_i(t) = \frac{1}{M} \int_{R^2} n\, x_i\, C(\mathbf{x}, t)\, d\mathbf{x}, i = 1, 2 \tag{D.2}$$

The second moment about the center of mass is a measure of the dispersion of the plume and is given by a second rank covariance tensor whose components are

$$X_{ij}(t) = \frac{1}{M}\int_{R^2} n\, x_i x_j\, C(\mathbf{x},t)\, d\mathbf{x} - X_i X_j,\ i,j = 1,2 \tag{D.3}$$

The third moment and the skewness coefficient are

$$X_{iii}(t) = \frac{1}{M}\int_{R^2} n\, (x_i - X_i(t))^3\, C(\mathbf{x},t)\, d\mathbf{x}, i = 1,2 \tag{D.4}$$

$$\text{Skewness} = \frac{X_{iii}}{X_{ii}^{3/2}} \tag{D.5}$$

The centroid coordinates, defined by the position vector $\mathbf{X}$(t) can be used to calculate the bulk velocity of the plume,

$$V_i(t) = \frac{dX_i(t)}{dt},\ i = 1,2 \tag{D.6}$$

Appendix E

PCE Simulation: Additional Results

We present the simulation results of PCE transport at the Borden site for the case where log K and log K_d are positively correlated with correlation coefficient of 0.5 and 1.0. These cases are also discussed in chapter 5 as PCRP5 and PCOR1.

We present the results for retardation factor (Figure E.1), longitudinal second moment (Figure E.2), longitudinal macrodispersivity (Figure E.3) and skewness coefficient (Figure E.4) for both the cases. In all the cases we find that the positively correlated cases do not show a good match with the field data.

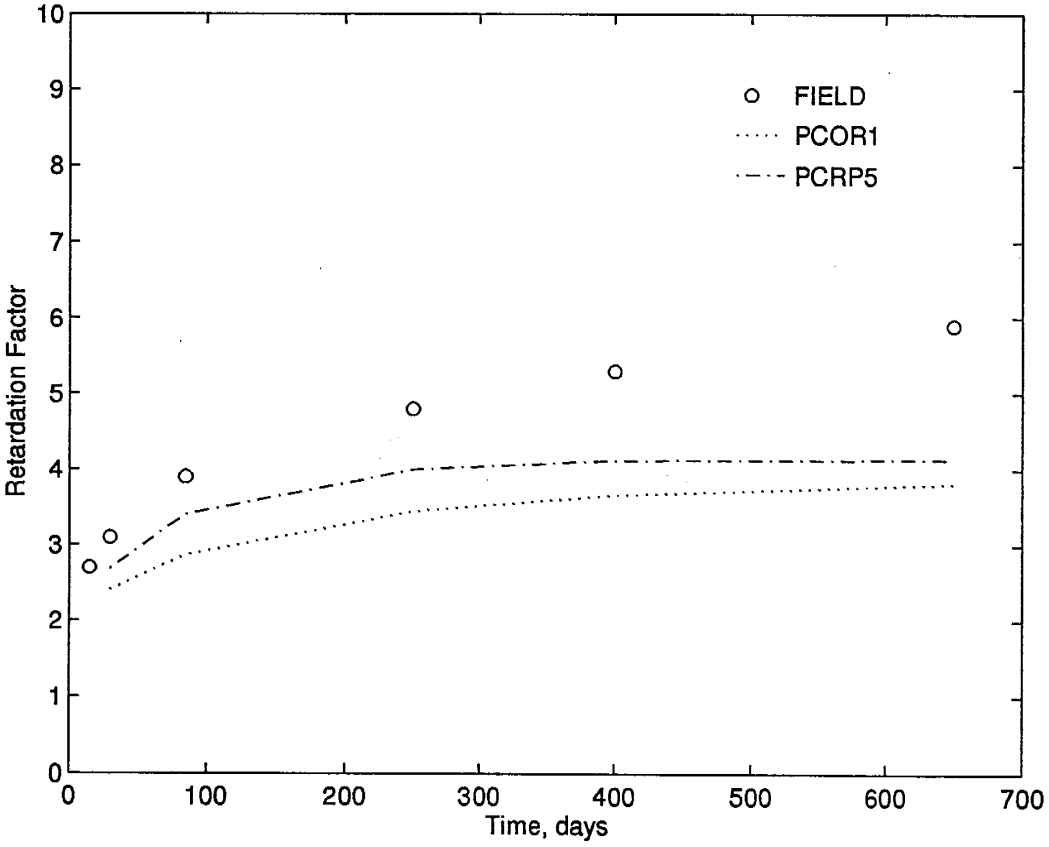

Figure E.1: Retardation factor for the case of positively correlated log $\mathring{\mathrm{K}}$ and log K_d.

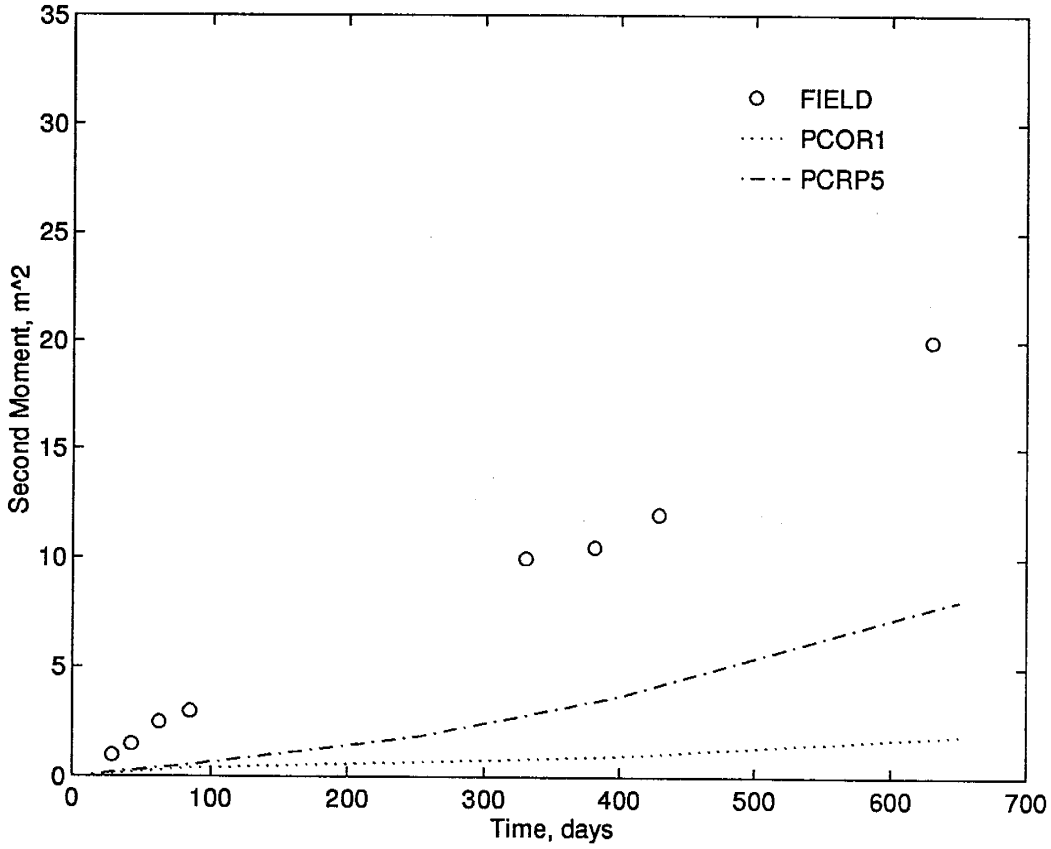

Figure E.2: Longitudinal second moment for the case of positively correlated log K and log K_d.

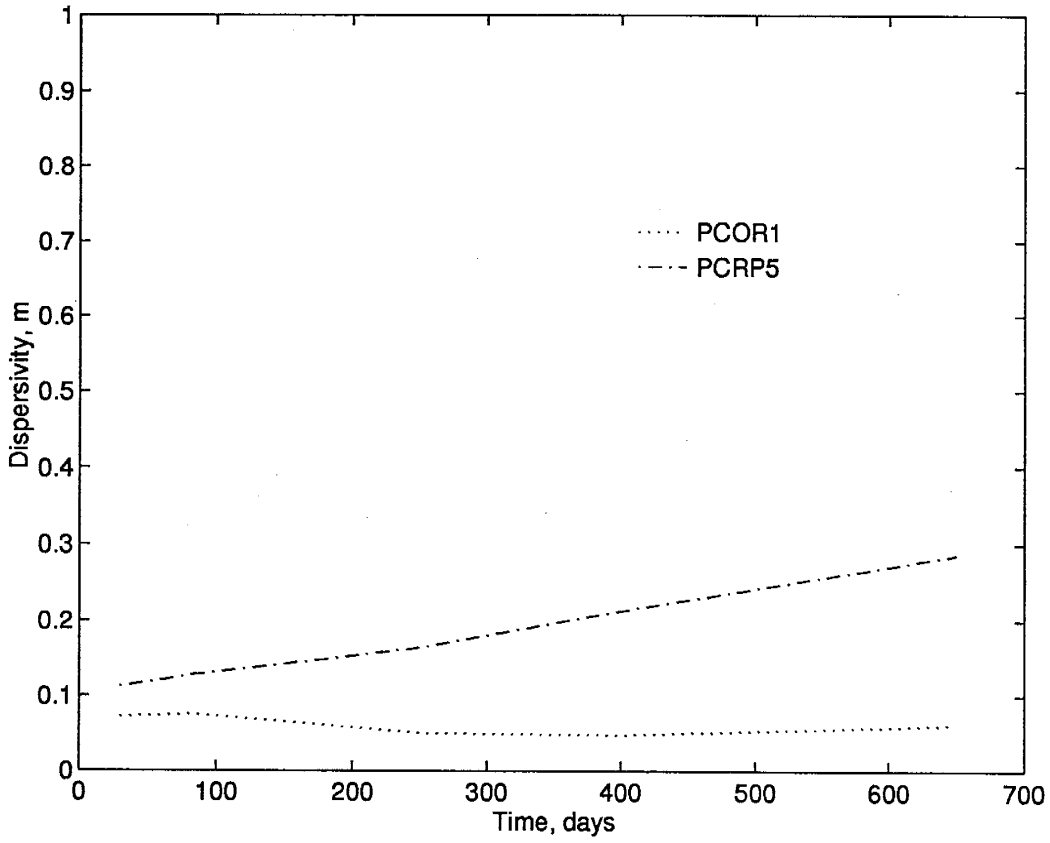

Figure E.3: Longitudinal macrodispersivity for the case of positively correlated log K and log K_d.

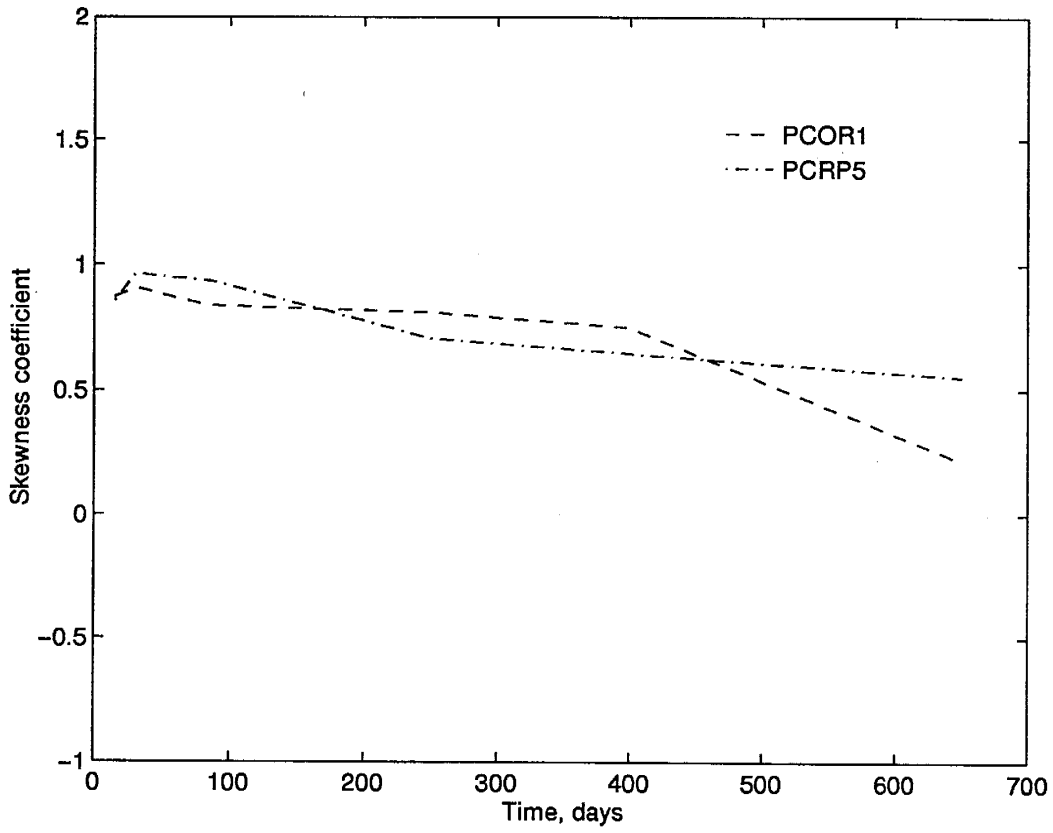

Figure E.4: Skewness coefficient for the case of positively correlated log K and log K_d.

Appendix F

A Probabilistic Model For γ

F.1 Overview

The solution of the transport problem for a linearly sorbing solute in a steady flow field in a heterogeneous aquifer where the velocity was assumed to be a random field was examined by Dagan and Cvetkovic [1993] and Cvetkovic and Dagan [1994]. They assume a uniform mean flow in the horizontal plane and a solute plume of constant concentration injected instantaneously into the formation. They then extend the results for a conservative solute [Dagan, 1984] to a more general form for a reactive solute undergoing kinetically controlled sorption with a constant K_d. The plume is characterized by the expected values of the first three spatial moments. Their approach is summarized below. We follow that by a simple alternate derivation of some important expressions required in the equations of Cvetkovic and Dagan [1994]. We further point out how the recursive approach can be used to extend all of the spatial moment analysis to the non-constant K_d case.

F.2 Previous Results

Cvetkovic and Dagan [1994] relate the moments of the reactive solute to the corresponding moments of the conservative case. The moments used are like those in

Appendix D (equations D.1 and D.2). For e.g.

$$M(t) = \int n\, C(\underline{x}, t) d\underline{x} \tag{F.1}$$

$$\underline{X}(t) = \frac{1}{M(t)} \int n\, \underline{x}\, C(\underline{x}, t) d\underline{x} \tag{F.2}$$

Equation F.2 is the first moment, and similar expressions hold for the other moments. In addition, expected values are applied to the moments to obtain the ensemble results. Thus, for example, the expected second moments, are

$$S_{ij}(t) = E\left[\frac{1}{M(t)} \int n[x_i - E[X_i(t)]]\ [x_j - E[X_j(t)]]\ C(\underline{x}, t) d\underline{x}\right] \tag{F.3}$$

In the Lagrangian framework, some of the basic results given by Cvetkovic and Dagan [1994] are equations for $S_{ij}(t)$ as well as other moments. We will focus primarily on $S_{11}(t)$ in this appendix, i.e. the expected longitudinal second moment. We let $R_{ij}(t)$ be the corresponding second moment for the conservative solute, namely the expectation in equation F.3 for the non-reactive case. For $S_{11}(t)$, Cvetkovic and Dagan [1994] obtain

$$S_{11}(t) = S_{11}(0) + U^2 \left[\frac{\Gamma_2(t)}{\Gamma_0(t)}\right] - U^2 \left[\frac{\Gamma_1(t)}{\Gamma_0(t)}\right]^2 + \frac{1}{\Gamma_0(t)} \int_0^\infty R_{11}(\tau)\gamma(t, \tau) d\tau \tag{F.4}$$

U is the constant mean velocity for the random velocity field. The functions $\Gamma_p(t)$ and $\gamma(t, \tau)$ are the focus of the discussion here and are explained below.

$\gamma(t, \tau)$ is a transfer function for the time it will take a particle to travel distance τ in a non-random unit velocity, one-dimensional field for the reactive case. More specifically, $\gamma(t, \tau)\ d\tau$ is the probability that a particle that starts in the aqueous phase at time 0 will have travelled a distance between τ and $\tau + d\tau$ and will again be in the aqueous phase at time t. Note the integral over τ will simply be the probability

that the particle is in the aqueous phase at time t. With this interpretation we see that $\gamma(t,\tau)\ d\tau$ is analogous to the recurrence formulation given in Chapter 3 for the unit velocity, one-dimensional constant rate case. There we solved for the travel time while here the interest is on travel distance.

The $\Gamma_p(t)$ terms are moments associated with $\gamma(t,\tau)$:

$$\Gamma_p(t) \equiv \int_0^\infty \tau^p \gamma(t,\tau)\ d\tau \tag{F.5}$$

Cvetkovic and Dagan [1994] find $\gamma(t,\tau)$ by solving the advective transport equation coupled with the first-order rate of sorption equation in a unit velocity, one-dimensional field:

$$\frac{\partial C}{\partial t} + \frac{\partial C}{\partial \tau} = -\frac{\partial S}{\partial t} \tag{F.6}$$

$$\frac{\partial C}{\partial t} = k_f\, C - k_r\, S \tag{F.7}$$

They obtain a general solution for the Laplace transform on t:

$$\hat{\gamma}(\tau,s) = exp\{-s[1+W^*(s)]\ \tau\} \tag{F.8}$$

where $W^*(s) = S^*(s)/C^*(s)$, and the asterisks indicate Laplace transforms. For a pulse injection the final solution is

$$\gamma(t,\tau) = exp(-k_f t)\ \delta(t-\tau) + k_f k_r \tau exp(-k_f\tau - k_r t + k_r\tau)\ \tilde{I}_1[k_f k_r \tau(t-\tau)]H(t-\tau) \tag{F.9}$$

$$\tilde{I}_1(Z) = I_1(2Z^{1/2})/Z^{1/2} \tag{F.10}$$

where I_1 is the modified Bessel function of the first kind of order one, H is the Heaviside function and δ is the delta function. Cvetkovic and Dagan [1994] then derive $\Gamma_p(t)$ by differentiating the Laplace transform on τ.

We derive these results based on purely a probabilistic argument which suggests some other ways to treat the spatially variable rate case. We also use a different approach for finding $\Gamma_p(t)$.

F.3 Alternative Derivations

Using the probabilistic interpretation and the exponential residence times implied in the first-order constant rate model, we can derive $\gamma(t,\tau)$ as describe below. The particle starts in the aqueous state at time 0. At time t, it is again set to be in the aqueous state. This can occur in several ways:

1. The particle never leaves the aqueous state. This occurs with probability $e^{-k_f t}$ or with probability density $\delta(t-\tau)\, e^{-k_f t}$;

2. The particle visits the sorbed state n $\geq$ 1 times and enters the aqueous state for the last time at time t-u (see Figure F.1). Then in all the n visits to the aqueous state it spent a total time $\tau - u$ in that state and in all the n visits to the sorbed state state it spent a total time t-τ there. Since these times are sums of independent exponentials each has a gamma distribution. Thus the joint probability density when there are n visits to the two states (aqueous and sorbed) and a final time of u in the aqueous state is

$$\frac{k_r[k_r(t-\tau)]^{n-1}}{(n-1)!}e^{-k_r(t-\tau)}\frac{k_f[k_f(\tau-u)]^{n-1}}{(n-1)!}e^{-k_f(\tau-u)}e^{-k_f u} \qquad \text{(F.11)}$$

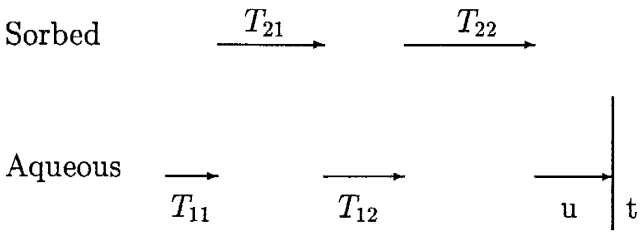

$T_{11} + T_{12} + u = \tau$

$T_{11} + T_{21} + T_{12} + T_{22} + u = t$

$T_{11} + T_{12}$=sum of two independent exponentials, rate k_f

$T_{21} + T_{22}$=sum of two independent exponentials, rate k_r

Figure F.1: Schematic representation of time spent in the aqueous and sorbed states for a sorbing solute with rates k_f, k_r. The number of transitions, n=2.

3. We need to integrate over all u and sum on n, the number of visits to the sorbed state. First integrating,

$$\int_0^\tau \frac{k_r[k_r(t-\tau)]^{n-1}}{(n-1)!} e^{-k_r(t-\tau)} e^{-k_f\tau} \frac{k_f[k_f(\tau-u)]^{n-1}}{(n-1)!} du \qquad \text{(F.12)}$$

$$= \frac{k_r[k_r(t-\tau)]^{n-1}}{(n-1)!} e^{-k_r(t-\tau)} e^{-k_f\tau} \frac{(k_f\,\tau)^n}{n!},\ t \geq \tau \quad . \qquad \text{(F.13)}$$

4. Since n, the number of transitions can range from 1 to infinity, we finally sum over n to get

$$\gamma(t,\tau) = e^{-k_f t}\delta(t-\tau) + \sum_{n=1}^{\infty} \frac{k_r[k_r(t-\tau)]^{n-1}}{(n-1)!} e^{-k_r(t-\tau)}\ e^{-k_f\tau} \frac{(k_f\,\tau)^n}{n!} H(t-\tau) \qquad \text{(F.14)}$$

Noting that

$$I_1(y) = \sum_{n=1}^{\infty} \frac{y^n}{(n-1)!n!} \tag{F.15}$$

we obtain the previous representation of Cvetkovic and Dagan [1994].

F.4 Evaluation of $\Gamma_p(t)$

Before discussing the ramfications of our derivation we note that to obtain the Γ_p's Cvetkovic and Dagan [1994] Laplace transformed γ over τ and needed to evaluate the derivatives given as

$$\Gamma_p(t) = (-1)^p \frac{d^p \hat{\gamma}}{ds^p} \mid_{s=0} \tag{F.16}$$

To find $\Gamma_p(t)$ we will instead use Laplace transform on t.

$$\Gamma_p(t) = \int_0^t \tau^p \gamma(t,\tau) d\tau \tag{F.17}$$

$$\begin{aligned} \Gamma_p(t) &= \int_0^t \tau^p \, e^{-k_f t} \, \delta(t-\tau) + \sum_{n=1}^{\infty} \int_0^t \frac{k_r[k_r(t-\tau)]^{n-1}}{(n-1)!} e^{-k_r(t-\tau)} \\ &\quad e^{-k_f \tau} \frac{k_f^n \tau^{n+p}}{n!} \, d\tau \qquad \text{(F.18)} \\ &= t^p e^{-k_f t} + \sum_{n=1}^{\infty} \int_0^t \frac{k_r[k_r(t-\tau)]^{n-1}}{(n-1)!} e^{-k_r(t-\tau)} \\ &\quad e^{-k_f \tau} \frac{k_f^{n+p+1} \tau^{n+p}}{(n+p)!} \frac{(n+p)\,(n+p-1)\cdots(n+1)}{k_f^{p+1}} \, d\tau \qquad \text{(F.19)} \end{aligned}$$

The Laplace transform on t gives

$$\Gamma_p^*(s) = \frac{p!}{(k_f+s)^{p+1}} + \sum_{n=1}^{\infty} \frac{(n+p)!}{k_f^{p+1}\, n!} \left(\frac{k_f}{k_f+s}\right)^{n+p+1} \left(\frac{k_r}{k_r+s}\right)^n \quad \text{(F.20)}$$

$$= \frac{p!}{(k_f+s)^{p+1}} + \frac{1}{(k_f+s)^{p+1}}$$

$$\left(\sum_{n=0}^{\infty} \frac{(n+p)!}{n!} \left[\frac{k_f k_r}{(k_f+s)\,(k_r+s)}\right]^n - p!\right) \quad \text{(F.21)}$$

$$= \frac{1}{(k_f+s)^{p+1}} \sum_{n=0}^{\infty} \frac{(n+p)!}{n!} \left[\frac{k_f k_r}{(k_f+s)\,(k_r+s)}\right]^n \quad \text{(F.22)}$$

The sum can be evaluated by noting that

$$\sum_{n=0}^{\infty} \frac{(n+p)!}{n!} a^n = \frac{d}{d\,a^p}\left[\frac{a^p}{1-a}\right] \quad \text{(F.23)}$$

and substituting a= $k_f\ k_r/(k_f+s)\ (k_r+s)$ after differentiation.

The moments $\Gamma_p(t)$ can now be evaluated for p=0, 1, 2, etc. For example for p=1;

$$\Gamma_1^*(s) = \frac{1}{(k_f+s)^2}\left(\frac{1}{(1-\frac{k_f k_r}{(k_f+s)(k_r+s)})^2}\right) \quad \text{(F.24)}$$

$$= \frac{(k_r+s)^2}{s^2\,[(k_f+k_r)+s]^2} - \frac{1}{(k_f+s)^2} \quad \text{(F.25)}$$

Inverting this expression using Laplace transform tables [Nixon, 1965] and simplifying we get

$$\Gamma_1(t) = \frac{t}{R^2} + \left(\frac{k_f}{k_r\,R}\right)^2 t\, e^{-(k_f+k_r)t} + \frac{2\,K_d}{k_r R^3}[1-e^{-(k_f+k_r)t}] \quad \text{(F.26)}$$

This agrees with the first spatial moment derived by Cvetkovic and Dagan [1994].

F.5 Consequences and Ramifications

The simpler approach that we present gives a clear insight to the evaluation of the various terms. We can use the same approach to evaluate the temporal

moments in a similar fashion. The physical analogy of γ now allows a very direct comparison with the semi-analytical solution along an individual streamline that we have developed. The significance of the alternate epxression of γ and evaluation of the spatial moments is that we can use our recursion formulation for the case of spatially varying rates and use it to obtain the various moments for the more generalized case of transport in a chemically heterogeneous media. Specifically we can use the variable k_f and k_r to derive γ along a given path. The result would be conditioned on the path. We would then need to generalize the result by unconditioning. This is proposed as part of future work.

References

[1] Adams, E. E., and L. W. Gelhar. Field study of dispersion in a heterogeneous aquifer 2. spatial moments analysis. *Water Resources Research*, 28(12):3293–3307, 1992.

[2] Anderson, M. P. Using models to simulate the movement of contaminants through groundwater flow systems. *CRC Critical Reviews in Environmental Control*, 9, Issue 1:97–156, 1979.

[3] Anderson, M. P., and W. W. Woessner. *Applied Groundwater Modeling, Simulation of flow and advective transport.* Academic Press, 1992.

[4] Andricevic, R., and E. Foufoula-Georgiou. Modeling kinetic non-equilibrium using the first two moments of the residence time distribution. *Journal of Stochastic Hydrology and Hydraulics*, 5:155–171, 1991.

[5] Bahr, J. M., and J. Rubin. Direct comparison of kinetic and local equilibrium formulations for solute transport affected by surface reactions. *Water Resources Research*, 23(3):438–452, 1987.

[6] Bakr, A. A., L. W. Gelhar, A. L. Gutjahr, and J. R. MacMillan. Stochastic analysis of spatial variablity in subsurface flows, 1, Comparison of one- and three-dimensional flows. *Water Resources Research*, 14:263–271, 1978.

[7] Ball, W. P., C. Buehler, T. C. Harmon, D. M. Mackay, and P. V. Roberts. Characterization of a sandy aquifer material at the grain scale. *Journal of Contaminant Hydrology*, 5(3):253–295, 1990.

[8] Ball, W. P., and P. V. Roberts. Long-term sorption of halogenated organic chemicals by aquifer material, 2. Intraparticle diffusion. *Environmental Science and Techology*, 25:1237–1249, 1991.

[9] Barber II, L. B., E. M. Thurman, and D. D. Runnells. Geochemical heterogeneity in a sand and gravel aquifer: Effect of sediment mineralogy and particle size on the sorption of chlorobenzenes. *Journal of Contaminant Hydrology*, 9:35–54, 1992.

[10] Bear, J. *Dynamics of fluids in porous media.* Elsevier, New York, 1972.

[11] Bellin, A., P. Salandin, and A. Rinaldo. Simulation of dispersion in heterogeneous porous formations: Statistics, first-order theories, convergence of computations. *Water Resources Research*, 28(9):2211–2227, 1992.

[12] Bellin, A., A. Rinaldo, W. J. P. Bosma, van der Zee, S. E. A. T. M., and Y. Rubin. Linear Equilibrium adsorbing solute transport in physically and chemically heterogeneous porous formation 1.Analytical solutions. *Water Resources Research*, 29(12):4019–4030, 1993.

[13] Bouchard, D. C., A. L. Wood, M. L. Campbell, P. Nkedi-Kizza, and P. S. C. Rao. Sorption non-equilibrium during solute transport. *Journal of Contaminant Hydrology*, 2:209–223, 1988.

[14] Bramlett, W., and R. C. Borden. Numerical generation of flow nets- the FLOWNS model. *Ground Water*, 28(6):946–950, 1990.

[15] Brusseau, M. L., R. E. Jessup, and P. S. C. Rao. Modeling the transport of solutes influenced by multiprocess non-equilibrium. *Water Resources Research*, 25(9):1971–1988, 1989.

[16] Brusseau, M. L., and P. Rao. Sorption nonideality during organic contaminat transport in porous media. *CRC Critical Reviews in Environmental Control*, 19, Issue 1:33–99, 1989a.

[17] Brusseau, M. L., and P. Rao. The influence of sorbate-organic matter interactions on sorption nonequilibrium. *Chemosphere*, 18, Nos. 9/10:1691–1706, 1989b.

[18] Brusseau, M. L. Transport of rate-limited sorbing solutes in heterogeneous porous media: Application of one-dimensional multifactor nonideality model to field data. *Water Resources Research*, 28:2485–2497, 1992.

[19] Bullard, B. E. Cross-correlated random field simulations using the spectral representation theorem. Master's thesis, New Mexico Institute of Mining and Technology, 1994. M.S. Thesis 69 pages.

[20] Burnett, R. D., and E. Frind. Simulation of contaminant transport in three-dimensions: 1, The alternating direction Galerkin technique. *Water Resources Research*, 23(4):683–694, 1987.

[21] Burr, D. T., E. A. Sudicky, and R. L. Naff. Nonreactive and reactive solute transport in three-dimensional heterogeneous porous media: Mean displace-

ment, plume spreading, and uncertainty. *Water Resources Research*, 30:791–816, 1994.

[22] Cameron, D. R., and A. Klute. Convective dispersive solute transport with a combined equilibrium and kinetic model. *Water Resources Research*, 13:183–188, 1977.

[23] Chen, W., and R. J. Wagenet. Solute transport in porous media with sorption-site heterogeneity. *Environmental Science and Techology*, 29:2725–2734, 1995.

[24] Chiou, C. T. Theoretical considerations of the partition uptake of nonionic organic compounds by soil organic matter. In B. L. Sawhney and K. Brown, editors, *Reactions and movement of organic chemicals in soils*, pages 1–29. Soil Science Society of America, Madison, WI, 1989. SSSA Special Publication 22.

[25] Chrysikopoulos, V. D., P. K. Kitanidis, and P. V. Roberts. Analysis of one-dimensional solute transport through media with spatially variable retardation factor. *Water Resources Research*, 26(3):437–446, 1990.

[26] Chrysikopoulos, V. D., P. K. Kitanidis, and P. V. Roberts. Macrodispersion of sorbing solutes in heterogeneous porous formations with spatially periodic retardation factor and velocity field. *Water Resources Research*, 28:1517–1530, 1992.

[27] Coats, K. H., and B. D. Smith. Dead-end pore volume and dispersion in porous media. *Journal of Society of Petroleum Engineering*, 4:73–84, 1964.

[28] Cunningham, A. B., W. G. Characklis, F. Abedeen, and D. Crawford. Influence of biofim accumulation on porous media hydrodynamics. *Environmental*

Science and Techology, 25:1305–1311, 1991.

[29] Curtis, G. P., P. V. Roberts, and M. Reinhard. A natural gradient experiment on solute transport in a sand aquifer, 4 Sorption of organic solute and its influence on mobility. *Water Resources Research*, 22(13):2059–2067, 1986.

[30] Cushman, J. H. Diffusion in fractal porous media. *Water Resources Research*, 27(4):643–644, 1991.

[31] Cushman, J. H. and T. R. Ginn. Nonlocal dispersion in media with continuously evolving scales of heterogeneity. *Transport in porous media*, 13:123–138, 1993.

[32] Cushman, J. H., B. X. Hu, and F. W. Deng. Nonlocal reactive transport with physical and chemical heterogeneity: Localization errors. *Water Resources Research*, 31(9):2219–2237, 1995.

[33] Cushman, J. H., B. X. Hu, and F. Deng. Comparison of Eulerian to Lagrangian expected moments for transport in a heterogeneous porous medium with deterministic linear nonequilibrium sorption. *Chem. Eng. Com.*, 146–150:5–21, 1996.

[34] Cvetkovic, V., and A. M. Shapiro. Mass arrival of sorptive solute in heterogeneous porous media. *Water Resources Research*, 26(5):2057–2067, 1990.

[35] Cvetkovic, V., and G. Dagan. Transport of kinetically sorbing solute by steady random velocity in heterogeneous porous formations. *Journal of Fluid Mechanics*, 265:189–215, 1994.

[36] Cvetkovic, V. Transport of reactive solutes. Subsurface flow and transport: the stochastic approach, 1995. UNESCO Kovacs Colloquium.

[37] Cvetkovic, V., and G. Dagan. Reactive transport and immiscible flow in geological media. 2 Application. *Proceedings of the Royal Soc. of London A*, 452:303–328, 1996.

[38] Dagan, G. Stochastic modeling of groundwater flow by unconditional and conditional probabiities, 2, The solute tranport. *Water Resources Research*, 18:835–848, 1982.

[39] Dagan, G. Solute transport in heterogeneous porous formations. *Journal of Fluid Mechanics*, 145:151–177, 1984.

[40] Dagan, G. Statistical theory of groundwater flow and transport: Pore to laboratory, laboratory to formation, and formation to regional scale. *Water Resources Research*, 22:120S–134S, 1986.

[41] Dagan, G. Theory of solute transport by groundwater. *Annual Reviews in Fluid Mechanics*, 19:183–215, 1987.

[42] Dagan, G. Time-dependent macrodispersion for solute transport in anisotropic heterogeneous formations. *Water Resources Research*, 24(9):1491–1500, 1988.

[43] Dagan, G. *Flow and transport through porous formations.* Springer-Verlag, 1989.

[44] Dagan, G., and S. P. Neuman. Nonasymptotic behavior of a common Eulerian approximation for transport in random velocity fields. *Water Resources Research*, 27(12):3249–3256, 1991.

[45] Dagan, G., and V. Cvetkovic. Spatial moments of a kinetically sorbing plume in a heterogeneous aquifer. *Water Resources Research*, 29(12):4053–4061, 1993.

[46] Daus, A. D., and E. O. Frind. An alternatinf direction Galerkin technique for simulation of contaminant transport in complex groundwater systems. *Water Resources Research*, 21(5):653–664, 1985.

[47] Deng, F. W., J. H. Cushman, and J. W. Dellur. A fast Fourier transform stochastic analysis of the contaminant transport problem. *Water Resources Research*, 29(9):3241–3247, 1993.

[48] Dougharty, N. A. Effect of adsorbent particle-size distribution in gas-solid chromatography. *American Institution of Chemical Engineering Journal*, 18(3):657–659, 1972.

[49] Dykaar, B. B., and P. K. Kitanidis. Macrotransport of a biologically reacting solute through porous media. *Water Resources Research*, pages 307–320, 1996.

[50] Fetter, C. W. *Contaminant Hydrogeology.* Prentice Hall, 1993.

[51] Fogg, G. E., and R. K. Senger. Automatic generation of flow nets with conventional ground-water modeling algorithms. *Ground Water*, 23(3):336–344, 1985.

[52] Freeze, R. A . A stochastic-conceptual analysis of one-dimensional groundwater flow in nonuniform homogeneous media. *Water Resources Research*, 11:725–741, 1975.

[53] Freyberg, D. L. A natural gradient experiment on solute transport in a sand aquier, 2, Spatial moments and the advection and dispersion of nonreactive tracers. *Water Resources Research*, 22(13):2031–2046, 1986.

[54] Friedly, J. C., and J. Rubin. Solute transport with multiple equilibrium-controlled or kinetically controlled chemical reactions. *Water Resources Research*, 28:1935–1953, 1992.

[55] Gamerdinger, A. P., R. J. Wagenet, and M. T. van Genuchten. Application of two-site/two-region models for studying simulataneous nonequilibrium transport and degradation of pesticides. *Soil Science Society of America Journal*, 54:957–963, 1990.

[56] Garabedian, S. P. *Large-scale dispersive transort in aquifers: Field experiments and reactive transport theory.* PhD thesis, Dep. of Civil Engg., Mass. Inst. of Technol., Cambridge, 1987. 290 pages.

[57] Garabedian, S. P., L. W. Gelhar, and M. A. Celia. Large scale dispersive transport in aquifers: Field experiments and reactive transport theory. Technical Report Rep. 315, Ralph M. Parsons Lab., Dep. of Civil Eng., M. I. T., Cambridge, 1988. 290 pages.

[58] Gardiner, C. W. *Handbook of stochastic methods for physics, chemistry and the natural sciences.* Springer Verlag, New York, 1990.

[59] Gelhar, L. W., A. L. Gutjahr, and R. L. Naff. Stochastic analysis of macrodispersion in a statified aquifer. *Water Resources Research*, 15(6):1387–1397, 1979.

[60] Gelhar, L. W., and C. L. Axness. Three-dimensional stochastic analysis of macrodispersion in aquifers. *Water Resources Research*, 19(1):161–180, 1983.

[61] Giddings, J. C., and H. Eyring. A molecular dynamic theory of chromatography. *Journal of Physical Chemistry*, 59:416–421, 1955.

[62] Goltz, M. N., and P. V. Roberts. Interpreting organic solute transport data from a field experiment using physical nonequilibrium models. *Journal of Contaminant Hydrology*, 1(1/2):77–93, 1986.

[63] Goltz, M. N., and P. V. Roberts. Simulation of physical nonequilibrium solute transport models: Application to a large-scale field experiment. *Journal of Contaminant Hydrology*, 3(1):37–63, 1988.

[64] Graham, W., and D. McLaughlin. Stochastic analysis of nonstationary subsurface solute transport 1. unconditional moments. *Water Resources Research*, 25(2):215–232, 1989a.

[65] Graham, W. and D. McLaughlin. Stochastic analysis of nonstationary subsurface solute transport 2. conditional moments. *Water Resources Research*, 25(11):2331–2335, 1989b.

[66] Grathwohl, P. Influence of organic matter from soild and sediments of various origins on the sorption of some chlorinated aliphatic hydrocarbons: Implications on K_{oc} correlations. *Environmental Science and Techology*, 24:1687–1693, 1990.

[67] Gutjahr, A. L. Fast Fourier transform for random field generation. Technical Report Contract Number 4-58-2690R, New Mexico Institute of Mining and Technology, 1989. Project Report for Los Alamos Grant.

[68] Gutjahr, A. L., B. Bullard, and S. Hatch. Joint conditional simulations and flow modeling. In R. Dimitrakopoulos, editor, *Geostatistics for the next century*, pages 185–96. Kluwer Academic Publishers, 1994.

[69] Gutjahr, A. L., B. Bullard, and S. Hatch. General joint conditional simulations using a Fast Fourier Transform method. *accepted for publication in Math. Geology*, 1996.

[70] Haggerty, R. and S. M. Gorelick. Multiple-rate mass transfer for modeling diffusion and surface reactions in media with pore-scale heterogeneity. *Water Resources Research*, 31(10):2383–2400, 1995.

[71] Harmon, T. C., and P. V. Roberts. Comparison of intraparticle sorption and desorption rates for a halogenated alkene in a sandy aquifer material. *Environmental Science and Techology*, 28:1650–1660, 1994.

[72] Harmon, T. C., L. Semprini, and P. V. Roberts. Simulating groundwater solute transport using laboratory determined sorption parameters. *Journal of Environmental Engineering*, 118(5):666–689, 1992.

[73] Hayes, M. H. B., and F. L. Himes. Nature and properties of humus-mineral complexes. In P. M. Huang and M. Schnitzer, editors, *Interactions of soil minerals with natural organics and microbes*, pages 103–158. Soil Science Society of America, Madison, WI, 1986.

[74] Hewett, T., and R. Behrens. Scaling laws in reservoir simulation and their use in a hybrid finite difference/streamtube approach to simulation of the effects of permeability heterogeneity. In L. Lake and J. Carroll, editors, *Reservoir Characterization II.* Academic Press, Inc., London, 1991.

[75] Hu, B. X., F. Deng, and J. H. Cushman. Nonlocal reactive transport with physical and chemical heterogeneity: Linear nonequilibrium sorption with random Kd. *Water Resources Research*, 31:2239–2252, 1995.

[76] Hu, B. X., and J. H. Cushman. Comparison of nonlocal-eulerian to lagrangian moments for transport in an anisotropic heterogeneous aquifer with deterministic linear nonequilibrium sorption. *Water Resources Research*, 33(4):891–896, 1997.

[77] Hu, B. X., F. Deng, and J. H. Cushman. Nonlocal reactive transport with physical and chemical heterogeneity: Linear nonequilibrium sorption with random rate coefficients. Recent Advances in Stochastic Hydrology, ed. G. Dagan and S. P. Neuman, Cambridge/UNESCO (in press), 1997.

[78] Hughson, D. *A Geostatistical inverse method for conditioning randomly heterogeneous transmissivity fields on transient hydraulic head data.* PhD thesis, New Mexico Inst. of Mining and Technology, Socorro, New Mexico, 1997.

[79] Huyakorn, P. S., and G. F. Pinder. *Computational methoda in subsurface flow.* Academic Press, 1983.

[80] James, R. V., and J. Rubin. Applicability of the local equilibrium assumption to transport through soils of solutes affected by ion exchange. In E. A. Jeanne, editor, *Chemical Modeling of Aqueous Systems*, pages 225–235. American Chemical Society, Washington, D.C., 1979.

[81] Kabala, Z. J., and G. Sposito. A stochastic model of reactive solute transport with time varying velocity in a heterogeneous aquifer. *Water Resources Research*, 27(3):341–350, 1991.

[82] Kent, D. B., J. A. Davis, L. D. Anderson, B. A. Rea, and T. D. Waite. Transport of chromium and selenium in the suboxic zone of a shallow aquifer: Influence

of redox and adsorption reactions. *Water Resources Research*, 30:1099–1114, 1994.

[83] Kinzelbach, W. The random walk method in pollutant transport simulation. In E. Custodio, A. Gurgui, and J. P. L. Ferreira, editors, *Groundwater flow and quality modeling*, pages 227–245. D. Reidel Publishing Company, 1988. Nato ASI series C, volume 224.

[84] Kinzelbach, W., and G. Uffink. The random walk method and extensions in groundwater modeling. In J. Bear and M. Y. Corapcioglu, editors, *Transport processes in porous media*, pages 761–787. Kluwer Academic, Massachusetts, 1991.

[85] Kitanidis, P. K. Particle Tracking equations for the solution of the advection-dispersion equation with variable coefficients. *Water Resources Research*, 30:3225–3227, 1994.

[86] Koch, D. L., and J. F. Brady. Nonlocal dispersion in porous media: Nonmechanical effects. *Chemical Engineering Science*, 42:1377–1392, 1987.

[87] Koch, D. L., and J. F. Brady. Anamolous diffusion in heterogeneous porous media. *Physics of Fluids*, 31:965–973, 1988.

[88] LaBolle, E. M., G. E. Fogg, and A. F. B. Tompson. Random-walk simulation of transport in heterogeneous porous media: Local mass-conservation problem and implementation methods. *Water Resources Research*, 32:583–593, 1996.

[89] Lake, L. W., J. R. Johnston, and G. L. Stegemeier. Simulation and performance prediction of a large-scale surfactant/polymer project. *Soc. Pet. Engg. Journal*,

21:731–739, 1981.

[90] LeBlanc, D. R., S. P. Garabedian, K. M. Hess, L. W. Gelhar, R. D. Quadri, K. G. Stollenwerk, and W. W. Wood. Large scale natural gradient tracer test in sand and gravel, Cape Cod, Massachusetts, 1, Experimental design and observed tracer movement. *Water Resources Research*, 27(5):895–910, 1991.

[91] Mackay, D. M., D. L. Freyberg, P. V. Roberts, and J. A. Cherry. A natural gradient experiment on solute transport in a sand aquifer 1. Approach and overview of plume movement. *Water Resources Research*, 22(13):2017–2029, 1986.

[92] Martin, J. C., and R. E. Wegner. Numerical simulation of multiphase, two-dimensional incompressible flow using streamtube relationships. *Soc. Petroleum Engg. Journal*, 19:313–323, 1979.

[93] Matanga, G. B. Pseudopotential functions in construction of flow nets for contaminant transport modeling. *Water Resources Research*, 24(4):553–560, 1988.

[94] Matanga, G. B. Stream functions in three-dimensional groundwater flow. *Water Resources Research*, 29(9):3125–3133, 1993.

[95] Matanga, G. B. Characteristics in evaluating stream functions in groundwater flow. *Journal of Hydrol. Eng. Am. Soc. Civ. Eng.*, 1(1):49–53, 1996.

[96] McNab, W. W., and T. N. Narasimhan. Modeling reactive transport of organic compounds in groundwater using a partial redox disequilibrium approach. *Water Resources Research*, 30:2619–2635, 1994.

[97] Miller, C. T., and W. J. Weber. Sorption of hydrophobic organic pollutants in saturated soil system. *Journal of Contaminant Hydrology*, 1:243–261, 1986.

[98] Mingelgrin, U. and Z. Gerstl. Reevaluation of partitioning as a mechanism of nonionic chemicals adsorption in soils. *Journal of Environmental Quality*, 12:1–11, 1982.

[99] Miralles-Wilhelm, F., and L. W. Gelhar. Stochastic analysis of sorption macrokinetics in heterogeneous aquifers. *Water Resources Research*, 32(6):1541–1550, 1996.

[100] Mizell, S. A., L. W. Gelhar, and A. L. Gutjahr. Stochastic analysis of spatial variability in two-dimensional steady groundwater flow assuming stationary and nonstationary heads. *Water Resources Research*, 18(4):1053–1068, 1982.

[101] Naff, R. L. On the nature of the dispersive flux in saturated heterogeneous porous media. *Water Resources Research*, 26(5):1013–1026, 1990.

[102] Neuman, S. P. Eulerian-Lagrangian theory of transport in space-time nonstationary velocity field: Exact nonlocal formalism by conditional moments and weak approximations. *Water Resources Research*, 29(3):633–645, 1993.

[103] Nixon, F. E. *Handbook of Laplace Transformation.* Prentice-Hall Inc., Engelwood Cliffs, N. J., 1965.

[104] Nkedi-Kizza, P., J. M. Biggar, M. T. van Genuchten, P. J. Wierenga, H. M. Selim, J. J. Davidson, and D. R. Nielson. Modeling tritium and chloride36 transport through an aggregated oxisol. *Water Resources Research*, 19:691–700, 1983.

[105] Pavlostathis, S. G., and G. N. Mathavan. Desorption kinetics of selected volatile organic compounds from field contaminated soils. *Environmental Science and Techology*, 26:532–538, 1992.

[106] Pignatello, J. J. Sorption dynamics of organic compounds in soils and sediments. In B. L. Sawhney and K. Brown, editors, *Reactions and movement of organic chemicals in soils*, pages 45–80. Soil Science Society of America, Madison, WI, 1989. SSSA Special Publication 22.

[107] Pignatello, J. J. Slowly reversible sorption of aliphatic halocarbons in soils 2. Mechanistic aspects. *Environmental Toxicology and Chemistry*, 9:1117–1126, 1990.

[108] Pignatello, J. J., and L. Q. Huang. Sorptive reversibility of Atrazine and Metachlor residues in field soil samples. *Journ. of Env. Quality*, 20:222–228, 1991.

[109] Pignatello, J. J. Recent advances in sorption kinetics. In A. J. Beck, K. C. Jones, M. Hayes, and U. Mingelrin, editors, *Organic substances in soil and water: Natural constituents and their influences on contaminant behavior*, pages 128–140. The Royal Society of Chemistry, Cambridge, UK, 1993. Special Publication 135.

[110] Pignatello, J. J., F. J. Ferrandino, and L. Q. Huang. Elution of aged and freshly added herbicides from a soil. *Environmental Science and Techology*, 27:1563–1571, 1993.

[111] Prickett, T. A., G. Naymik, and C. G. Lonnquist. A random-walk solute transport model for selected groundwater quality evaluations. Technical report, Illinois State Water Survey, Urbana, Illinois, 1981.

[112] Ptacek, C. J., and R. W. Gilham. Laboratory and field measurements of non-equilibrium transport in the Borden aquifer, Ontario, Canada. *Journal of Contaminant Hydrology*, 10:119–158, 1992.

[113] Quinodoz, H. M., and A. J. Valocchi. Stochastic analysis of the transport of kinetically sorbing solutes in aquifers with randomly heterogeneous hydraulic conductivity. *Water Resources Research*, 29(9):3227–3240, 1993.

[114] Rajaram, H., and L. W. Gelhar. Plume-scale dependent dispersion in heterogeneous aquifers: 1. Lagrangian analysis in a stratified aquifer. *Water Resources Research*, 29(9):3249–3260, 1993.

[115] Rajaram, H. Time and scale dependent effective retardation factors in heterogeneous aquifers. *Advances in Water Resources*, 20(4):217–230, 1997.

[116] Rao, P. S. C., R. E. Jessup, D. E. Rolston, J. M. Davidson, and D. P. Kilerease. Experimental and mathematical description of non-adsorbed solute transfer by diffusion in spherical aggregates. *Soil Science Society of America Journal*, 44:684–688, 1980a.

[117] Rao, P. S. C., D. E. Rolston, R. E. Jessup, and J. M. Davidson. Solute transport in aggregated porous media: Theoretical and experimental evaluation. *Soil Science Society of America Journal*, 44:1139–1146, 1980b.

[118] Rittmann, B. E. The significance of biofilms in porous media. *Water Resources Research*, 29:2195–2202, 1993.

[119] Roberts, P. V., M. N. Goltz, and D. M. Mackay. A natural gradient experiment on solute transport in a sand aquifer, 3, Retardation estimates and mass balances for organic solutes. *Water Resources Research*, 22(13):2047–2058, 1986.

[120] Roberts, P. V., and D. M. Mackay. A natural gradient experiment on solute transport in a sand aquifer. Technical Report Rep. No. 292, Dep. of Civil Eng., Stanford University, 1986.

[121] Robin, M. J. L. *Migration of reactive solutes in three-dimensional heterogeneus porous media.* PhD thesis, Dept. of Earth Sciences, Univ. of Waterloo, Waterloo, Ontario, Canada, 1991. Ph. D. thesis.

[122] Robin, M. J. L., E. A. Sudicky, R. W. Gilham, and R. G. Kachanoski. Spatial variability of strontium distribution coefficients and their correlation with hydraulic conductivity in the Canadian Forces Base Borden aquifer. *Water Resources Research*, 27:2619–2632, 1991.

[123] Ross, N. G. *Introduction to probability models.* Academic Press, 1989.

[124] Rubin, J. Transport of reacting solutes in porous media: relation between mathematical nature of problem formulation and chemical nature of reactions. *Water Resources Research*, 19(5):1231–1252, 1983.

[125] Sardin, M., D. Schweich, F. J. Leij, and M. T. van Genuchten. Modeling the nonequlibrium transport of linearly interacting solutes in porous media: A review. *Water Resources Research*, 27(9):2287–2307, 1991.

[126] Scheidegger, A. E. Statistical hydrodynamics in porous meida. *Journal of Geophysical Research*, 66(10):3273–3278, 1954.

[127] Scribner, S. L., T. R. Benzig, S. Sun, and S. A. Boyd. Desorption and bioavailability of aged Simazine residues in soil from a continuous corn field. *Journal of Environmental Quality*, 21:115–120, 1992.

[128] Selroos, J. O., and V. Cvetkovic. Modeling solute advection coupled with sorption kinetics in heterogeneous formations. *Water Resources Research*, 28:1271–1278, 1992.

[129] Simmons, C. S., T. R. Ginn, and B. D. Wood. Stochastic-convective transport with nonlinear reaction: Mathematical framework. *Water Resources Research*, 31:2675–2689, 1995.

[130] Steinberg, S. M., J. J. Pignatello, and B. L. Sawhney. Persistence of 1,2-dibromomethane in soils: Entrapment in intraparticle micropores. *Environmental Science and Techology*, 21:1201–1208, 1987.

[131] Stollenwerk, K. G. Modeling adsorption of molybdate. *Water Resources Research*, 31(2):347–357, 1995.

[132] Sudicky, E. A., J. A. Cherry, and E. O. Frind. Migration of contaminants in groundwater at a landfill: A case study 4. A natural-gradient dispersion test. *Journal of Hydrology*, 63:81–108, 1983.

[133] Sudicky, E. A . A natural gradient experiment on solute transport in a sand aqifer: Spatial variability of hydraulic conductivity and its role in the dispersion process. *Water Resources Research*, 22(13):2069–2082, 1986.

[134] Sudicky, E. A. The Laplace transform Galerkin technique: A time- continuous finite element theory and application to mass transport in groundwater. *Water Resources Research*, 25(8):1833–1846, 1989.

[135] Sudicky, E. A. The Laplace transform Galerkin technique for large-scale simulation of mass transport in discretely fractured porous formations. *Geoderma*, 46:209–232, 1990.

[136] Taylor, G. I. Diffusion by continuous movements. *Proc. London Math. Soc.*, 2(20):196–214, 1921.

[137] Taylor, S. W., and P. R. Jaffe'. Biofilm growth and the related changes in the physical properties of a porous medium, 1, Experimental investigation. *Water Resources Research*, 26:2153–2159, 1990.

[138] Therrien, R., E. A. Sudicky, and M. L. Brusseau. Three-dimensional analysis of solute transport in heterogeneous aquifers under multiprocess nonequilibrium. In *International Conference and workshop on transport and mass exchange processes in sand and gravel aquifers: Field and modeling studies*, Ottawa, Ontario, Canada, 1990. AGU.

[139] Thiele, M. R., R. P. Batycky, M. J. Blunt, and F. M. Orr. Simulating flow in heterogeneous systems using stremtubes and streamlines. *SPE Reservoir Engineering*, February:5–12, 1996.

[140] Tompson, A. F. B. Numerical simulation of solute transport in three-dimensional, randomly heterogeneous porous media. *Water Resources Research*, 26:2541–2562, 1987.

[141] Tompson, A. F. B., and L. Gelhar. Numerical simulation of solute transport in three-dimensional, randomly heterogeneous porous media. *Water Resources Research*, 26:2541–2562, 1990.

[142] Tompson, A. F. B. Numerical simulation of chemical migration in physically and chemically heterogeneous porous media. *Water Resources Research*, 29(11):3709–3726, 1993.

[143] Tsang, C. F., L. W. Gelhar, G. Marsily, and J. Andersson. Solute transport in heterogeneous media: A discussion of technical issues coupling site characterization and predictive assessment. *Advances in Water Resources*, 17:259–264, 1994.

[144] Uffink, G. J. M. A random-walk method for the simulation of macrodispersion in a stratified aquifer. In *Relation of groundwater quality and quantity.* Proceedings of IUGG-IASH symposium in Hamburg, 1983, IASH Publication 146, 1985.

[145] Valocchi, A. J. Spatial moment analysis of the transport of kinetically adsorbing solutes through stratified aquifers. *Water Resources Research*, 25:273–279, 1989.

[146] Valocchi, A. J. Use of temporal moment analysis to study reactive solute transport in aggregated porous media. *Geoderma*, 46:233–247, 1990.

[147] van Genuchten, M. T., D. H. Tang, and R. Guennelon. Some exact solutions for solute transport through soils containing large cylindrical macropores. *Water Resources Research*, 20(3):335–346, 1984.

[148] van Genuchten, M. T., and R. J. Wagnet. Two site/ two region models for pesticide transport and degradation: Theoretical development and analytical solution. *Soil Science Society of America Journal*, 53:1303–1310, 1989.

[149] Van Kampen, N. G. *Stochastic processes in physics and chemistry.* North-Hollan Publishing Company, 1981.

[150] Vandervivere, P. and P. Baveye. Saturated hydraulic conductivity reduction caused by aerobic bacteria in sand column. *Soil Science Society of America Journal*, 156:1–13, 1992.

[151] Villermaux, J. Theory of linear chromatography. In A. E. Rodrigues and D. Tondeur, editors, *Percolation processes, Theory and Applications*, pages 83–140. NATO ASI Series E, 33, 1981.

[152] Villermaux, J. Chemical engineering approach to dynamic modelling of linear chromatography: A flexible method for representing complex phenomena from simple concepts. *Journal of Chromatography*, 406:11–26, 1987.

[153] Villermaux, J. Dynamics of linear interactions in heterogeneous media: A systems approach. *Journal of Petroleum Science and Engineering*, 4:21–30, 1990.

[154] VomVoris, E. G. *Concentration variability in transport in heterogeneous aquifers: A stochatic analysis.* PhD thesis, Dep. of Civil and Environ. Eng., Mass. Inst. of Technology, Cambridge, 1986. Ph.D thesis.

[155] Weber Jr., W. J., P. M. McGinley, and L. E. Katz. Sorption phenomena in subsurface systems: Concepts, models and effects on contaminant fate and

transport. *Water Resources*, 25(5):499–528, 1991.

[156] Weber Jr., W. J., P. M. McGinley, and L. E. Katz. A distributed reactivity model for sorption by soils and sediments 1, Conceptual basis and equilibrium assessments. *Environmental Science and Techology*, 26:1955–1962, 1992.

[157] Wood, W. W., T. F. Kraemer, and P. P. Hearn Jr. Intragranular diffusion: An important mechanism influencing solute transport in clastic aquifers? *Science*, 247:1569–1572, 1990.

[158] Woodbury, A. D., and E. A. Sudicky. A reexamination of the geostatistical characteristics of the Borden aquifer. *Water Resources Research*, 27(4):533–546, 1991.

[159] Wu, S. C., and P. M. Gschwend. Sorption kinetics of hydrophobic organic compounds to natural sediments and soils. *Environmental Science and Techology*, 20:717–725, 1986.

[160] Yeh, G. T., and V. S. Tripathi. A model for simulating transport of reactive multispecies components: Model development and demonstration. *Water Resources Research*, 27:3075–3094, 1991.

[161] Zheng, C., and G. D. Bennett. *Applied Contaminant Transport Modeling.* Van Nostrand Reinhold, 1996.

This dissertation is accepted on behalf of the faculty of the Institute by the following committee

John L Wilson — Allan Stuhyr
Adviser

Robert A. Bowman

Fred M Phillips

June 23, 1997
Date

I release this document to New Mexico Institute of Mining and Technology.

Amit Kumar Mishra — June 25, 1997

Student's Signature — Date